

Naval Surface Warfare Center Carderock Division

West Bethesda, MD 20817-5700

NSWCCD-50-TR-2011/049 September 2011

Hydromechanics Department Report

Mission Assessment Investigation Based on Seakeeping Criteria for the Joint High-Speed Sealift Monohull and Trimaran Designs

by

J.T. Klamo

S.S. Lee

A. L. Silver

201101294



Approved for public release; distribution unlimited.

REPORT DOCUMENTATION PAGE

Form Approved
OMB No. 0704-0188

Public reporting burden for this collection of information is estimated to average 1 hour per response, including the time for reviewing instructions, searching existing data sources, gathering and maintaining the data needed, and completing and reviewing this collection of information. Send comments regarding this burden estimate or any other aspect of this collection of information, including suggestions for reducing this burden to Department of Defense, Washington Headquarters Services, Directorate for Information Operations and Reports (0704-0188), 1215 Jefferson Davis Highway, Suite 1204, Arlington, VA 22202-4302. Respondents should be aware that notwithstanding any other provision of law, no person shall be subject to any penalty for failing to comply with a collection of information if it does not display a currently valid OMB control number. **PLEASE DO NOT RETURN YOUR FORM TO THE ABOVE ADDRESS.**

1. REPORT DATE (DD-MM-YYYY) 7-Sep-2011			2. REPORT TYPE Final		3. DATES COVERED (From - To) 1-Jun-2008 - 30-Sep-2008	
4. TITLE AND SUBTITLE Mission Assessment Investigation Based on Seakeeping Criteria for the Joint High-Speed Sealift Monohull and Trimaran Designs					5a. CONTRACT NUMBER	
					5b. GRANT NUMBER	
					5c. PROGRAM ELEMENT NUMBER	
6. AUTHOR(S) Klamo, J.T., Lee, S.S., and Silver, A.L.					5d. PROJECT NUMBER	
					5e. TASK NUMBER	
					5f. WORK UNIT NUMBER 08-1-2125-146/-147	
7. PERFORMING ORGANIZATION NAME(S) AND ADDRESS(ES) AND ADDRESS(ES) Naval Surface Warfare Center Carderock Division Code 5500, Seakeeping 9500 MacArthur Boulevard West Bethesda, MD 20817-5700					8. PERFORMING ORGANIZATION REPORT NUMBER NSWCCD-50-TR-2011/049	
9. SPONSORING / MONITORING AGENCY NAME(S) AND ADDRESS(ES) Commander Naval Sea Systems Command Attn PMS 385 1333 Isaac Hull Ave SE Washington Navy Yard DC 20376-5100					10. SPONSOR/MONITOR'S ACRONYM(S)	
					11. SPONSOR/MONITOR'S REPORT NUMBER(S)	
12. DISTRIBUTION / AVAILABILITY STATEMENT Public release; distribution unlimited.						
13. SUPPLEMENTARY NOTES						
14. ABSTRACT Joint High-Speed Sealift (JHSS) vessel concepts were recently investigated by the Navy for inter-theater transport. A monohull and a trimaran design were produced in order to further technology development and reduce technical risks. This report documents ship motion assessment studies using each of these two preliminary hull configurations. These assessment studies covered three diverse potential mission profiles in an effort to investigate the ship performance over a range of plausible scenarios. The three missions considered were an open ocean high-speed transit; a coastal waters, zero-speed helicopter cargo transfer; and an open ocean, stricken vessel in large waves survival. The simulation software used to perform the ship motion calculations was the ShipX Vessel Response program (VERES).						
15. SUBJECT TERMS mission assessment, seakeeping criteria, VERES, monohull, trimaran						
16. SECURITY CLASSIFICATION OF:			17. LIMITATION OF ABSTRACT	18. NUMBER OF PAGES	19a. NAME OF RESPONSIBLE PERSON	
a. REPORT UNCLASSIFIED	b. ABSTRACT UNCLASSIFIED	c. THIS PAGE UNCLASSIFIED			Klamo, J.T.	
			SAR	82	19b. TELEPHONE NUMBER (include area code) (301)227-5523	

THIS PAGE INTENTIONALLY LEFT BLANK

Contents

	<i>Page</i>
Nomenclature	x
Abstract	1
Administrative Information	1
Introduction	1
VERES Theory	2
Frequency Domain Calculations	2
Single Significant Amplitude Value	2
Roll, Pitch, and Acceleration Statistics	3
Slamming	3
Motion Sickness Incidence	4
Motion Induced Interruptions	4
Simulation Details	5
Input Geometry	5
Ship Points of Interest	5
Mission Assessment Criteria	5
Verification of Hydrostatics	9
Simulation Conditions	9
Dynamic Sinkage and Trim	11
Wave Orientation Descriptions	12
Uncertainty Discussion	13
Transfer Function Resolution	14
Dynamic Sinkage and Trim	14
Relative Displacement and Velocity	14
Motion Sickness Incidence and Motion Induced Interruptions	15
Survival Mission Assessment Simplifications	15
Transit Mission Assessment Monohull Results	15
Accelerations	16
Motion Events	16
Roll and Pitch Motion Limits	20
Deck Wetness and Bow Slams	20
Transit Mission Assessment Trimaran Results	24
Accelerations	24
Motion Events	24
Roll and Pitch Motion Limits	27
Deck Wetness and Bow Slams	32
Transfer Mission Assessment	32

Accelerations	32
Motion Events	32
Roll and Pitch Motion Limits	36
Survival Mission Assessment	43
Critical Roll	43
Sensitivity of Results	44
Summary and Conclusions	49
Summary of Transit Mission Assessment	49
Summary of Transfer Mission Assessment	52
Summary of Survival Mission Assessment	52
Overall Conclusions	52
Acknowledgements	54
Appendix A - Random Seaway Description	55
Appendix B - Dynamic Sinkage and Trim Determination	61
Appendix C - Comparison of 2D and 2.5D Strip Theory for the Monohull at 36 knots	65
Appendix D - Comparison of 2D and 2.5D Strip Theory for the Trimaran at 36 knots	73
References	81

Figures

	<i>Page</i>
1. Orthogonal views of the JHSS monohull.	6
2. Orthogonal views of the JHSS trimaran.	7
3. Wave orientation descriptions.	13
4. Acceleration components oriented in the ship reference frame at the pilothouse for the JHSS monohull during a simulated ocean transit.	17
5. Acceleration components oriented in the ship reference frame at the forward spot for the JHSS monohull during a simulated ocean transit.	18
6. MSI and MII results at the pilothouse for the JHSS monohull during a simulated ocean transit.	19
7. MSI and MII results at the forward spot for the JHSS monohull during a simulated ocean transit.	21
8. Vessel roll and pitch results for the JHSS monohull during a simulated ocean transit.	22
9. Water on the deck and bow slam results for the JHSS monohull during a simulated ocean transit.	23
10. Acceleration components oriented in the ship reference frame at the pilothouse for the JHSS trimaran during a simulated ocean transit.	25
11. Acceleration components oriented in the ship reference frame at the forward spot for the JHSS trimaran during a simulated ocean transit.	26
12. MSI and MII results at the pilothouse for the JHSS trimaran during a simulated ocean transit.	28
13. MSI and MII results at the forward spot for the JHSS trimaran during a simulated ocean transit.	29
14. Vessel roll and pitch results for the JHSS trimaran during a simulated ocean transit.	30
15. Water on the deck and bow slam results for the JHSS trimaran during a simulated ocean transit.	31
16. Acceleration components oriented in the ship reference frame at helicopter spot 1 for both the JHSS monohull and trimaran during a simulated cargo transfer.	33
17. Acceleration components oriented in the ship reference frame at helicopter spot 2 for both the JHSS monohull and trimaran during a simulated cargo transfer.	34
18. Acceleration components oriented in the ship reference frame at helicopter spot 3 for both the JHSS monohull and trimaran during a simulated cargo transfer.	35
19. MSI and MII results at helicopter spot 1 for both the JHSS monohull and trimaran during a simulated cargo transfer.	37
20. MSI and MII results at helicopter spot 2 for both the JHSS monohull and trimaran during a simulated cargo transfer.	38
21. MSI and MII results at helicopter spot 3 for both the JHSS monohull and trimaran during a simulated cargo transfer.	39
22. Vessel roll and pitch results for both the JHSS monohull and trimaran during a simulated cargo transfer.	40

23. Study of appendage effects on the roll motions of the monohull geometry with zero forward speed in various sea states.	41
24. Comparison of the predicted roll motions for different geometry monohulls in a Sea State 5.	42
25. Vessel roll results for both the JHSS monohull and trimaran during a simulated survival situation.	44
26. Comparison of vessel pitch angles predicted using the traditional 2D strip theory and the high-speed 2.5D strip theory for a 36 knot simulation for both the JHSS monohull and trimaran.	46
27. Comparison of hull slams predicted using the traditional 2D strip theory and the high-speed 2.5D strip theory for a 36 knot simulation for both the JHSS monohull and trimaran.	47
28. Comparison of hull slams predicted using the traditional Ochi critical velocity relationship and a $V_{cr} = 0$ for a 20 knot simulation for both the JHSS monohull and trimaran.	48
29. Composite results of the transit mission for the JHSS monohull.	50
30. Composite results of the transit mission for the JHSS trimaran.	51
31. Composite results of the transfer mission for both the JHSS monohull and trimaran.	53
32. Composite results for the survival mission for both the JHSS monohull and trimaran.	54
A.1. Bretschneider Sea State 5 spectral shape used in the “transit” portion of the mission assessment.	56
A.2. Bretschneider Sea State 6 spectral shape used in the “transit” portion of the mission assessment.	56
A.3. Bretschneider Sea State 7 spectral shape used in the “transit” portion of the mission assessment.	57
A.4. Bretschneider Sea State 8 spectral shape used in the “survival” portion of the mission assessment.	57
A.5. Comparison of the spectral shapes for Bretschneider Sea States 5 through 8 used during the “transit” and “survival” portion of the mission assessment study.	58
A.6. JONSWAP Sea State 2 spectral shape used in the “transfer” portion of the mission assessment.	58
A.7. JONSWAP Sea State 3 spectral shape used in the “transfer” portion of the mission assessment.	59
A.8. JONSWAP Sea State 4 spectral shape used in the “transfer” portion of the mission assessment.	59
A.9. JONSWAP Sea State 5 spectral shape used in the “transfer” portion of the mission assessment.	60
A.10. Comparison of the spectral shapes for JONSWAP Sea States 2 through 5 used during the cargo “transfer” portion of the mission assessment study.	60
B.1. Experimentally measured dynamic sinkage and trim of the JHSS monohull.	61

B.2. Experimentally measured dynamic sinkage and trim of a similar trimaran model to the JHSS trimaran.	62
B.3. Extrapolated dynamic sinkage value for 20 and 36 knots for different longitudinal side hull spacing ratios.	63
B.4. Extrapolated dynamic trim values for 20 and 36 knots for different longitudinal side hull spacing ratios.	63
C.1. Comparison of longitudinal accelerations at the pilothouse for the JHSS monohull using 2D and 2.5D strip theory at $F_n = 0.347$	65
C.2. Comparison of lateral accelerations at the pilothouse for the JHSS monohull using 2D and 2.5D strip theory at $F_n = 0.347$	66
C.3. Comparison of the vertical accelerations at the pilothouse for the JHSS monohull using 2D and 2.5D strip theory at $F_n = 0.347$	66
C.4. Comparison of longitudinal accelerations at the general helicopter spot for the JHSS monohull using 2D and 2.5D strip theory at $F_n = 0.347$	67
C.5. Comparison of lateral accelerations at the general helicopter spot for the JHSS monohull using 2D and 2.5D strip theory at $F_n = 0.347$	67
C.6. Comparison of vertical accelerations at the general helicopter spot for the JHSS monohull using 2D and 2.5D strip theory at $F_n = 0.347$	68
C.7. Comparison of MSI at the pilothouse for the JHSS monohull using 2D and 2.5D strip theory at $F_n = 0.347$	68
C.8. Comparison of MII at the pilothouse for the JHSS monohull using 2D and 2.5D strip theory at $F_n = 0.347$	69
C.9. Comparison of MSI at the general helicopter spot for the JHSS monohull using 2D and 2.5D strip theory at $F_n = 0.347$	69
C.10. Comparison of MII at the general helicopter spot for the JHSS monohull using 2D and 2.5D strip theory at $F_n = 0.347$	70
C.11. Comparison of vessel roll angles for the JHSS monohull using 2D and 2.5D strip theory at $F_n = 0.347$	70
C.12. Comparison of vessel pitch angles for the JHSS monohull using 2D and 2.5D strip theory at $F_n = 0.347$	71
C.13. Comparison of deck wetness at the bow for the JHSS monohull using 2D and 2.5D strip theory at $F_n = 0.347$	71
C.14. Comparison of hull slams at the bow for the JHSS monohull using 2D and 2.5D strip theory at $F_n = 0.347$	72
D.1. Comparison of longitudinal accelerations at the pilothouse for the JHSS trimaran using 2D and 2.5D strip theory at $F_n = 0.364$	73
D.2. Comparison of lateral accelerations at the pilothouse for the JHSS trimaran using 2D and 2.5D strip theory at $F_n = 0.364$	74
D.3. Comparison of vertical accelerations at the pilothouse for the JHSS trimaran using 2D and 2.5D strip theory at $F_n = 0.364$	74

D.4. Comparison of longitudinal accelerations at the general helicopter spot for the JHSS trimaran using 2D and 2.5D strip theory at $F_n = 0.364$	75
D.5. Comparison of lateral accelerations at the general helicopter spot for the JHSS trimaran using 2D and 2.5D strip theory at $F_n = 0.364$	75
D.6. Comparison of vertical accelerations at the general helicopter spot for the JHSS trimaran using 2D and 2.5D strip theory at $F_n = 0.364$	76
D.7. Comparison of MSI at the pilothouse for the JHSS trimaran using 2D and 2.5D strip theory at $F_n = 0.364$	76
D.8. Comparison of MII at the pilothouse for the JHSS trimaran using 2D and 2.5D strip theory at $F_n = 0.364$	77
D.9. Comparison of MSI at the general helicopter spot for the JHSS trimaran using 2D and 2.5D strip theory at $F_n = 0.364$	77
D.10. Comparison of MII at the general helicopter spot for the JHSS trimaran using 2D and 2.5D strip theory at $F_n = 0.364$	78
D.11. Comparison of vessel roll angles for the JHSS trimaran using 2D and 2.5D strip theory at $F_n = 0.364$	78
D.12. Comparison of vessel pitch angles for the JHSS trimaran using 2D and 2.5D strip theory at $F_n = 0.364$	79
D.13. Comparison of deck wetness at the bow for the JHSS trimaran using 2D and 2.5D strip theory at $F_n = 0.364$	79
D.14. Comparison of hull slams at the bow for the JHSS trimaran using 2D and 2.5D strip theory at $F_n = 0.364$	80

Tables

	<i>Page</i>
1. Risk level of MIIs and their corresponding per minute values.	4
2. Points of interest for the monohull geometry used for the mission assessment. . . .	8
3. Points of interest for the trimaran geometry used for the mission assessment. . . .	8
4. Listing of the mission assessment criteria for the “transit”, “transfer”, and “survival” portions of the mission assessment.	9
5. Design and realized hydrostatic values for the JHSS monohull. Bold numbers are inputs to VERES and are not independently calculated.	10
6. Design and realized hydrostatic values for the JHSS trimaran. Bold numbers are inputs to VERES and are not independently calculated.	11
7. Sea state definitions using significant wave height and modal period.	12
8. Dynamic sinkage and trim values applied to the monohull and trimaran designs during the transit portion of the mission assessment study.	13

Nomenclature

Abbreviations

CG	center of gravity
JHSS	Joint High-Speed sealift
JONSWAP	Joint North Sea Wave Project
MSI	motion sickness incidence
MII	motion induced interruptions
NAVSEA	Naval Sea Systems Command
RMS	root-mean square
RSLs	Rapid Strategic Lift Ship
SSA	single significant amplitude
VERES	Vessel Responses program

Symbols

F	freeboard
F_n	Froude Number
g	acceleration due to gravity
H_s	significant wave height (meters)
$H_\eta(\omega)$	transfer function of the η degree of freedom
$m_{k,\eta}$	the k^{th} moment of the η degree of freedom
n	number of slams per hour
P_{slam}	probability of a slam event
$R_\eta(\omega)$	vessel response spectrum
$S(\omega)$	wave spectrum
T_m	modal wave period (seconds)
V_{cr}	critical vertical velocity
η	a given degree of freedom
γ	peakedness parameter
$\psi_{\text{sig},\eta}$	single significant amplitude value in the η direction
σ	spectral width parameter
σ_V	standard deviation of the relative vertical velocity
σ_F	standard deviation of the relative vertical displacement
θ_η	vessel rotation in the η direction
ω	wave frequency (radians/second)
ω_m	modal wave frequency (radians/second)

Abstract

Joint High-Speed Sealift (JHSS) vessel concepts were recently investigated by the Navy for inter-theater transport. A monohull and a trimaran design were produced in order to further technology development and reduce technical risks. This report documents ship motion assessment studies using each of these two preliminary hull configurations. These assessment studies covered three diverse potential mission profiles in an effort to investigate the ship performance over a range of plausible scenarios. The three missions considered were an open ocean high-speed transit; a coastal waters, zero-speed helicopter cargo transfer; and an open ocean, stricken vessel in large waves survival. The simulation software used to perform the ship motion calculations was the ShipX Vessel Response program (VERES).

Administrative Information

The work described in this report was funded by the Joint High Speed Sealift (JHSS) program office of the Naval Sea Systems Command (NAVSEA) PMS 385. The results contained in this report were performed by the Seakeeping Division, Code 5500, of the Hydromechanics Department at the Naval Surface Warfare Center, Carderock Division (NSWCCD) under work unit numbers 08-1-2125-146 and 08-1-2125-147.

Introduction

The Joint High Speed Sealift (JHSS) project investigated concepts for rapidly transporting low-density, high value cargo over strategic distances. This study assessed shipboard motions for a 290 meter monohull and a 264 meter trimaran, each designed to cruise at 36 knots. The monohull displaces 34,843 tonnes and has 151,000 kilowatt installed propulsion power driving four fixed pitch propellers. The trimaran displaces 31,173 tonnes, and has 144,000 kilowatt installed propulsion power driving four waterjets.

This shipboard motions assessment used established criteria to evaluate mission performance in various North Atlantic and North Pacific Ocean scenarios. Three potential missions were explored. The first was a high-speed transit at 20 and 36 knots across the open ocean. The parameters of interest for this mission were motions, accelerations, hull slams, deck wetness, motion sickness incidence (MSI), and motion induced interruptions (MII). The second mission considered was a cargo transfer using helicopters in coastal waters at zero speed. For this portion, the relevant parameters were motions, accelerations, hull slams, deck wetness, MSI, and MII. The final mission considered was a stricken vessel in the open ocean with large waves. The only parameter of interest for this portion was the vessel roll angle. For all three missions considered, a range of wave conditions that are representative of the ocean environments in which each mission would be conducted was considered. This evaluation was also conducted over a range of ship operating conditions, i.e., combinations of various speeds and headings. The output of this study will be useful for establishing future high-speed ship hullform design and arrangement priorities.

VERES Theory

Vessel Responses (VERES) is an optional plug-in program for the Marintek ShipX Workbench. The ShipX Workbench provides the necessary graphical user interface to create the input for VERES as well as run it. VERES is a linear, potential flow, two-dimensional strip theory ship motion simulation program that is able to accommodate both monohull and multihull vessels. Besides the traditional two-dimensional strip theory that follows the commonly used Salvensen-Tuck-Faltinsen^{1†} formulation, and is usually employed for low ship speeds, VERES also contains a high-speed 2.5D strip theory² for use at higher ship speeds. There is not a single universally accepted Froude number that delineates when each of the two methods should be used. However, the VERES manual³ suggests that the high-speed strip theory should be used when vessel speeds reach or surpass a Froude number in the general range of 0.30 to 0.40. VERES also allows for the input of dynamic sinkage and trim values for a given vessel speed. The linear theory formulation within VERES means that the code is best suited to predict moderate ship motions caused by moderate wave heights.

Frequency Domain Calculations

For a given hull geometry at various user-prescribed vessel speeds and wave encounter frequencies, VERES determines the hydrodynamic coefficients necessary to predict ship motions in the frequency domain and provides the various transfer functions, $H_\eta(\omega)$, where η refers to one of the six degrees of freedom and ω is frequency. VERES determines the response spectrum, $R_\eta(\omega)$, by combining the relevant transfer function with the provided wave spectrum, $S(\omega)$, as follows

$$R_\eta(\omega) = |H_\eta(\omega)|^2 S(\omega). \quad (1)$$

The statistics of the responses can be calculated from the various moments of these response spectrum. The moments are given by

$$m_{k,\eta} = \int_0^\infty \omega^k R_\eta(\omega) d\omega \quad (2)$$

where $m_{k,\eta}$ is the k^{th} moment of the η degree of freedom.

Single Significant Amplitude Value

The standard deviations of the responses of interest are obtained within VERES by calculating the square-root of the k^{th} order moment of the corresponding response spectrum. The value of k will be determined by whether one is seeking the statistics of the displacements, velocities, or accelerations. For a zero mean process, such as the case in this study when the movement of each point of interest is considered from its corresponding static location, the standard deviation equals the root-mean square (RMS) value.

For this mission assessment study, the criteria threshold values were based on the single significant amplitude (SSA) value of the responses. Single significant amplitude values are simply

[†]References are found beginning on page 81

twice the standard deviation, or RMS, value and represent the average of the one-third highest amplitudes in the sample. Therefore, we have the simple relationship

$$\psi_{\text{sig},\eta} = 2\sqrt{m_{k,\eta}} \quad (3)$$

where $\psi_{\text{sig},\eta}$ is the single significant amplitude value. All roll and pitch angle results, as well as longitudinal, transverse, and vertical acceleration results, are given in terms of their SSA value throughout this study.

Roll, Pitch, and Acceleration Statistics

Translational and angular displacement statistics of ship motion are calculated using the 0th moment in Equation 2. The pitch and roll motion statistics described in this report were determined in this manner. The velocity statistics of ship motions can be calculated using the 2nd moment of Equation 2 and the acceleration statistics by using the 4th moment of the same equation. These displacements, velocities, and accelerations are referenced to a coordinate system that is fixed to the moving vessel at the mean waterline.

The effect of gravity on the ship motion accelerations is also considered. The linear formulation means that the transformation of gravity effects into the ship frame of reference is $g\theta_\eta$, where g is the acceleration due to gravity and θ_η is either pitch angle, for longitudinal accelerations, or roll angle, for transverse accelerations. This correction allows the code to predict the acceleration an object or person moving with the vessel would experience at its current location. The longitudinal and lateral acceleration parameters are deviations from zero, making them identical to RMS values, while the vertical acceleration parameter is a deviation about the acceleration due to gravity. All accelerations can be easily nondimensionalized by gravity within VERES. The mission assessment criteria of accelerations were based on the gravity corrected acceleration parameters.

Slamming

Slamming is determined within VERES by considering two separate parameters: the relative vertical displacement and the relative vertical velocity. The relative vertical displacement in VERES is determined by subtracting the projected undisturbed wave height at a point of interest from the vertical displacement of that point. This vertical displacement has heave displacement and pitch and roll angle contributions included. The other consideration in the slamming calculation is the relative vertical velocity. This is calculated in VERES by subtracting the undisturbed wave velocity at a point of interest from the vertical velocity of that point on the vessel. The vertical velocity of the vessel has both pitch and roll rate contributions included as well as the vertical component of the vessel forward speed when pitched at an angle.

VERES determines the number of slams per hour by first determining the statistics of relative vertical displacement and velocity using the moments of the responses as discussed in Equation 2. This allows the estimation of the standard deviations of the relative vertical displacement and velocity. Since the relative motion and relative velocity are statistically independent, we can express the probability of the slamming as a joint probability of the two considerations. The probability is therefore calculated using

$$P_{\text{slam}} = e^{-\frac{1}{2} \left[\left(\frac{V_{cr}}{\sigma_V} \right)^2 + \left(\frac{F}{\sigma_F} \right)^2 \right]} \quad (4)$$

where P_{slam} is the probability of slamming, V_{cr} is the critical velocity, σ_V is the standard deviation of the relative vertical velocities, F is the freeboard, and σ_F is the standard deviation of the relative vertical displacement. Once the probability of slamming, P_{slam} , is known, the number of slams per hour, n , is estimated from the number of encounters using

$$n = \frac{3600\sigma_F}{2\pi\sigma_V} P_{\text{slam}} \quad (5)$$

Motion Sickness Incidence

The motion sickness incidence, or MSI, represents the percentage of the crew, after a certain exposure time, that would experience motion sickness having been exposed to the vessel motions at the location of interest. One way to calculate MSI involves treating it as a function of the frequency, acceleration, and exposure time of the vertical motion as suggested by O’Hanlon and McCauley⁴. This idea was later refined in McCauley *et al.*⁵ and a mathematical model was proposed. This model has been implemented in VERES, and calculates the percentage MSI for a certain exposure time; exposure times of two and four hours are frequently used in the literature. For all of our mission assessment calculations, the threshold criteria were based on 20 percent of the crew becoming sick over an exposure time of four hours.

Motion Induced Interruptions

Motion induced interruptions, or MIIs, can be thought of as a sufficient loss of balance by a crew member to require him or her to stop working on the current task. In order to compare the operational performance of different vessels when no specific deck operation is being analyzed, Graham⁶ proposed establishing a standard deck operation for comparison purposes. This standard operation is defined as a one-minute operation with a tipping coefficient of 0.25 resulting in the unit “MIIs per minute” for deck operations criteria. Proposed values for different risk levels are shown in Table 1. It is suggested by Graham⁶ that deck operations be considered substantially degraded when the MII incidence value exceeds one per minute.

Table 1. Risk level of MIIs and their corresponding per minute values according to Graham⁶.

Risk level	MIIs per minute
possible	0.1
probable	0.5
serious	1.5
severe	3.0
extreme	5.0

In order to calculate the motion induced interruptions, or MII, the lateral and vertical accelerations that are perceived in the plane of the ship's deck by an object must be known. These are the gravity corrected lateral and vertical accelerations and are determined internally by VERES as described in Section **Roll, Pitch, and Acceleration Statistics**. These accelerations cause objects to topple or slide across the deck, and people to lose their balance.

Simulation Details

Input Geometry

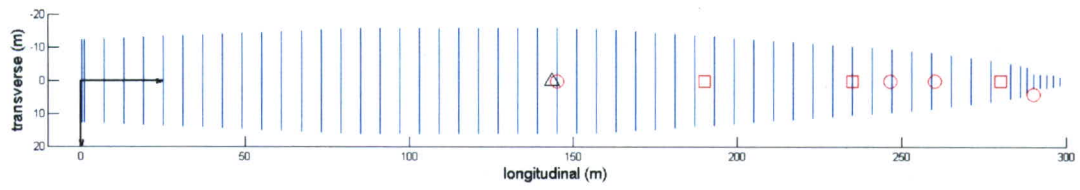
A vessel geometry is provided to VERES as a point definition file containing the offset points along numerous hull lines of the vessel, referred to as stations. Essentially, each station occurs at a constant longitudinal value and offset points, representing the transverse and vertical locations, are used to create the three-dimensional hull curve. For the monohull, the FY05 "Best of Show" Baseline JHSS monohull was used. This hull was represented by 56 stations each containing approximately 35 offset points per hull line. Within VERES, bilge keels and a stern trim tab were modeled as lifting foils. The full monohull vessel geometry, minus the internal VERES lifting foils, can be seen in Figure 1. For the trimaran hull, the RSLs Trimaran FY05 was used. This hull was represented by 68 stations with the central hull body containing approximately 35 offset points and each side hull containing approximately 35 offset points as well. The corresponding full vessel geometry can be seen in Figure 2.

Ship Points of Interest

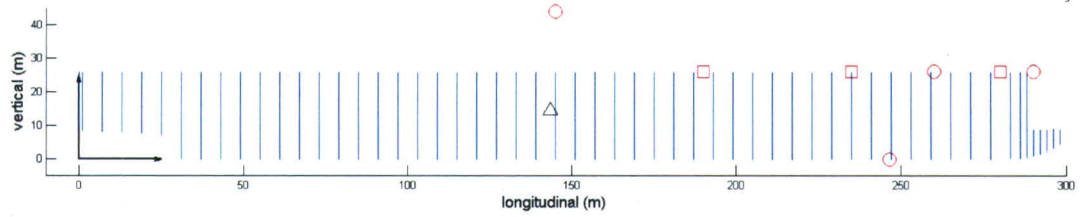
Eight locations on each vessel were identified as being important when determining mission assessments and are shown in Tables 2 and 3. The first two locations are subjected to bow wetness, labeled BW, and bow slams, labeled BS. Three more locations are areas of the ship where helicopter operations are conducted and are labeled H1, H2, and H3. Another point, FS, in the forward part of the ship is located longitudinally between two helicopter operations points. The last two points of interest are the pilothouse, labeled PH, and the vessel center of gravity, labeled CG. For the monohull these points were based on the RSLs FY05 "Best of Show" feasibility study but were adjusted for the JHSS 2006 Hull form offsets. The locations of the trimaran points were based on the RSLs FY05 trimaran feasibility study and are adjusted for the the RSLs FY05 trimaran hull form offsets. The eight points of interest are shown graphically in Figures 1 and 2 for the monohull and trimaran respectively. In each figure, the triangle marks the location of the center of gravity for the vessel. The circles mark the locations of the points used in the transit portion of the mission assessment while the squares denote points used in the cargo transfer portion of the mission assessment. VERES employs a left handed input coordinate system such that the x-axis points forward from the aft perpendicular, the y-axis points starboard from the centerline, and the z-axis points upward from the baseline.

Mission Assessment Criteria

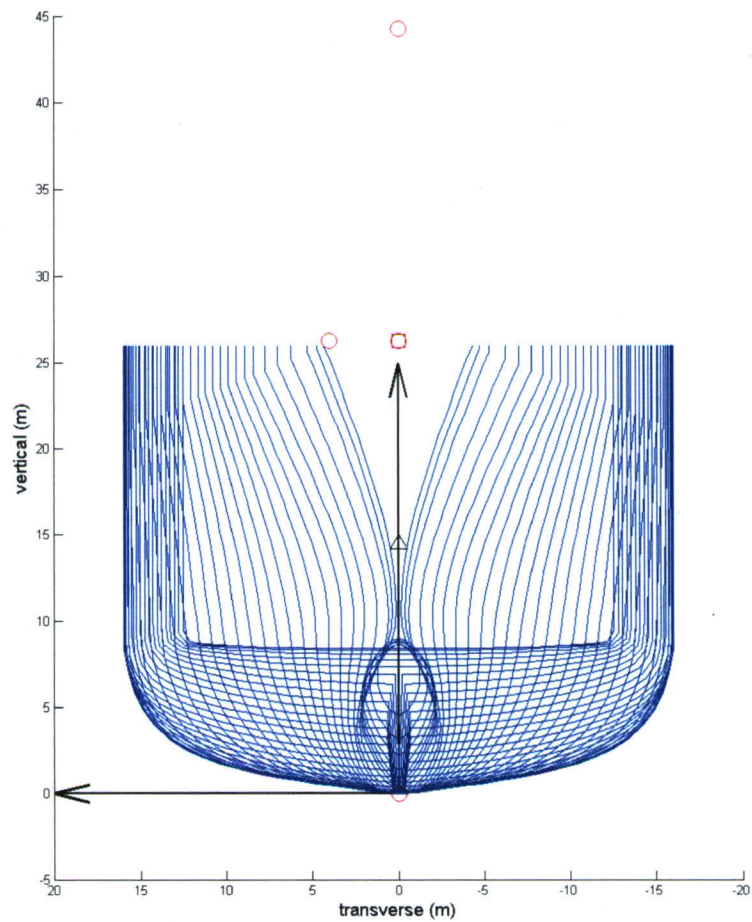
In order to determine if a vessel is capable of completing a given mission, three entities must be determined: a set of measurable parameters that affect the mission, the quantitative values that those parameters must not exceed, and the locations on the vessel to evaluate those parameters.



(a) top view, XY-plane

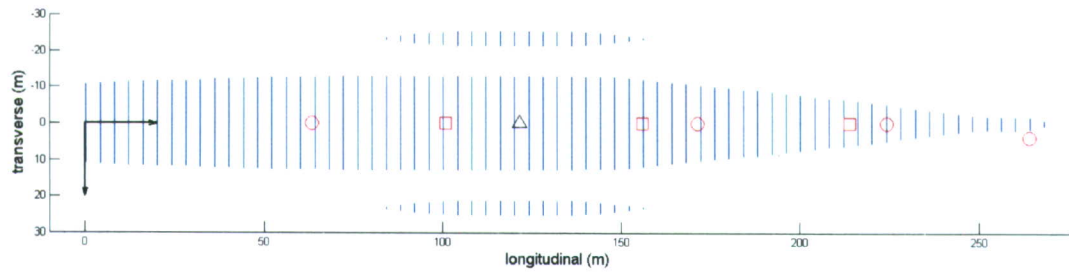


(b) side view, XZ-plane

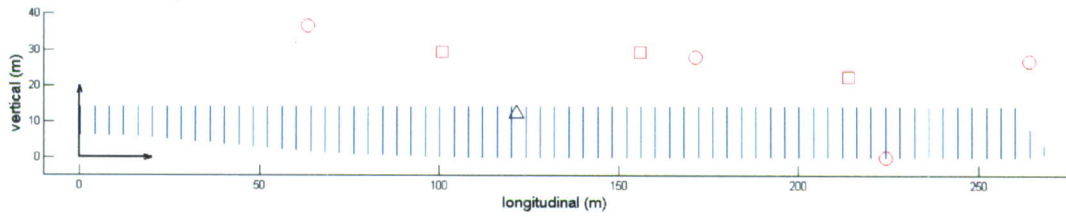


(c) front view, YZ-plane

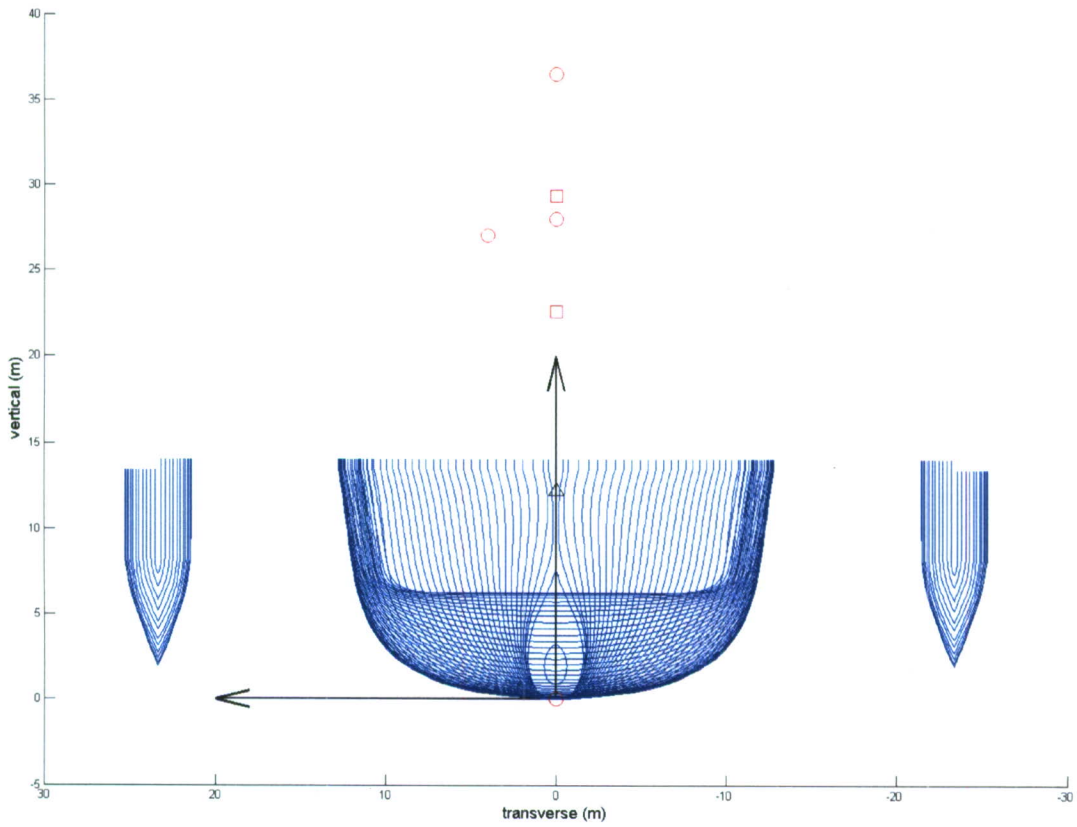
Fig. 1. Orthogonal views of the JHSS monohull. \circ : points used for transit portion; \square : points used for transfer portion; \triangle : center of gravity.



(a) top view, XY-plane



(b) side view, XZ-plane



(c) front view, YZ-plane

Fig. 2. Orthogonal views of the JHSS trimaran. \circ : points used for transit portion; \square : points used for transfer portion; \triangle : center of gravity.

Table 2. Points of interest for the monohull geometry used for the mission assessment.

point description	point label	X (m)	Y (m)	Z (m)
bow wetness	BW	290.00	4.00	26.30
helicopter spot 1	H1	280.00	0.00	26.30
forward spot	FS	260.00	0.00	26.30
bow slams	BS	246.50	0.00	0.00
helicopter spot 2	H2	235.00	0.00	26.30
helicopter spot 3	H3	190.00	0.00	26.30
pilothouse	PH	145.00	0.00	44.30
center of gravity	CG	143.53	0.00	14.36

Table 3. Points of interest for the trimaran geometry used for the mission assessment.

point description	point label	X (m)	Y (m)	Z (m)
bow wetness	BW	263.46	4.00	27.00
bow slams	BS	223.86	0.00	0.00
helicopter spot 1	H1	214.00	0.00	22.60
forward spot	FS	170.96	0.00	28.00
helicopter spot 2	H2	156.00	0.00	29.35
center of gravity	CG	120.93	0.00	12.20
helicopter spot 3	H3	101.00	0.00	29.35
pilothouse	PH	62.79	0.00	36.52

The criteria used to determine whether a vessel is able to perform a given mission is somewhat arbitrary and depends on how well the three selected entities represent the actual mission. For this investigation, three different missions were considered. The first mission, referred to as “transit,” is an attempt to represent the vessel as it moves from its loading location to its unloading location. Therefore, this mission involves the vessel moving at fairly high speeds, 20 and 36 knots, in open-ocean high sea states. The second mission considered, referred to as “transfer,” is an attempt to represent the vessel loading or unloading cargo through helicopter operations, essentially a helicopter-based cargo transfer. This mission involves the vessel at zero forward speed in lower sea states in a fetch limited, close to shore, location. The final mission considered, referred to as “survival,” attempts to capture a worst case scenario of the vessel, at zero speed, in the open ocean in extremely large waves.

The mission assessment criteria used in this investigation were based on standard Navy guidelines for the various types of mission investigated^{7,8}. All the determined criteria and their threshold values are listed in Table 4. In order for the vessel to be considered able to accomplish its current mission for a given speed and heading while in a given sea state, the single significant amplitude response or events per length of time, whichever is relevant, of each of the criteria of interest must be below the threshold level.

Table 4. Listing of the mission assessment criteria for the “transit”, “transfer”, and “survival” portions of the mission assessment.

transit portion criteria		
parameter	location	threshold criteria
roll angle	CG	8.0°
pitch angle	CG	3.0°
longitudinal acceleration	PH, FS	0.2g
lateral acceleration	PH, FS	0.2g
vertical acceleration	PH, FS	0.4g
MSI	PH, FS	20% of crew after 4 hour duration
MII	PH, FS	1 per minute
deck wetness	BW	30 submergences per hour
bow slams	BS	20 slams per hour
transfer portion criteria		
parameter	location	threshold criteria
roll angle	CG	4.0°
pitch angle	CG	2.0°
longitudinal acceleration	H1, H2, H3	0.1g
lateral acceleration	H1, H2, H3	0.1g
vertical acceleration	H1, H2, H3	0.4g
MSI	H1, H2, H3	20% of crew after 4 hour duration
MII	H1, H2, H3	1 per minute
survival portion criteria		
parameter	location	threshold criteria
roll angle	CG	30.0°

Verification of Hydrostatics

Before computing the vessel response with VERES, the hydrostatic calculations were examined to insure that the geometry was properly oriented within the program as well as ballasted for the right displacement and static trim. The hydrostatics parameters that it determined are compared to the estimated design values. The results for the monohull geometry can be seen in Table 5 and the trimaran geometry in Table 6.

Simulation Conditions

Each of the three portions of the mission assessment had a unique set of simulation conditions. The “transit” portion involved vessel speeds of 20 knots ($F_n = 0.193$ monohull and $F_n = 0.202$ trimaran) and 36 knots ($F_n = 0.347$ monohull and $F_n = 0.364$ trimaran). Since the latter speed put both vessels above $F_n = 0.30$, the high-speed VERES 2.5D strip theory was also investigated and compared with the traditional 2D strip theory to see the effects of theory formulation on the

Table 5. Design and realized hydrostatic values for the JHSS monohull. Bold numbers are inputs to VERES and are not independently calculated.

parameter	Design Value	Input Geometry
length overall, LOA (m)		297.86
length between perpendiculars, LBP (m)	290.00	290.00
beam, waterline (m)		31.76
draft amidship (m)	8.59	8.59
displacement (tonne)	34843.00	35852.03
heel to starboard (deg)	0.00	0.00
trim, + stern down (m)	0.00	0.00
wetted area (m ²)		9568.92
waterplane area (m ²)		6723.05
LCB from AP, + fwd (m)	145.77	145.77
LCF from AP, + fwd (m)		119.15
LCG from AP, + fwd (m)	145.77	145.79
KB (m)		5.306
KG (m)	14.36	14.36
GMt (m)		3.46
GMI (m)		1028.71
KMt (m)		17.79
KMI (m)		
immersion (tonne/cm)		68.91
r44 (m)		12.10
r55 (m)		70.81
r66 (m)		70.85
r46 (m)		1.90

results for that speed. The seaway used for this operation investigation was a long-crested, irregular seaway with a Bretschneider spectral shape for sea states five through seven. For the helicopter cargo “transfer” portion of the mission assessment only zero vessel speed was considered. The seaway used for this mission was a long-crested, irregular seaway with a JONSWAP spectral shape for sea states two through five. The JONSWAP spectrum was chosen to better represent the fetch limited wind conditions that are prevalent closer to shore. The JONSWAP spectrum considered had a fixed γ value of 3.3 (see Appendix A for more details on JONSWAP spectrum). For the “survival” portion of the mission assessment, again, only zero vessel speed was considered. The seaway was a long-crested, irregular seaway with a Bretschneider spectral shape for Sea State 8.

For all three scenarios of the mission assessment, the wave headings considered were from 0 to 345 degrees by 15 degree increments. Also, the modal periods and significant wave heights used for each of the sea states used in all three missions were obtained from Lee and Bales⁹ and are listed in Table 7. The spectral shape for each sea state can be seen in the figures of Appendix A and

Table 6. Design and realized hydrostatic values for the JHSS trimaran. Bold numbers are inputs to VERES and are not independently calculated.

parameter	Design Value	Input Geometry
length overall, LOA (m)		268.00
length between perpendiculars, LBP (m)	263.60	263.46
beam, waterline (m)	50.50	50.50
draft amidship (m)	8.60	8.60
displacement (tonne)	31173.00	31171.66
heel to starboard (deg)	0.00	0.00
trim, + stern down (m)	0.70	0.70
wetted area (m ²)	8987.50	10619.80
waterplane area (m ²)	5276.50	5304.49
LCB from AP, + fwd (m)	121.10	120.61
LCF from AP, + fwd (m)	109.40	108.74
LCG from AP, + fwd (m)	121.10	120.61
KB (m)	5.40	5.33
KG (m)	12.20	12.20
GMt (m)	7.50	7.605
GMI (m)	630.10	685.91
KMt (m)	19.70	19.82
KMI (m)	642.30	698.11
immersion (tonne/cm)	54.10	54.37
r44 (m)		19.69
r55 (m)		65.90
r66 (m)		68.54
r46 (m)		0.00

a comparison of the sea states is shown in Figure A.5 for the Bretschneider spectra and Figure A.10 for the JONSWAP spectra.

Dynamic Sinkage and Trim

Since the “transit” portion of the mission assessment involved forward vessel speeds, approximate dynamic sinkage and trim values were applied to both the monohull and trimaran. For the monohull, the dynamic sinkage and trim values were obtained from the JHSS Model 5653-3 experimental test by Cusanelli and Chesnakas¹⁰ conducted at NSWCCD. During this test, the sinkage and trim of the model was recorded from 15 to 45 knots in one knot increments. Therefore, the two speeds used in this simulation, 20 and 36 knots, were actually tested and the corresponding sinkage and trim values measured. These measured values were used in the simulation.

For the trimaran, no data existed from an experimental model test using a trimaran hull similar to the one used in this simulation. Therefore, the values for the trimaran were estimates based

Table 7. Sea state definitions using significant wave height and modal period.

transit portion sea states		
Sea State	mean H_s (m)	most probable T_m (sec)
5	3.25	9.7
6	5.00	12.4
7	7.50	15.0
transfer portion sea states		
Sea State	mean H_s (m)	most probable T_m (sec)
2	0.30	6.9
3	0.88	7.5
4	1.88	8.8
5	3.25	9.7
survival portion sea state		
Sea State	mean H_s (m)	most probable T_m (sec)
8	11.50	16.4

on experimental results from a model test conducted by Carr and Dvorak¹¹ at the Webb Institute using a trimaran hull that was similar to the one used for this study. The major differences between the two trimaran hulls were that the Carr and Dvorak model had the side hulls farther aft and a smaller static trim than the JHSS model. In their experiment, they measured the changes in hull draft and trim, from their static values, over a range of speeds for various side hull locations. Their measured values can be found in Appendix B along with the extrapolated results, at the two speeds used in this simulation, for amidship side hulls; the position used in these simulations. The two extrapolated values for the change in draft were used as the dynamic sinkage for the JHSS trimaran at the corresponding speeds. The two extrapolated values for the change in trim were applied to the +0.15 degrees of static trim, that the JHSS trimaran is designed to have, to approximate the dynamic trim at the corresponding speeds. The dynamic sinkage and trim values used during this mission assessment investigation for both the monohull and trimaran can be seen in Table 8.

Wave Orientation Descriptions

In VERES, the wave heading convention is zero degrees for head seas, 90 degrees for port beam seas, and 180 degrees for following seas. This wave heading convention is shown in Figure 3. For clarity when describing the mission assessment results, we also adopted the phrase “general” in front of head, beam, or following seas to denote the entire general area of such a wave orientation. For instance, general beam seas would refer to any wave heading from between 45 to 135 degrees as well as 225 to 315 degrees. This nomenclature is also shown in Figure 3.

Table 8. Dynamic sinkage and trim values applied to the monohull and trimaran designs during the transit portion of the mission assessment study.

monohull design		
speed (knots)	sinkage, + up (m)	trim, + stern down (deg)
20	-0.163	-0.050
36	-0.602	-0.230
trimaran design		
speed (knots)	sinkage, + up (m)	trim, + stern down (deg)
20	-0.175	0.125
36	-0.800	0.200

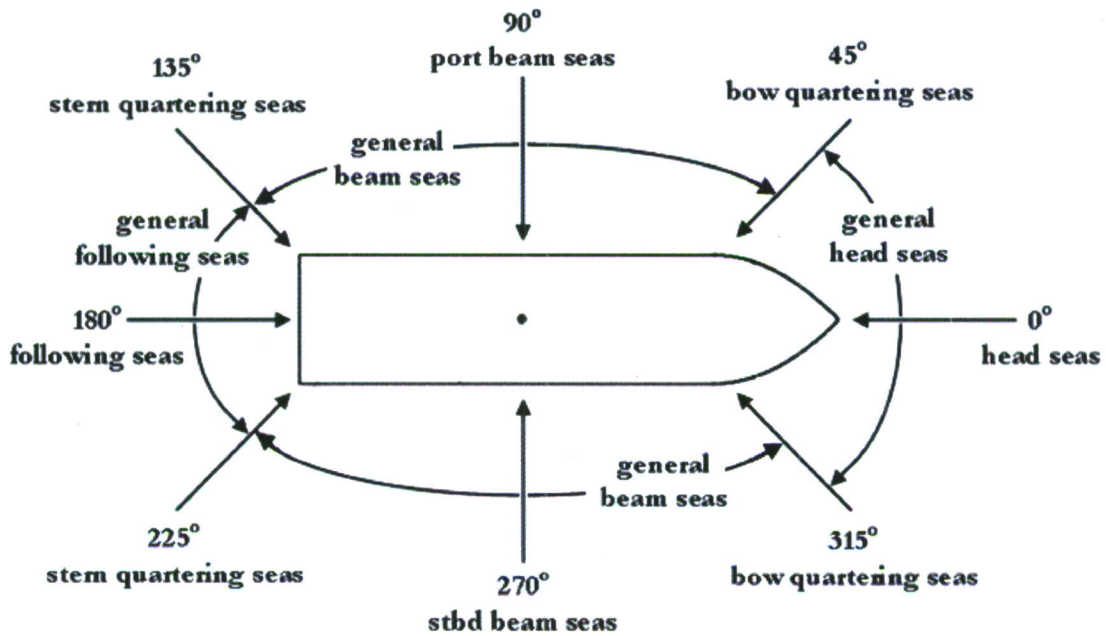


Fig. 3. Wave orientation descriptions.

Uncertainty Discussion

The fact that VERES is based on linear, potential flow, strip theory introduces a certain amount of error into the results. As mentioned in Section **VERES Theory**, the linear nature of the code means that it is best suited for moderate ship motions caused by medium wave heights. Numerous multihull vessel geometries, particularly trimarans, have been simulated at NSWCCD using VERES to obtain their response transfer functions. These simulation transfer functions have been correlated with regular wave model test results, as reported by O’Dea¹², and were found to qualitatively predict the motions of a trimaran. Therefore, when simulating irregular sea conditions that allow for the prediction of overall ship motions through the superposition of the individual motion

at each corresponding frequency, the VERES predictions should be realistic. However, the larger waves seen in the highest sea states, and the large induced motions that result, require nonlinear terms to capture the correct behavior and therefore restrict the validity of the VERES results. The following sections introduce various factors that could potentially increase the uncertainty of the VERES output, but do not attempt to quantify that uncertainty.

Transfer Function Resolution

In order to calculate the statistics of the response spectrum, it is extremely important that the resolution of the transfer function be sufficiently robust. Namely, the transfer function must contain a sufficient number of wave periods in the range where the wave spectrum contains most of its energy in order to smoothly resolve the behavior of the transfer function there. Violation of this may lead to meaningless results from the calculations of statistics. In an effort to ensure sufficient coverage of the transfer functions in the wave periods where the wave spectrum contained its energy, two different transfer function resolutions were used: one resolution for the lower sea state JONSWAP spectrum and a different resolution for the higher sea state Bretschneider spectrum. The frequency resolution of the transfer functions can be seen in Appendix A.

Dynamic Sinkage and Trim

Dynamic sinkage and trim considerations also introduced uncertainty within the results. For the monohull, the model test conducted by Cusanelli and Chesnakas¹⁰ was able to provide experimentally measured dynamic sinkage and trim values. However, the report shows how these values can change depending on how the hull is configured with regards to trim tabs, propeller struts, and bulbs, for instance. Therefore, although the overall hullform is set, the most accurate values to use in the simulation do depend on the details of how the hull is ultimately configured. For the trimaran design, the dynamic sinkage and trim estimates were arrived at by *extrapolating* a model test that used a similar trimaran hull form. One issue is how accurate the extrapolations are since the side hulls for the JHSS are approximately amidship while the side hulls for the model tested were approximately three-quarters of the way to stern. The second issue is what effect the static trim plays on the realization of dynamic sinkage and trim. The Carr and Dvorak model had zero static trim while the current design of the JHSS trimaran calls for a 0.7 meter static trim (stern down).

Relative Displacement and Velocity

There is a certain amount of uncertainty in the results that involve probabilities, such as deck wetness and bow slams, due to the exponential nature of the probability calculation. The exponential relationship in the probabilities cause these results to be extremely sensitive to the relative motions and velocities. This explains why there can be large changes in deck wetness and bow slams when comparing the different theory formulations.

Another component of uncertainty in the relative displacement and velocity predictions for VERES is the determination of the wave field near a portion of the hull. The actual wave field near the hull is difficult to compute and is influenced by both diffracted and radiated waves as well as other effects such as water run up and splashing. This is especially true for the trimaran. In VERES,

the wave field near the hull is simplified down to the determination of what the undisturbed wave field would be at each point.

Motion Sickness Incidence and Motion Induced Interruptions

By the very nature of its definition, MSI has inherent uncertainty. For it attempts to predict what percentage of a population would experience motion sickness for a given combination of acceleration amplitudes and frequencies. This is highly dependent on the physiology of the subjects being studied. As the sample size in the studies becomes larger, the topology of the MSI surface will be better defined. However, the study by McCauley *et al.*⁵, upon which the VERES results are based, used approximately 20 subjects for each amplitude and frequency combination.

Furthermore, as the McCauley *et al.*⁵ report notes, they were not able to cover the full amplitude frequency space of sinusoidal accelerations. This meant that the percentage of cases of motion sickness monotonically increased as the frequency of the motion was decreased over the range of their test conditions. However, in the limit of no motion, or zero frequency, the percentage of motion sickness must be zero. Therefore, there must be a local maximum somewhere outside the range of their test. To compensate for a lack of data in this region, they assumed a parabolic profile and performed a least-squares fit to the data. Only by having more data in this low acceleration frequency region would one be able to determine how accurate these predicted results are.

The calculated motion induced interruptions also contain uncertainty. In order to determine how the crew would be affected by the lateral and vertical accelerations, basic assumptions about the “average” crew member and typical deck surface must be made. These assumptions include an estimate of both the vertical distance between the deck surface and the center of gravity of the crew member along with how wide a stance the crew member takes when performing an average task. There must also be an estimation of the friction coefficient between the deck surface and the shoes of the crew member. These values will obviously depend on the type of task being performed and the location where the task is performed.

Survival Mission Assessment Simplifications

The survival portion of the mission assessment involves Sea State 8 and its corresponding large wave fields. The large waves presumably induce extreme ship motions, which severely test, if not exceed, the capabilities of such a linear frequency domain code. The solution would be to run a nonlinear time-domain code which is much more time consuming. Therefore, the survival portion of this study should be viewed as a rough approximation to how the vessel might respond in such a situation.

Transit Mission Assessment Monohull Results

The results of the JHSS monohull design for the “transit” mission assessment study are presented in four subsections. The first section deals with the accelerations at the pilothouse (PH) and the forward spot (FS). The next section examines both motion sickness incidence, MSI, and motion induced interruptions, MII, collectively denoted henceforth as *motion events*, at those same two locations on the vessel. The third section looks at the roll and pitch motions of the vessel and the final section explores issues of deck wetness and bow slams.

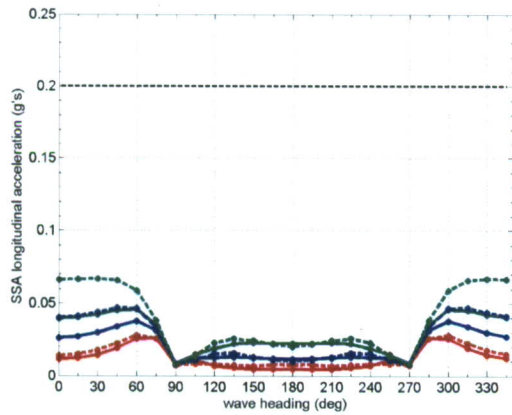
Accelerations

The three components of acceleration were examined at both the pilothouse and the forward spot. The results for the pilothouse can be seen in Figure 4 while Figure 5 shows the results at the forward spot. For both 20 and 30 knots, in all three sea states, and all headings, the longitudinal acceleration at the pilothouse is well below the threshold criteria of 0.2g's. The worst case, 36 knots in head seas in a Sea State 7, the longitudinal acceleration in the pilot house is only predicted to be 0.07g's. The same is true for the vertical acceleration; that is, all speeds, sea states, and headings are below the threshold criteria. For vertical accelerations, the maximum occurs when the waves are coming from approximately 60 degrees off the bow; for 36 knots in Sea State 7 the predicted magnitude is about 0.2g's. The transverse accelerations, however, can begin to limit mission capability. The threshold criteria are nearly met if the vessel goes at 36 knots in a Sea State 7 in beam seas. Even in a Sea State 6 in beam seas, the transverse accelerations are fairly high. The vessel is well below the threshold criteria in a Sea State 5 conditions, however.

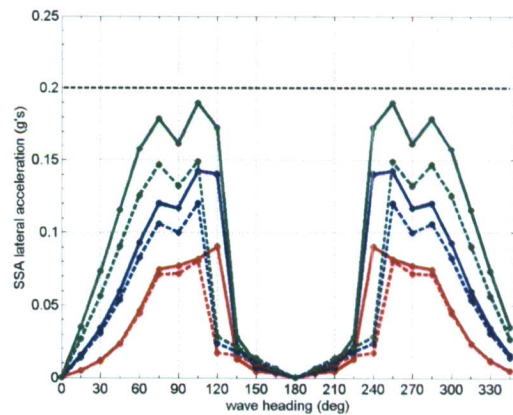
The accelerations at the forward spot have similar effects on the mission assessment. The longitudinal accelerations are again well below the threshold criteria for all speeds, sea states, and wave headings. The transverse accelerations are also below the threshold criteria although for Sea State 7 in beam seas, the accelerations are in the range of 0.13g's. The limiting accelerations at the forward spot are the vertical accelerations this time. Similar to the pilothouse, for the 36 knot speed in Sea State 7, the threshold criteria is reached. In lower sea states or at slower speeds, the accelerations decrease below the threshold criteria although they remain fairly high in beam seas for all cases, except for a Sea State 5.

Motion Events

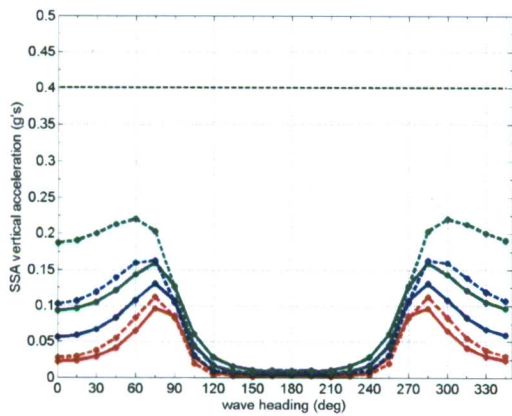
The motion events at the pilothouse are examined first and can be seen in Figure 6. If the vessel is able to maintain a general following seas wave heading, then MSI and MII are not a concern in the pilothouse. However, waves coming from any other direction could severely limit the mission capabilities. For instance around beam seas, every speed and sea state explored except a speed of 20 knots in Sea State 5 would put the vessel very close to, or cause the vessel to exceed, the MSI threshold of 20 percent crew sickness after four hours. Even at this one safe condition, the results still predict that almost 15 percent of the crew will experience sickness after four hours. The MII in beam seas for all speeds and sea states are also significant. The results predict multiple MII events which greatly exceed the threshold criteria of one event per minute. MII events diminish as the wave heading approaches head seas, headings less than 30 degrees away from zero, and in fact all speeds and sea states are apparently within the MII threshold criteria. However, MSI is still an important consideration in head sea conditions. Even though all speeds and sea states, except the 36 knots, Sea State 7 case, are under the threshold criteria for MSI in head seas, a significant amount of MSI still occurs.



(a) longitudinal



(b) transverse



(c) vertical

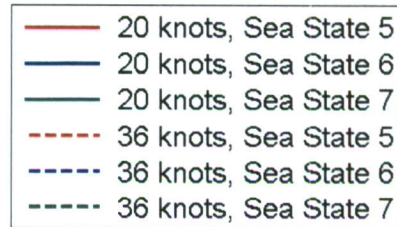


Fig. 4. Acceleration components oriented in the ship reference frame at the pilothouse for the JHSS monohull during a simulated ocean transit.

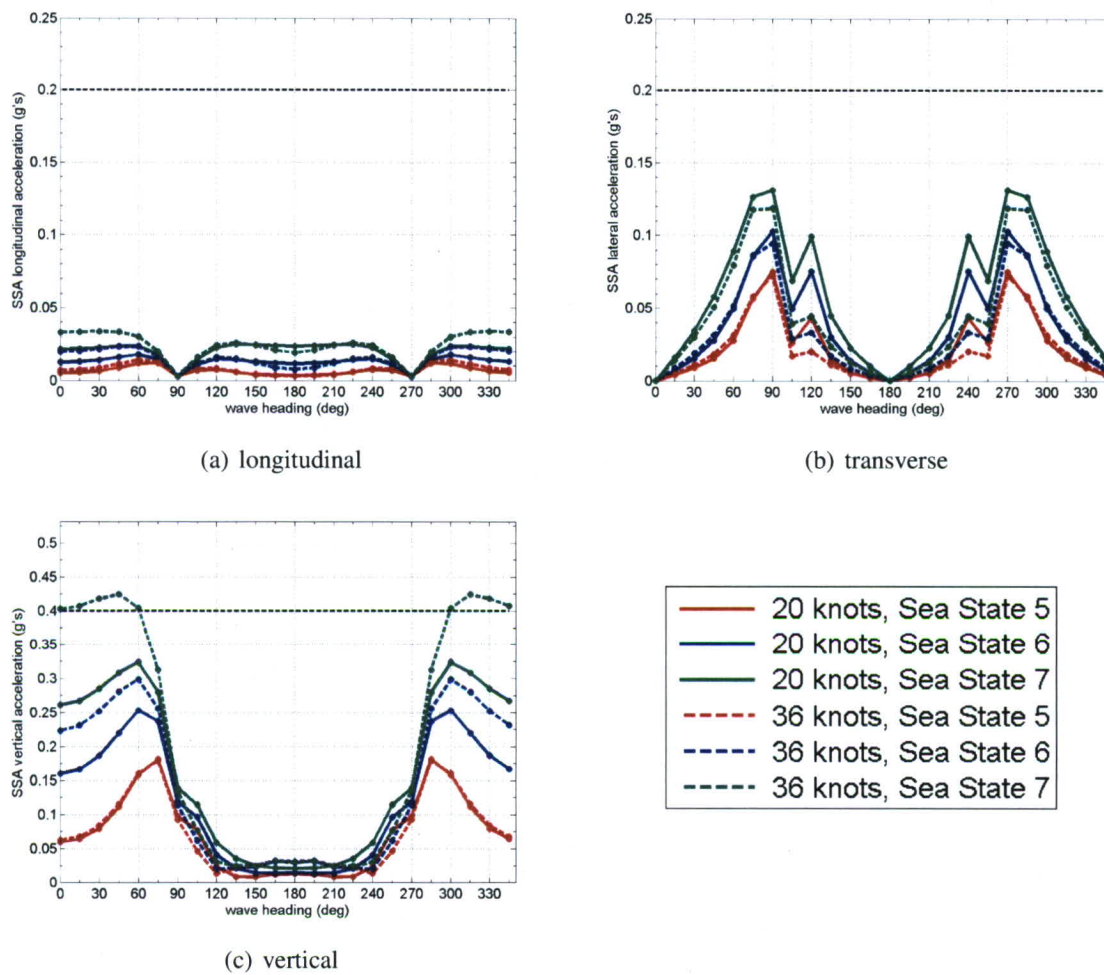
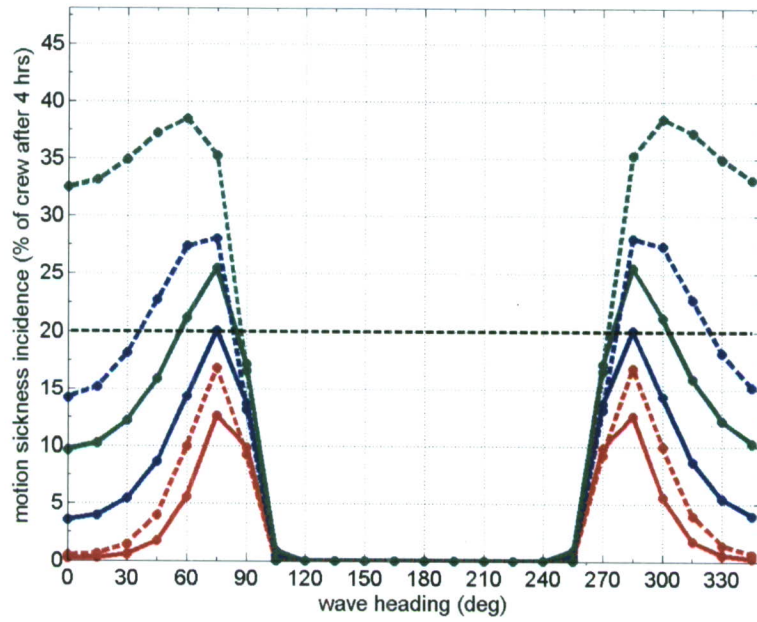
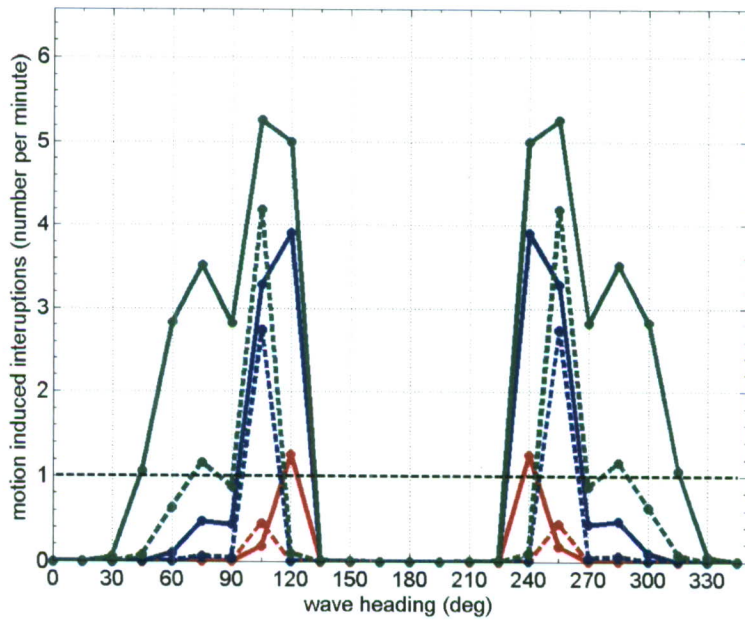


Fig. 5. Acceleration components oriented in the ship reference frame at the forward spot for the JHSS monohull during a simulated ocean transit.



(a) motion sickness incidence



(b) motion induced interruption



Fig. 6. MSI and MII results at the pilothouse for the JHSS monohull during a simulated ocean transit.

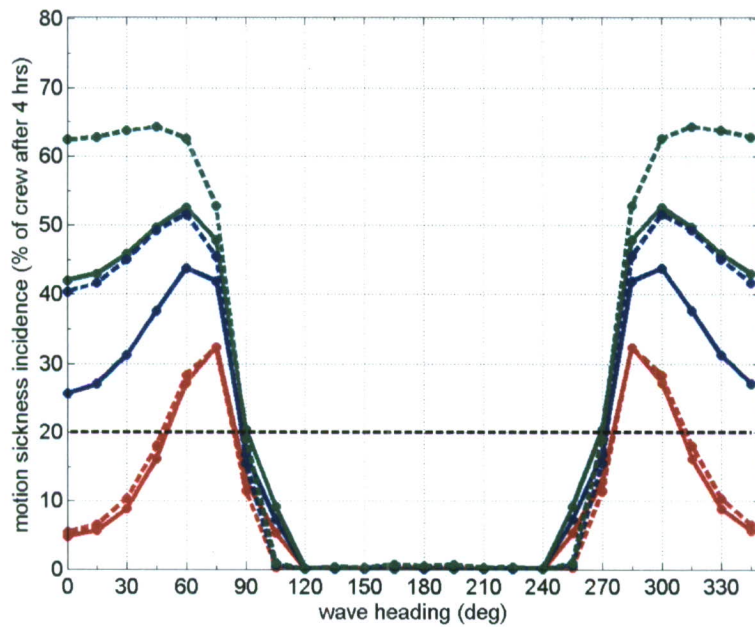
The motion interruption trends at the forward spot are similar to what was observed for the pilothouse; however, the MSI results are even more severe. This can be seen in the results shown in Figure 7. Like for the pilothouse, if the vessel is able to maintain a following seas orientation, then there does not appear to be any MSI or MII concerns. Both are nearly zero. However, in general beam seas, every speed and sea state caused the MSI criteria to be exceeded, and most also caused the MII criteria to be exceeded as well. Also like the pilothouse, as the vessel orients itself to head seas, MII considerations are no longer a concern. However, unlike the pilothouse, the MSI considerations still exceed the mission threshold for both speeds in Sea States 6 and 7.

Roll and Pitch Motion Limits

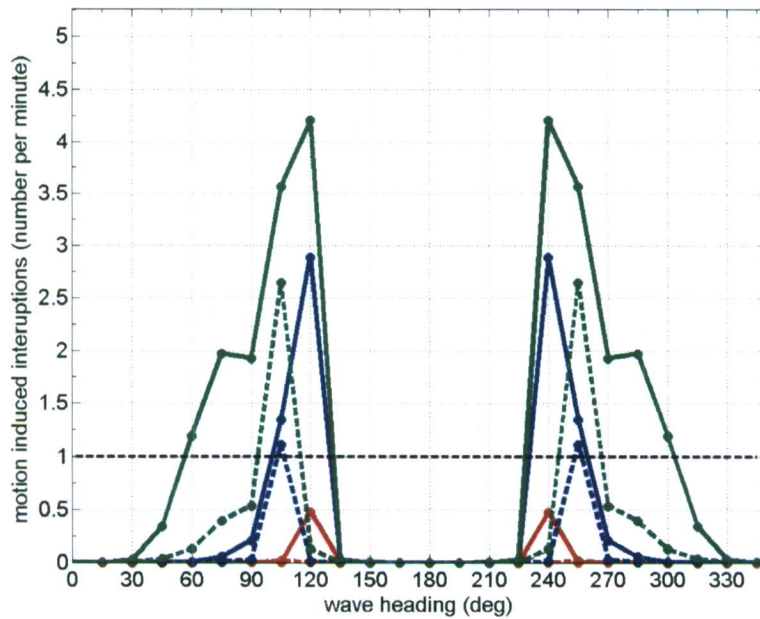
The predictions for roll and pitch can be seen in Figures 8(a) and 8(b), respectively. If the monohull is not in general beam sea conditions, then roll does not affect the mission capability except for the most severe case explored here, a speed of 36 knots in Sea State 7. For that case, the wave heading has to be less than 60 degrees to be under the threshold criteria. If the monohull is experiencing beam seas, then all the speeds and sea states explored here cause the roll criteria limit to be either reached or exceeded. In fact, for high speed or high sea states, the roll can be as large as 20 degrees. On the other hand, for the monohull, for every speed, sea state, and heading investigated, the pitch of the vessel remained under the threshold criteria. The worst case was pure head seas, wave heading of 0 degrees, at a speed of 36 knots in Sea State 7. In that situation, the pitch was predicted to be around 2 degrees.

Deck Wetness and Bow Slams

Mission assessment deck wetness was investigated at the bow of the ship. The results are shown in Figure 9(a) as the predicted number of submergences per hour. For all ship speeds, sea states, and headings examined, the number of deck submergences at the bow is well below the threshold criteria of 30 submergences per hour. The most submergences per hour, two or three, occur at 36 knots in Sea State 7 in approximate head seas, 330 to 30 degrees. Bow slam occurrences affect mission capability the same as deck wetness. Again, for all speeds, sea states, and headings, the number of hull slams per hour was well below the limiting criteria of 20 slams per hour. The maximum number of slams per hour occurred in the same operating speed, sea state, and wave heading as deck wetness and totaled approximately five.



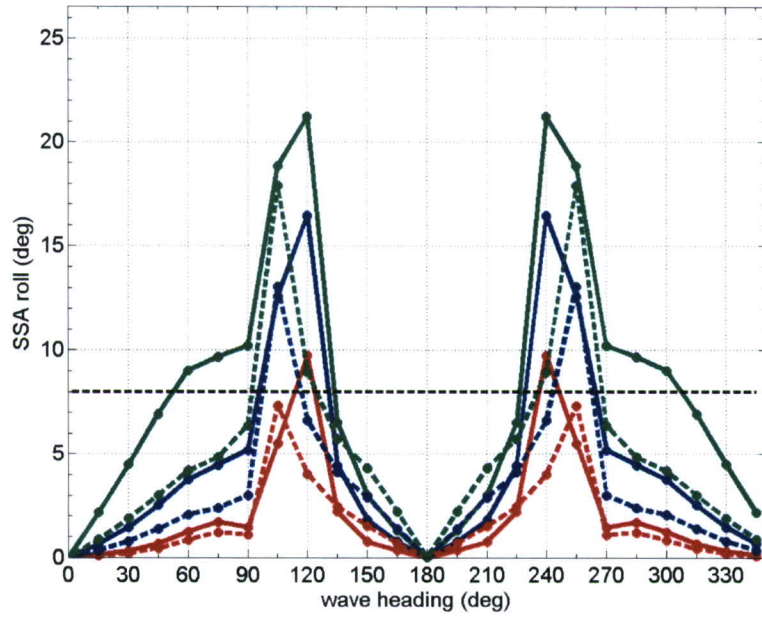
(a) motion sickness incidence



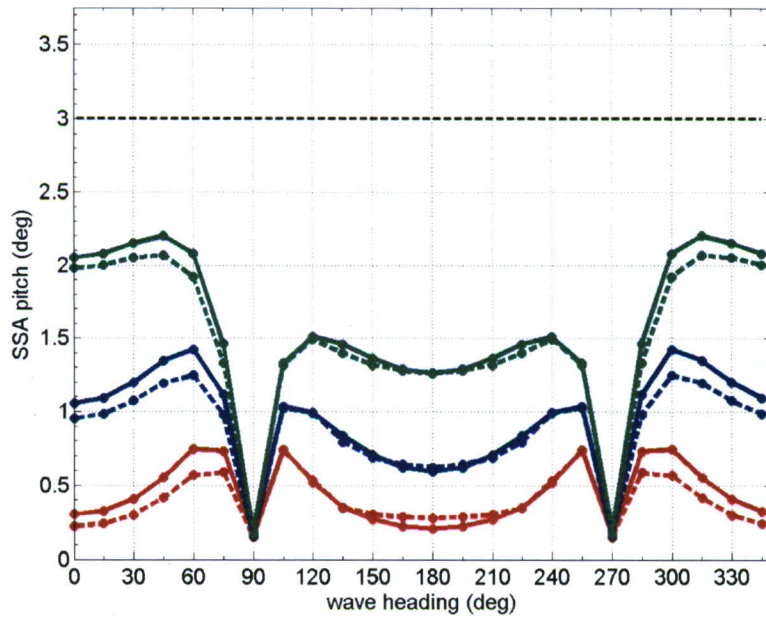
(b) motion induced interruption



Fig. 7. MSI and MII results at the forward spot for the JHSS monohull during a simulated ocean transit.



(a) vessel roll



(b) vessel pitch

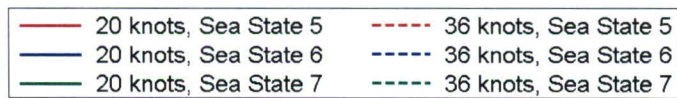
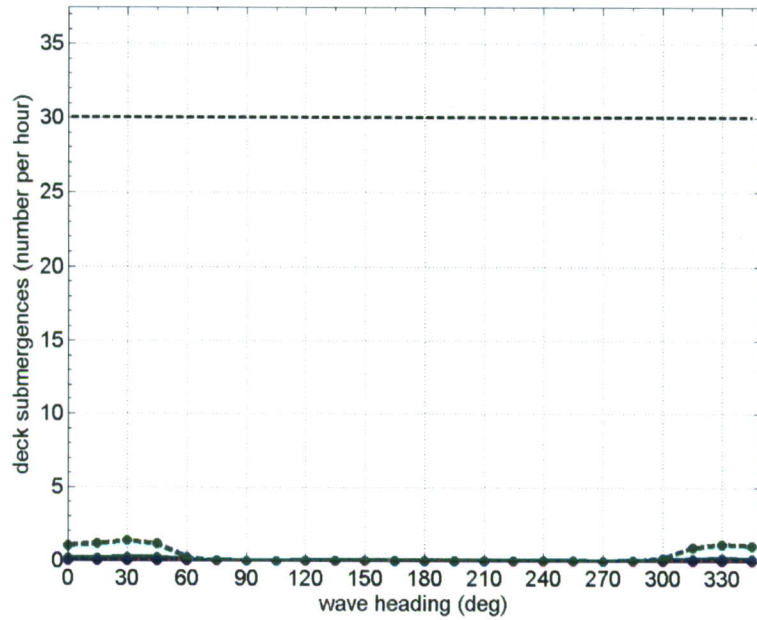
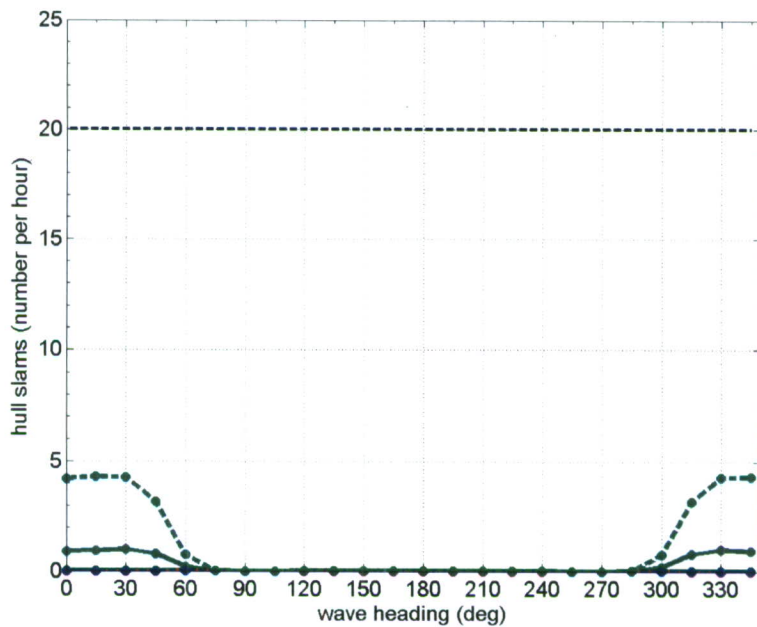


Fig. 8. Vessel roll and pitch results for the JHSS monohull during a simulated ocean transit.



(a) deck wetness



(b) bow slams

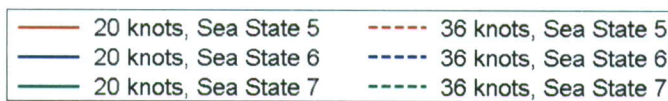


Fig. 9. Water on the deck and bow slam results for the JHSS monohull during a simulated ocean transit.

Transit Mission Assessment Trimaran Results

The results of the JHSS trimaran hull design for the “transit” mission assessment study are similarly presented in four subsections. The first section deals with the accelerations at the pilothouse (PH) and the forward spot (FS). The next section examines motion events, MSI and MII, at those same two locations on the vessel. The third section looks at the roll and pitch motions of the vessel and the final section explores issues of deck wetness and bow slams. Many of the results and trends from the monohull are also observed with the trimaran. These similarities and differences will be highlighted.

Accelerations

The longitudinal, transverse, and vertical components of the acceleration were examined at both the pilothouse and the forward spot. The results for the pilothouse can be seen in Figure 10 while Figure 11 shows the results at the forward spot.

When looking at the accelerations in the pilothouse with the vessel in a general following seas condition, all three components of the acceleration are close to 0g's. The longitudinal and vertical accelerations, have distinct values in wave headings up to 90 degrees, on either side, away from zero degrees, but they are still well below the criteria. The limits to mission capability at the pilothouse occur due to the transverse accelerations. For a vessel orientation to the waves of general beam seas, every speed and sea state surpassed the mission criteria threshold. For the lower sea state, Sea State 5, once the vessel is removed from a pure beam seas wave heading (90 degrees), the transverse acceleration drops below the threshold. However, for larger sea states, the vessel heading must be closer to a general head or following sea heading in order for the transverse acceleration to decrease below the threshold criteria. And for Sea State 7, the vessel must be at least 45 degrees away from pure beam seas to drop below the threshold criteria.

The accelerations at the forward spot have almost identical trends on the mission assessment capability those at the pilothouse. First, the vessel accelerations are again well below the threshold criteria in a general following seas orientation. Also identical to the pilothouse location, the longitudinal component of the acceleration does not limit the mission over any speed, sea state, or wave heading, and its maximum value is only approximately half the limiting mission assessment value. Again, the major limiting factor on the mission capability is the transverse accelerations. For all speeds, sea states, and headings, if the vessel is in a pure beam seas then the threshold criteria will be surpassed. In some cases, for instance in Sea State 7, the transverse acceleration is more than three times larger than the threshold value. The major difference between the acceleration in the pilothouse compared to the forward spot is in the vertical component. Whereas for the pilothouse, this component never seriously approached the threshold criteria, at the forward spot for the high speed and largest sea state, the vertical acceleration comes very close to reaching the threshold criteria value.

Motion Events

In this section, motion events refers to both motion sickness incidence and motion induced interruptions. Due to the fact that MSI and MII are dependent on the accelerations that occur at a certain location on a vessel, the results here refer to the number of MII that would occur in the

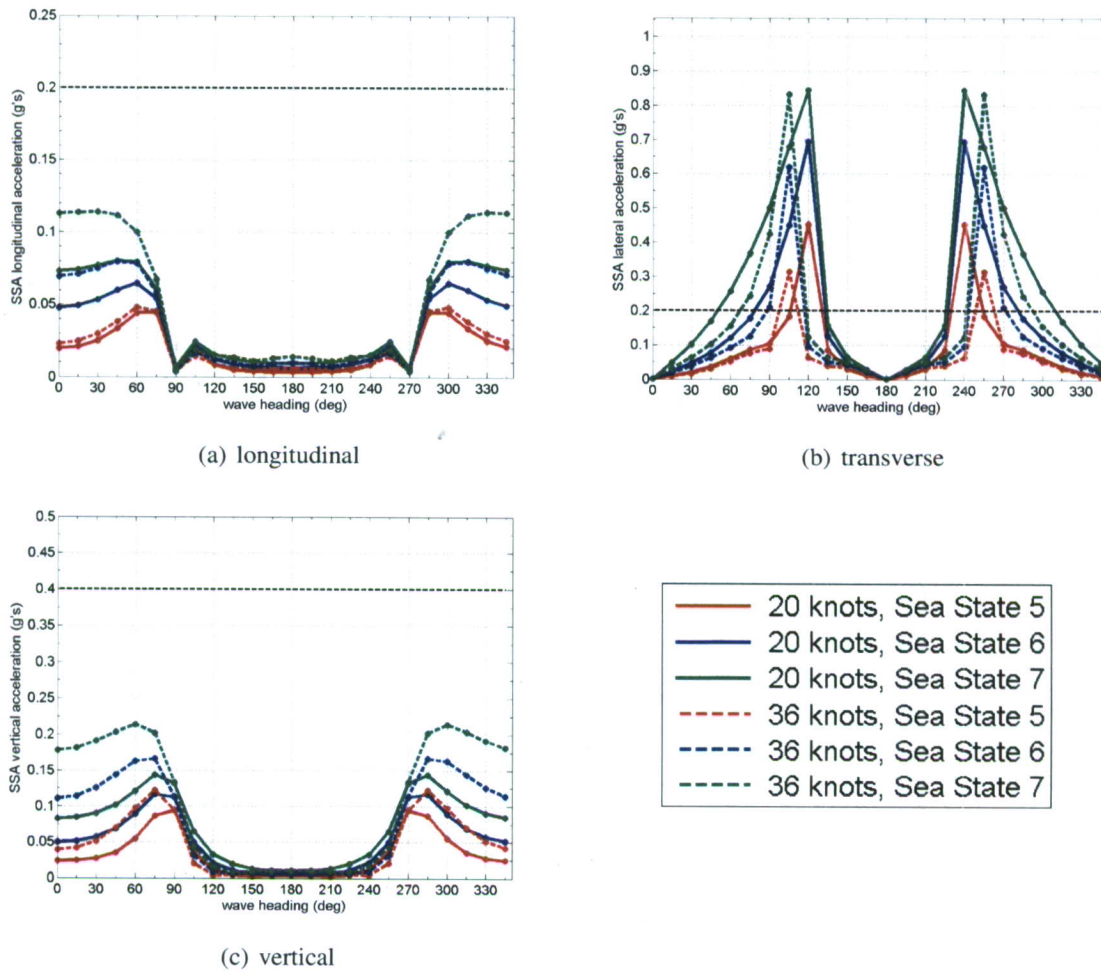
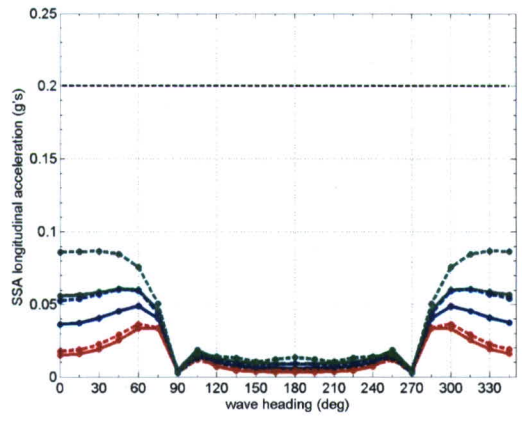
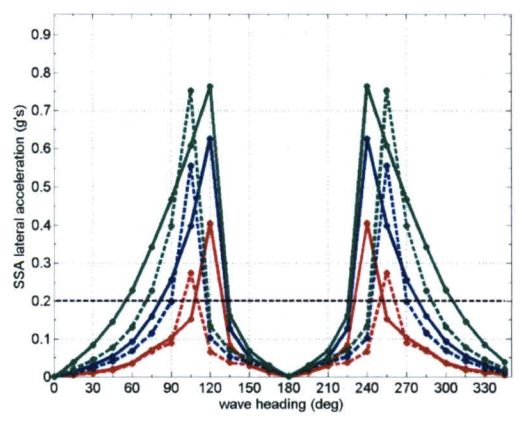


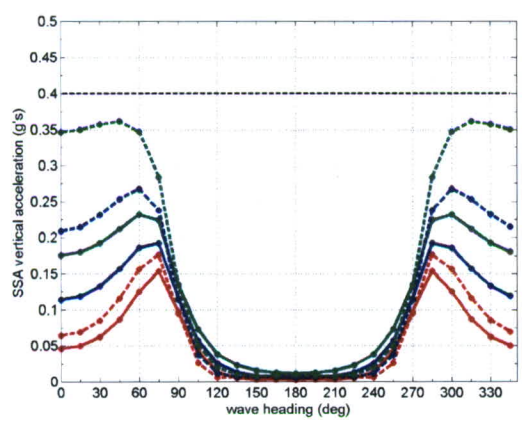
Fig. 10. Acceleration components oriented in the ship reference frame at the pilot-house for the JHSS trimaran during a simulated ocean transit.



(a) longitudinal



(b) transverse



(c) vertical

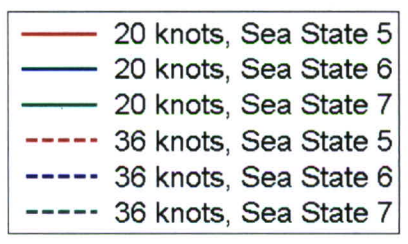


Fig. 11. Acceleration components oriented in the ship reference frame at the forward spot for the JHSS trimaran during a simulated ocean transit.

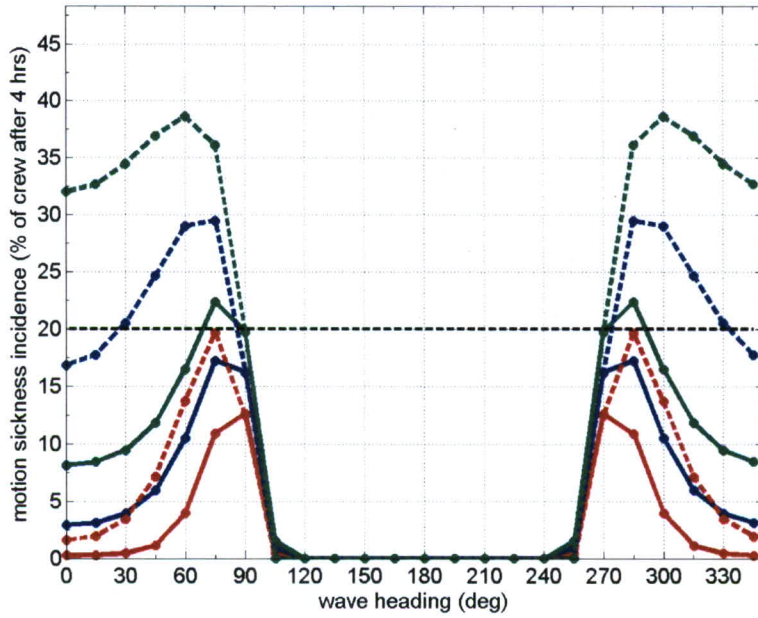
very near vicinity to that point of the ship or the percent of the crew that would experience MSI at the specific location.

The results for MSI at the pilothouse can be seen in Figure 12(a) while the results for MII are shown in Figure 12(b). For both of these parameters, if the trimaran is able to maintain a general following seas orientation, then neither of the mission capabilities are impacted because, in this set of wave headings, the predicted percentage of MSI or number of MII is effectively zero. In a general beam seas orientation however, MSI and MII will limit the mission capability severely. For all speeds and sea states in this general vessel orientation, the threshold value of one motion induced interruption per minute is exceeded and, in most cases, there are several interruptions per minute. Also, for all speeds and sea states except the least severe case, 20 knots in Sea State 5, the percent of local crew experiencing MSI also exceeds the threshold limit. Even the least severe case, it is predicted that approximately fifteen per cent of the crew will experience MSI. Finally, when the vessel is in a general head seas orientation, MII considerations no longer limit mission capability since the number of interruptions is effectively zero. However, the percentage of MSI can still be a limiting parameter. For the higher speed runs, 36 knots, in Sea States 6 and 7, the threshold criteria is exceeded.

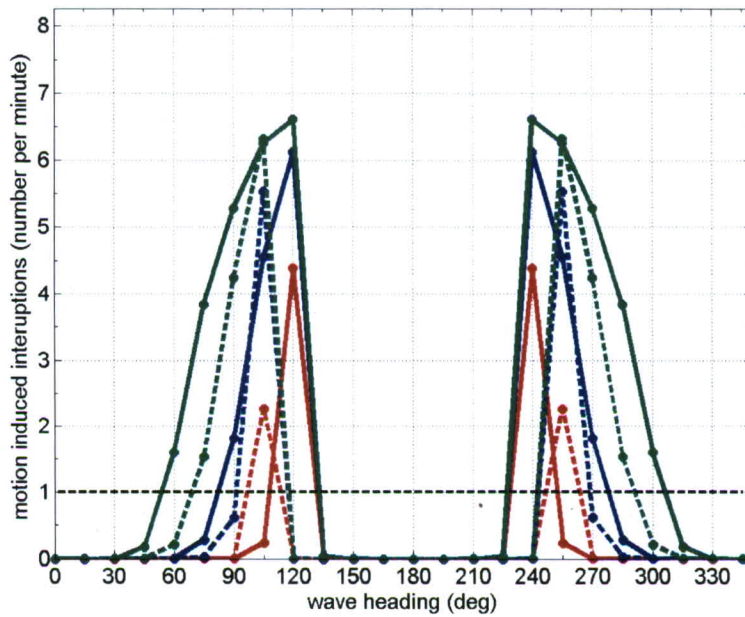
The monohull MII results at the forward spot are similar to what was observed for the pilothouse. Also, similar to the monohull results, the MSI results are even more severe at this vessel location. The trimaran MSI and MII results at the forward spot are shown in Figures 13(a) and 13(b). Similar to the pilothouse location, if the vessel is able to maintain an approximate following seas orientation, then there does not appear to be any MSI or MII concerns; both are nearly zero at the forward spot. However, in approximate beam seas, every speed and sea state caused both the MSI and MII criteria are exceeded. The number of motion induced interruptions can be as much as six times above the threshold criteria for the most extreme case. As was shown for the monohull at both locations as well as the trimaran at the pilothouse, as the vessel orients itself to head seas, MII considerations are no longer a concern. However, unlike the trimaran pilothouse, the MSI considerations now exceed the mission threshold for all cases except the lowest sea state cases.

Roll and Pitch Motion Limits

The predictions for roll can be seen in Figure 14(a) and for pitch in Figure 14(b). For the trimaran, in wave headings of less than 75 degrees or greater than 135 degrees, then roll does not affect the mission capability. For the most severe cases explored here, however, roll motion can approach the limiting criteria as the heading tends toward beam seas. If the trimaran is in a beam sea condition, then all the speeds and sea states explored cause the roll motion to exceed the roll criteria limit. In fact for high speed or high sea states, the roll angle can be as large as 35 degrees. In regards to pitch, as was discovered for the monohull, the pitch criteria is not exceeded by the trimaran for any speed, sea state, or heading investigated. The worst case was an approximate head seas orientation, wave headings of 330 to 30 degrees, at a speed of 36 knots in Sea State 7. In such a situation, the pitch was predicted to be around 2.5 degrees.



(a) motion sickness incidence



(b) motion induced interruption

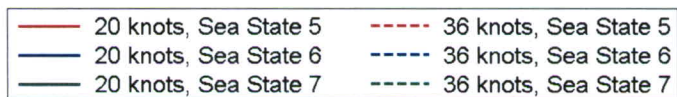
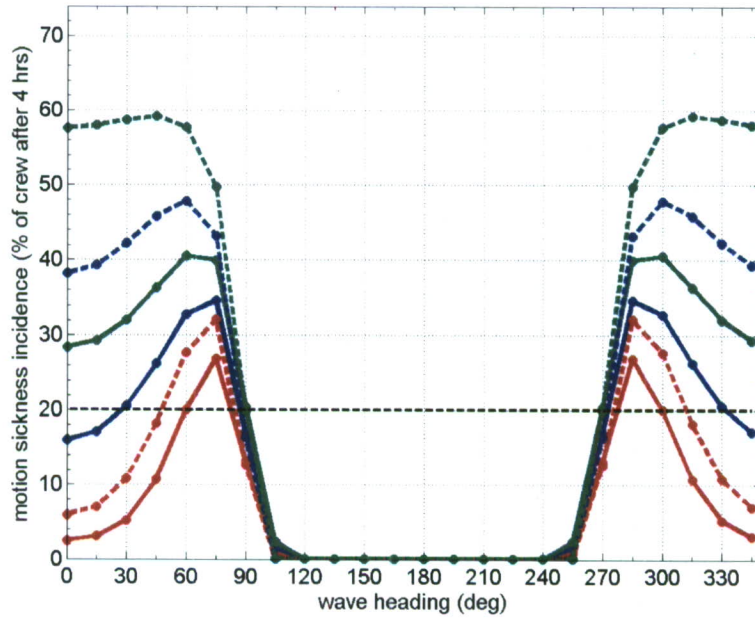
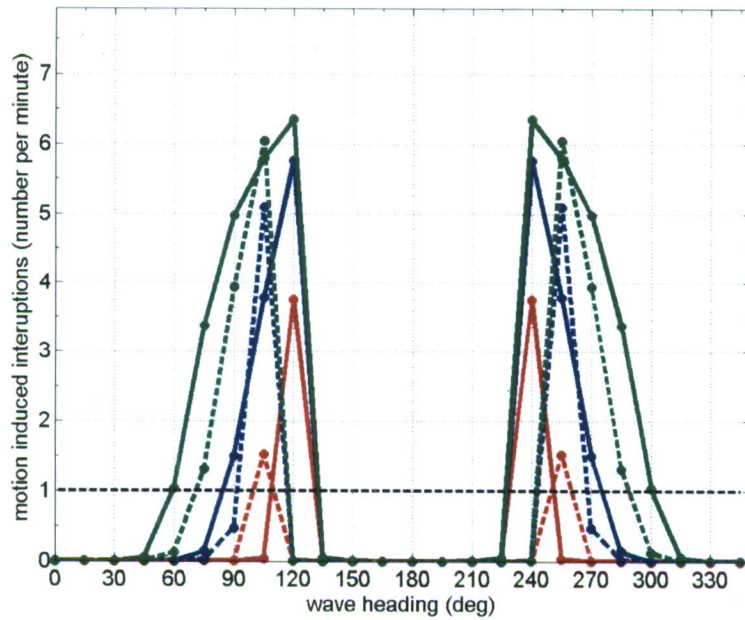


Fig. 12. MSI and MII results at the pilothouse for the JHSS trimaran during a simulated ocean transit.



(a) motion sickness incidence



(b) motion induced interruption

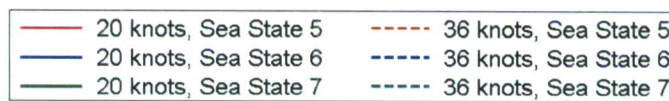
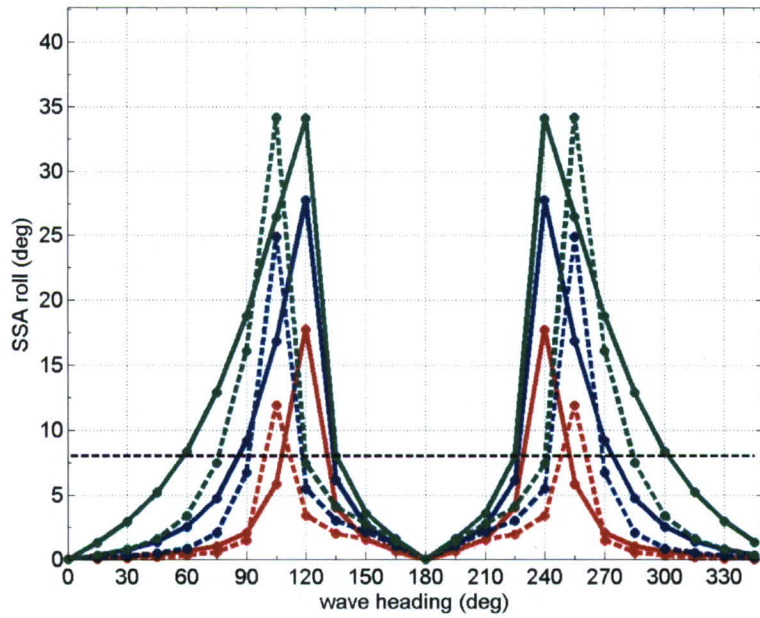
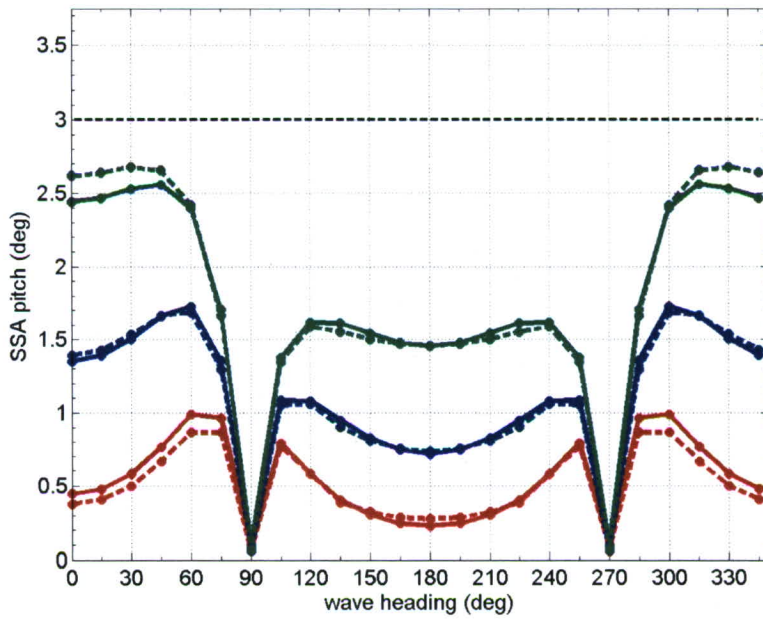


Fig. 13. MSI and MII results at the forward spot for the JHSS trimaran during a simulated ocean transit.



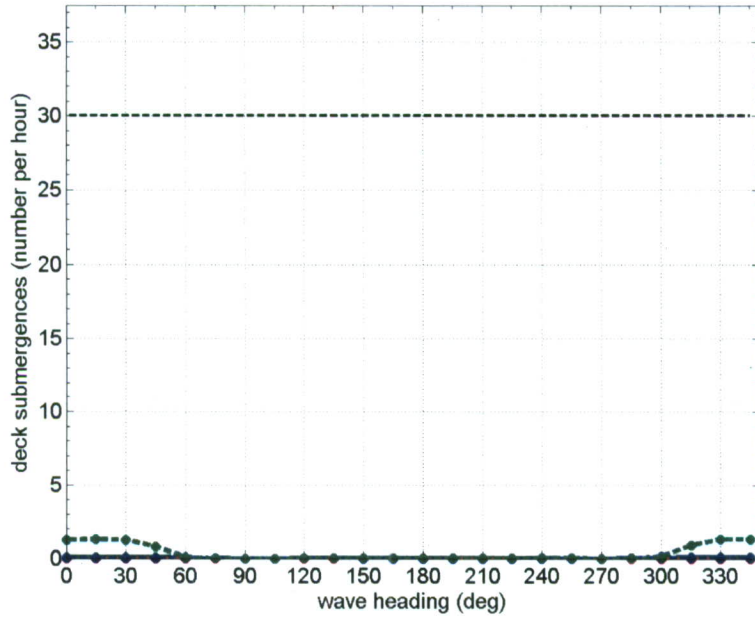
(a) vessel roll



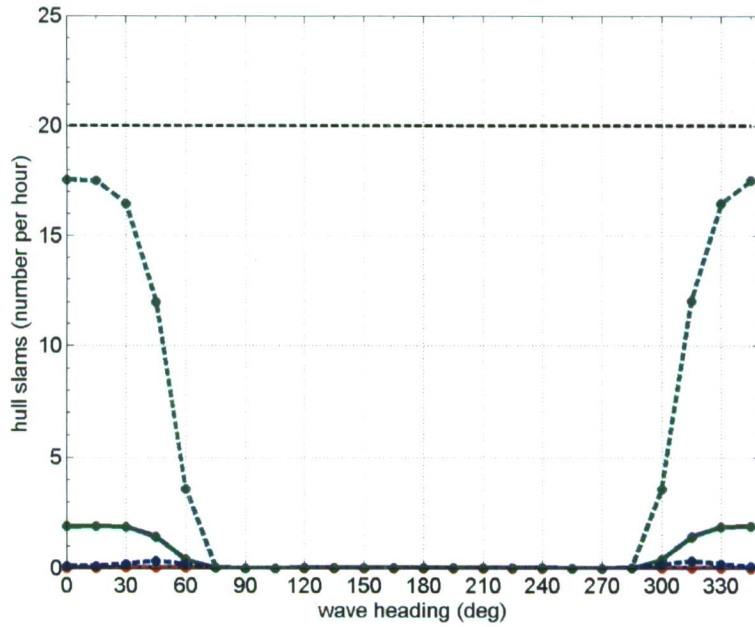
(b) vessel pitch



Fig. 14. Vessel roll and pitch results for the JHSS trimaran during a simulated ocean transit.



(a) deck wetness



(b) bow slams

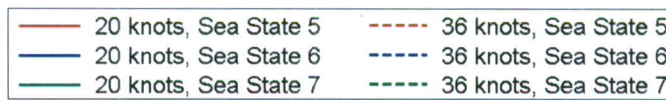


Fig. 15. Water on the deck and bow slam results for the JHSS trimaran during a simulated ocean transit.

Deck Wetness and Bow Slams

Mission assessment deck wetness was investigated at the bow of the ship. The results are shown in Figure 15(a) as the predicted number of submergences per hour. Of all the parameters investigated for the mission assessment capability, deck wetness had the least influence since for all conditions examined, the number of deck submergences at the bow is effectively zero. The bow slam effects on mission capability were also minimal and are shown in Figure 15(b). The only condition that might begin to affect mission performance was pure head seas at 36 knots in Sea State 7. For this situation, the number of slams per hour was approximately seventeen which is approaching the limiting criteria of twenty. For all other cases examined however, the number of hull slams per hour was well below the limiting criteria and in many cases was effectively zero.

Transfer Mission Assessment

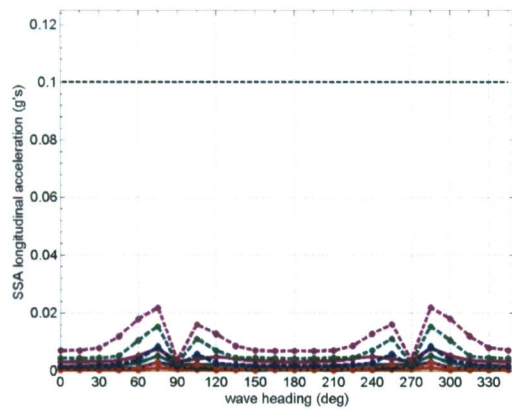
The results of both the JHSS monohull and trimaran designs for the “transfer” portion of the mission assessment study are presented here in three subsections. For the transfer mission, the motion criteria are limited by helicopter operation considerations which results in more stringent criteria as shown in Table 4. The first section deals with the accelerations at the three different helicopter spots, H1, H2, and H3. The next section examines motion events, or MSI and MII, at those same location on the vessel. The third section looks at the roll and pitch motions of the vessel. The sea states used for the mission assessment for the transfer of equipment was limited to a maximum of Sea State 5.

Accelerations

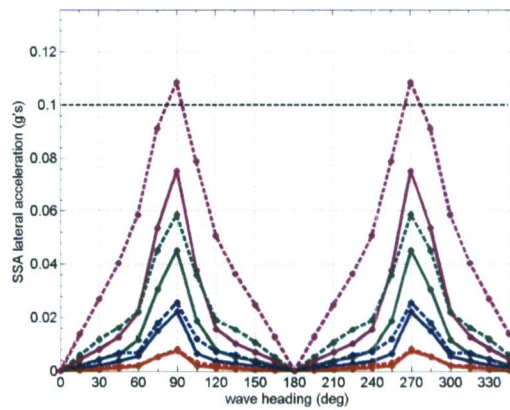
The behavior of the accelerations at each of the three helicopter spots is very similar for both the monohull and trimaran designs. First, both the longitudinal and vertical components of acceleration are well below the threshold criteria for both ships in all headings and sea states. Second, the transverse component of the acceleration in beam seas and Sea State 5 could cause the threshold criteria value to be exceeded. For the trimaran, the simulation predicts that the acceleration criteria will be exceeded and for the monohull, while below the limit, the accelerations are close to them. As long as general beam seas are avoided in Sea State 5, then the transverse accelerations are also not a concern for either vessel. These similarities found at all three helicopter spots can be seen in Figure 16 for helicopter spot 1, in Figure 17 for helicopter spot 2, and in Figure 18 for helicopter spot 3. The biggest difference between the three helicopter spots regarding accelerations is seen in the vertical component. Going from the third helicopter spot, near the center of the vessels, toward the first helicopter spot, near the bow of the vessels, the vertical component increases. This increase can be seen by noting the vertical component in Figure 18(c) of approximately 0.1g's at helicopter spot 3 while at helicopter spot 1 the value is approximately 0.15g's as seen in Figure 16(c).

Motion Events

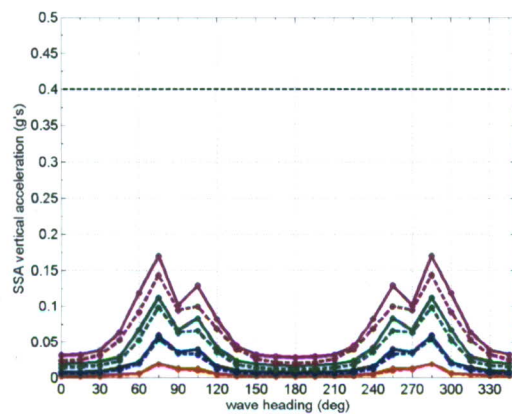
MSI considerations are shown in Figures 19(a), 20(a), and 21(a) for helicopter spots 1, 2, and 3, respectively. Both hull types are well below the threshold criteria for all sea states except in the general beam sea heading. However, if beam seas are encountered, then the mission could be



(a) longitudinal



(b) transverse



(c) vertical

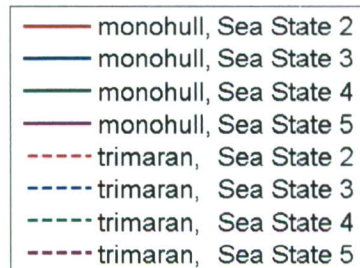
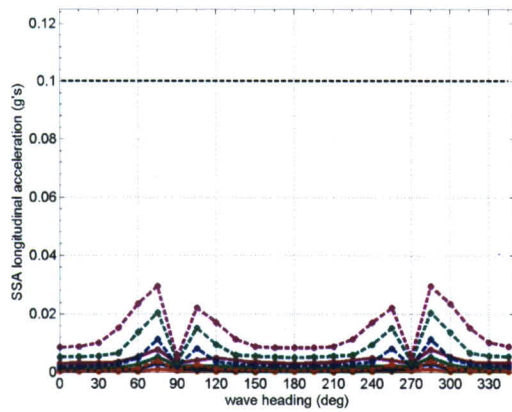
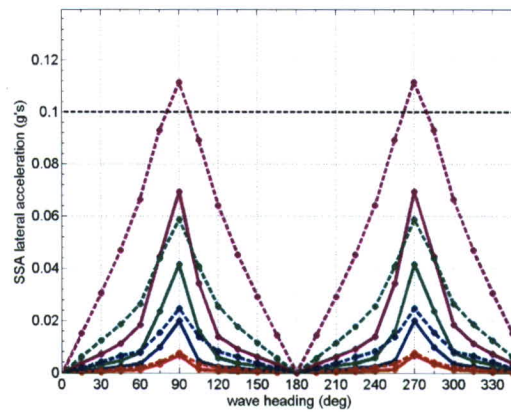


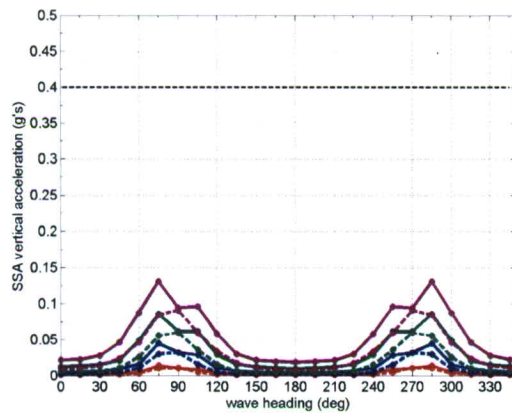
Fig. 16. Acceleration components oriented in the ship reference frame at helicopter spot 1 for both the JHSS monohull and trimaran during a simulated cargo transfer.



(a) longitudinal



(b) transverse



(c) vertical

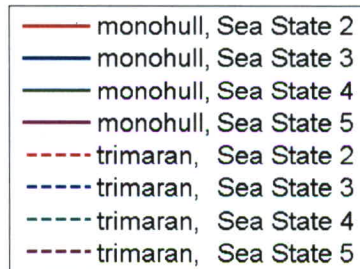
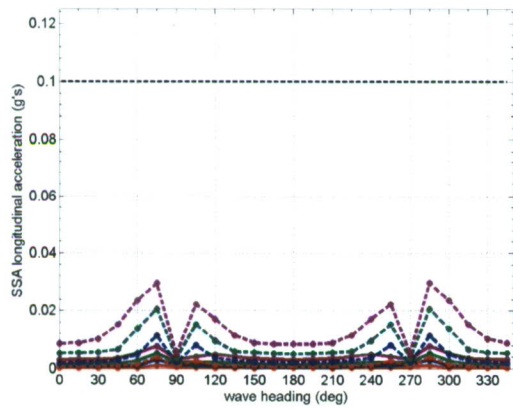
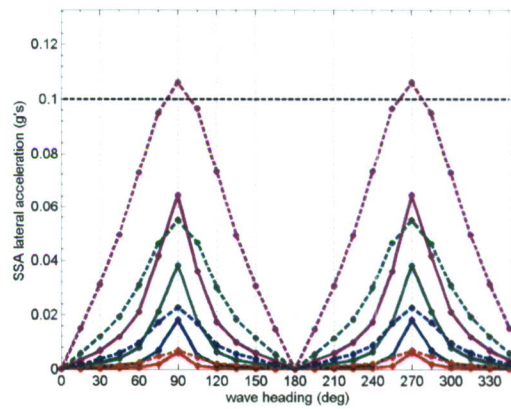


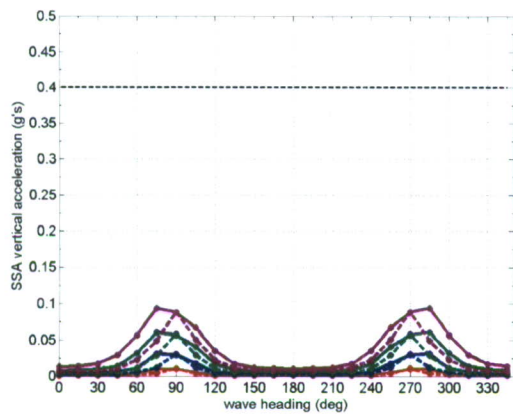
Fig. 17. Acceleration components oriented in the ship reference frame at helicopter spot 2 for both the JHSS monohull and trimaran during a simulated cargo transfer.



(a) longitudinal



(b) transverse



(c) vertical

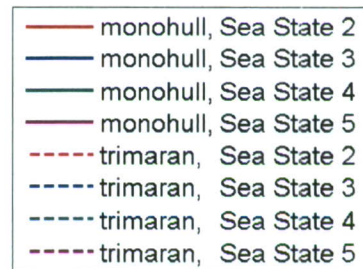


Fig. 18. Acceleration components oriented in the ship reference frame at helicopter spot 3 for both the JHSS monohull and trimaran during a simulated cargo transfer.

compromised. Both the monohull and the trimaran exceed the threshold MSI criteria in Sea State 5 at the forward helicopter spot, but are not exceeded for the lower sea states. Also, the helicopter locations towards the center of the vessel show a decrease in the percentage of MSI for a given sea state. At the second helicopter spot, the MSI criteria is not exceeded for the trimaran and right at the limit for the monohull while at the third helicopter spot, all sea states and headings for both vessel are well below the MSI threshold criteria.

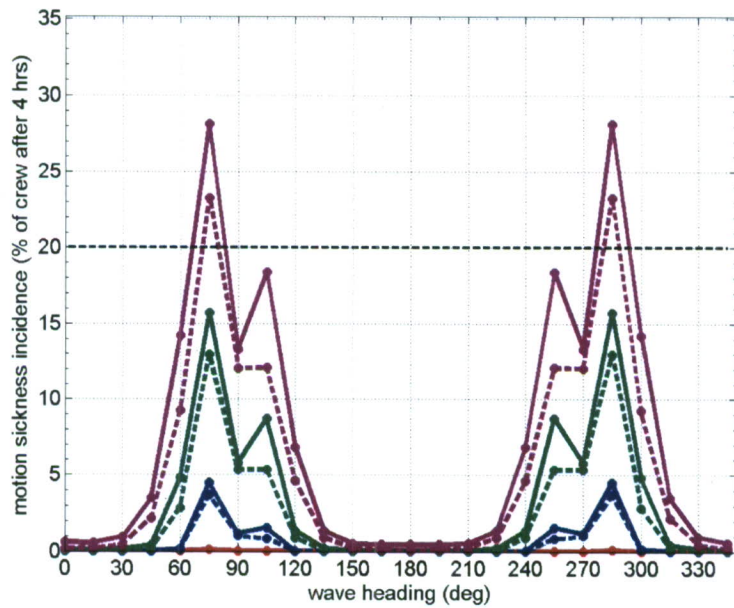
For MII incidents, which are shown in Figures 19(b), 20(b), and 21(b) for helicopter spots 1, 2, and 3, respectively, both vessels can successfully complete the transfer mission for all headings and sea states. In fact, the simulation predicts that there will be practically zero events at all three helicopter locations.

Roll and Pitch Motion Limits

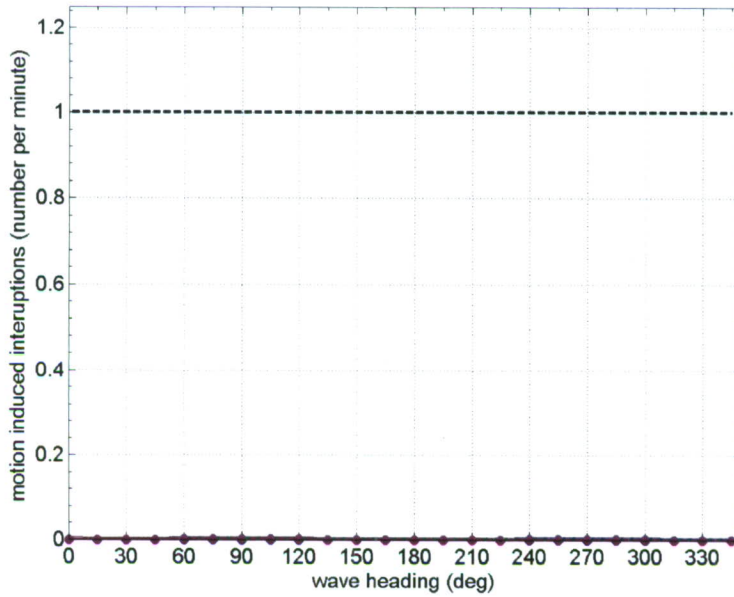
The predictions for both hull designs can be seen in Figure 22(a) for roll and in Figure 22(b) for pitch. As has been the case throughout this mission assessment study, vessel pitch is less of a concern than vessel roll for the transfer portion of the mission assessment as well. For both hull designs, the ship pitch is much lower than the threshold criteria and is the largest for bow quartering waves with a value of approximately 1 degree. The ship roll, on the other hand, is a concern for mission capability. For Sea State 4 or lower, roll motion is predicted to be significantly below the threshold criteria. However, in Sea State 5, roll could potentially be a concern for both hull designs. The predicted roll angles for both hulls are below the threshold criteria, but they come close in beam seas; within 1 degree for the monohull and 1.5 degrees for the trimaran. This is significant because it is the only parameter that limits the mission capability of either hull in the transfer mission portion.

An unexpected feature that appears in the predicted roll motions for the monohull is a decrease in roll that occurs around a wave heading of 90 degrees. This decrease in roll is not seen in the trimaran results; the maximum roll occurs at pure beam seas. Unlike the trimaran though, for the monohull geometry, rudders and a trim tab were modeled and treated as lifting surfaces and the bilge keels were modeled using a roll damping module within VERES. In order to verify that one of these appendage models was not contaminating the simulation predictions, roll results were re-simulated on JHSS monohull geometries that contained only one appendage at a time, along with a geometry that contained no appendages. The results of this appendage study can be seen in Figure 23.

For Sea States 2 through 4, the presence or lack of a given appendage does not change the resultant predicted roll motion. In Sea State 5, however, the effects of the given appendages becomes apparent. For a given wave heading, the cases that do not contain a bilge keel model (green, purple, and orange lines) produce a slightly larger roll angle than the two cases that contain bilge keel models (red and blue lines). Furthermore, the case with all the appendages modeled (red line) is nearly identical to the case with only the bilge keels modeled (blue line). Therefore, it appears that the bilge keels are the only appendage that noticeably affect the roll angle. Although this is an interesting result in its own right, the study clearly shows that, in each of the sea states considered, all the various appendage models contained the unexpected decrease in roll motion around beam seas thus eliminating any appendage model as the cause.



(a) motion sickness incidence



(b) motion induced interruption

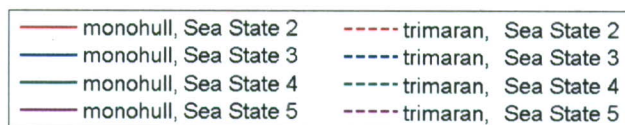
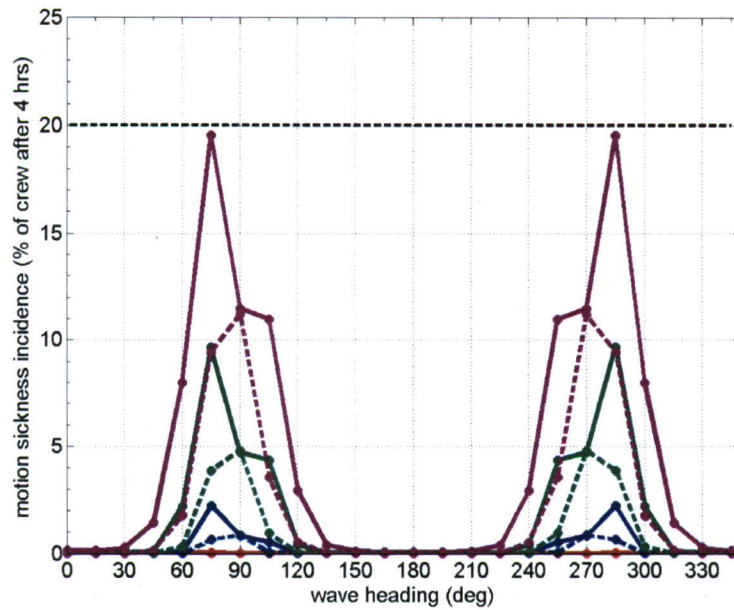
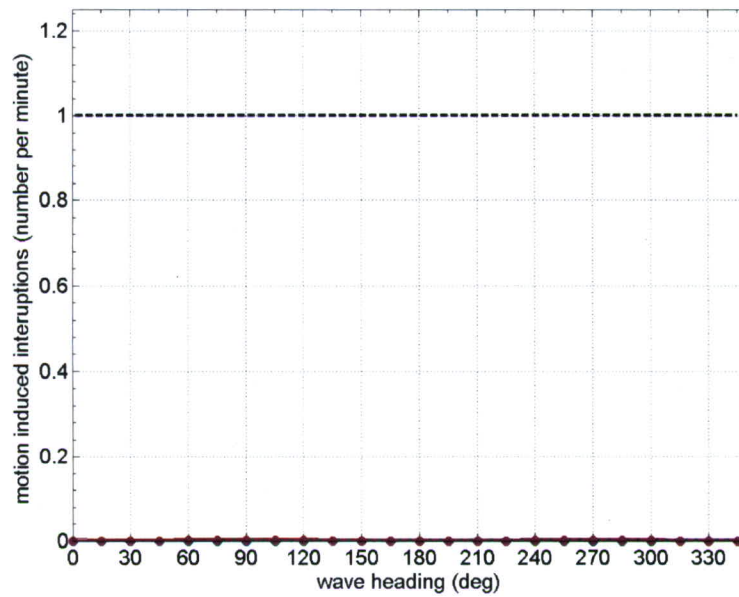


Fig. 19. MSI and MII results at helicopter spot 1 for both the JHSS monohull and trimaran during a simulated cargo transfer.



(a) motion sickness incidence



(b) motion induced interruption

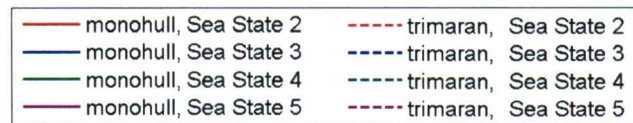
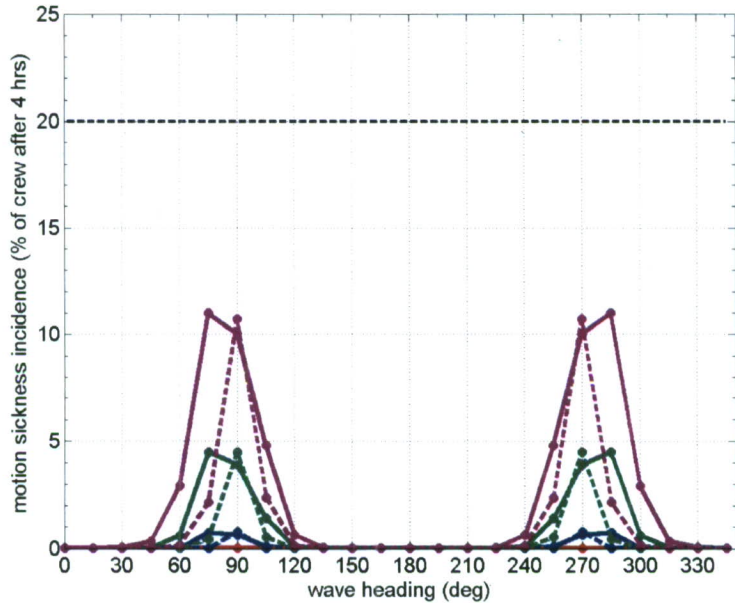
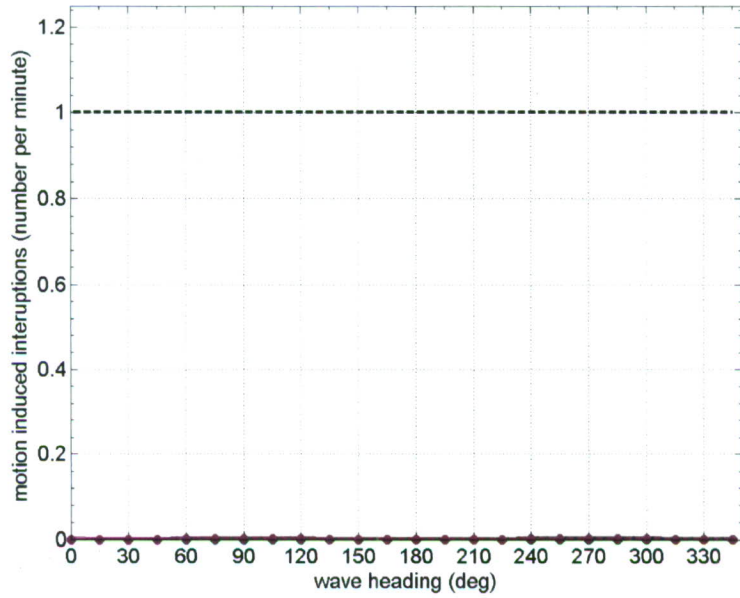


Fig. 20. MSI and MII results at helicopter spot 2 for both the JHSS monohull and trimaran during a simulated cargo transfer.



(a) motion sickness incidence



(b) motion induced interruption

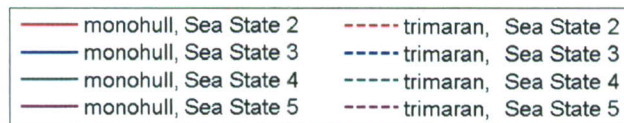
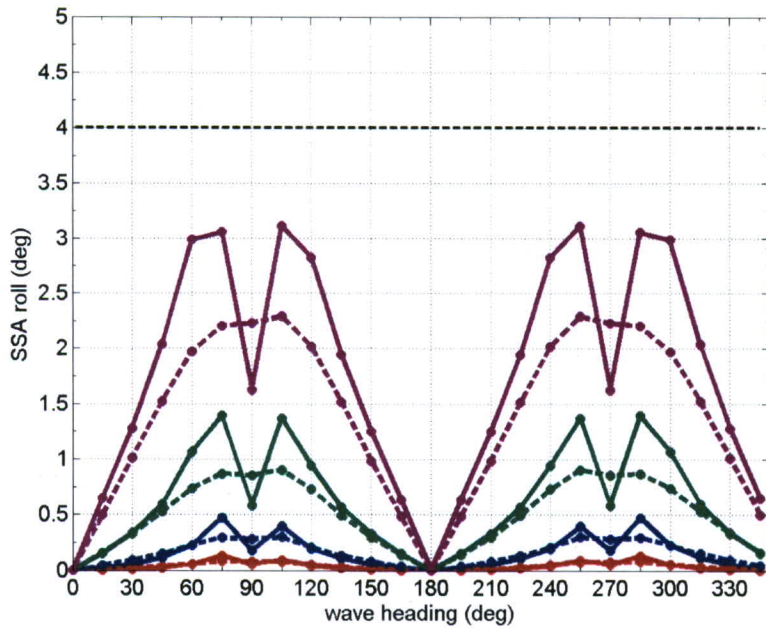
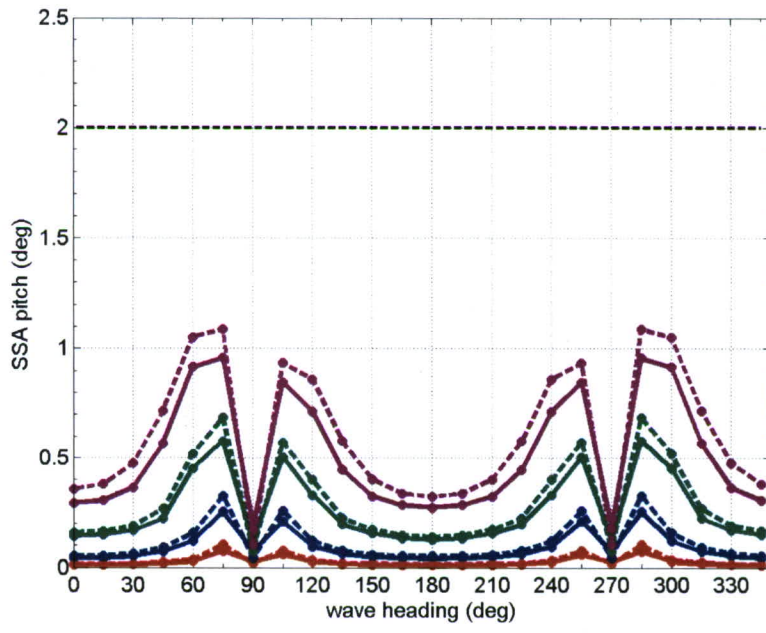


Fig. 21. MSI and MII results at helicopter spot 3 for both the JHSS monohull and trimaran during a simulated cargo transfer.



(a) vessel roll



(b) vessel pitch

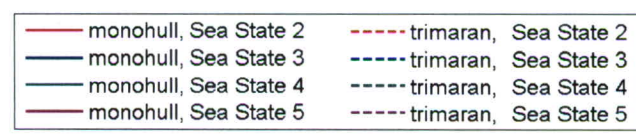


Fig. 22. Vessel roll and pitch results for both the JHSS monohull and trimaran during a simulated cargo transfer.

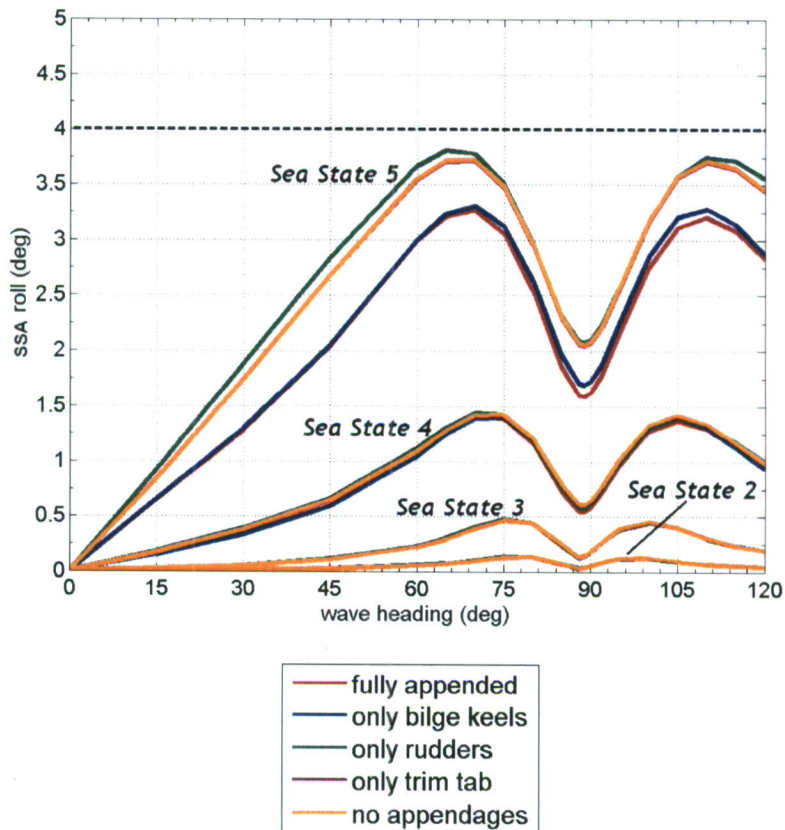
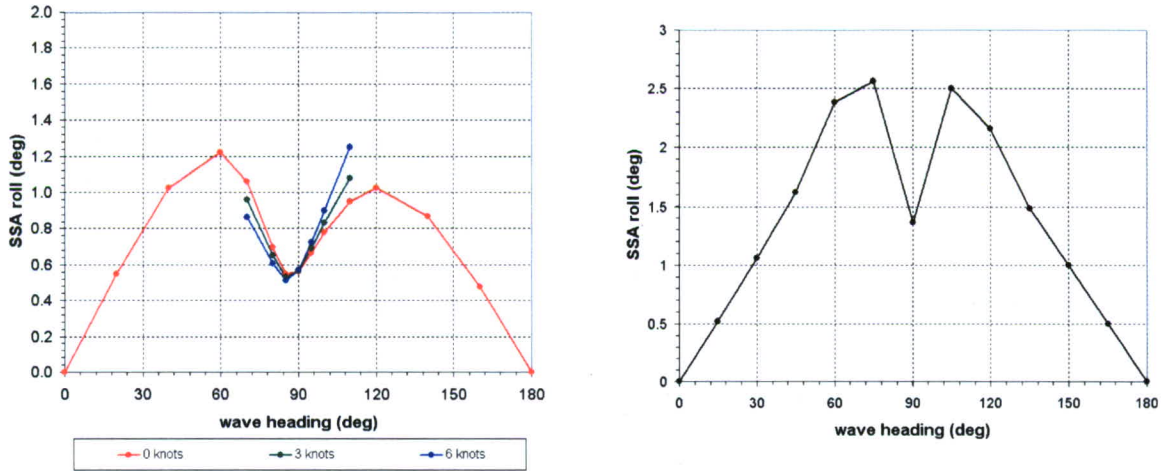


Fig. 23. Study of appendage effects on the roll motions of the monohull geometry with zero forward speed in various sea states.

Another result of the appendage study was that the unexpected drop in predicted roll occurs over a range of headings in general beam seas. The predicted drop in roll for the “transfer” portion of the mission assessment study, shown in Figure 22(a), was caused by a single point, the 90 degree wave heading value. The two nearest neighboring points, at 75 and 105 degrees, followed the expected trend of increasing roll as the wave heading tended toward 90 degrees. The appendage study, however, had finer wave heading increments in the 75 to 105 degrees region than did the mission assessment study. These finer increments showed that the predicted roll is being affected in the entire region, with the largest decrease occurring at 90 degrees.

To further investigate the unexpected drop in roll, another readily available hull form was simulated in VERES. This hull form was the S-175 hull, which resembles a high-speed containership and is the sample input file provided for VERES by Marintek. The predicted roll motions from VERES were obtained over a wide range of wave headings at zero speed for Sea State 5 and can be seen in Figure 24(a). As the results (red line) clearly show, a decrease in roll around 90 degrees exists. Little attention should be paid to the actual predicted SSA roll magnitudes since the physical hull dimensions are quite different between the two hulls and the wave parameters, such as

ratio of beam to wavelength and ratio of hull draft to wave height, were not scaled to make them consistent across the hulls. Instead, the *behavior* of the predicted roll over wave headings is of principle interest. In order to determine if the drop occurs only for zero speed, the S-175 was also simulated at 3 knots (green line) and 6 knots (blue line) in a Sea State 5 for wave headings between 75 and 105 degrees. These results are also shown in Figure 24(a). The decrease in roll is present at these slow forward speeds as well.



(a) S-175 containship ship hull at both zero and forward speed using VERES with viscous roll damping but no appendages modeled.

(b) JHSS hull at zero speed using SMP95 with appendages modeled.

Fig. 24. Comparison of the predicted roll motions for different geometry monohulls in a Sea State 5.

The effects of the viscous roll damping models used in VERES were also investigated. These models involve the work of Kato¹³ for frictional roll damping and the work of Ikeda et al.¹⁴ for bare hull eddy damping. The JHSS monohull was simulated with and without the viscous roll damping terms in a Sea State 5 at zero forward speed over a wave heading range of 75 to 105 degrees. For any given wave heading over the range explored, the viscous roll damping caused a decrease of only approximately one percent in the predicted roll motion compared to the predicted motion without the viscous models and the overall behavior was the same.

The motions of numerous monohulls have been previously simulated at NSWC Carderock using the Standard Ship Motion Program (SMP), which is also based on traditional strip theory. Some of these simulated monohulls include the CG-47, CVN-70, FFG-7, DDG-51, and CV-66. A survey of all these previous studies showed that the following general trend existed: for reasonably long wavelengths relative to a given ship length, the maximum roll did occur at 90 degrees, however, for shorter wavelengths, the decrease in roll around beam seas emerged again. For instance, for the CVN-70, for wavelengths longer than roughly 450 meters (modal periods greater than 17 seconds), the maximum roll angle did occur at 90 degrees. However, for shorter wavelengths, the unexpected decrease in roll around a wave heading of 90 degrees was present. To directly compare

to these previous results, the JHSS monohull was simulated using SMP95 at zero forward speed in a Sea State 5 and the predicted roll motion results can be seen in Figure 24(b). The SMP predicted roll shows the same trend of decreasing roll near beam seas.

The results of the appendage and S-175 hull studies along with the SMP simulations captured many aspects of this unexpected roll behavior. First, the decrease in predicted roll angle was not the result of using an appendage model or viscous roll damping models within VERES. Furthermore, this behavior was seen over a broad wave heading region, between 75 and 105 degrees and occurs at zero speed as well as at slow speeds, up to six knots at least. Also, our studies showed that these results are not unique to the JHSS monohull, nor to VERES, and were seen over a wide range of other monohulls and a second simulation program. Finally, this behavior appears to occur for short wavelengths relative to the given ship length and disappears at longer wavelengths.

Taking all the various results into account, it appears that the unexpected roll decrease in beam seas with short wavelengths is inherent to the traditional strip theory formulation. Unfortunately, without model test data at zero speed in beam seas, which is a nontrivial testing arrangement since the model orientation relative to the waves tends to wander, it is currently impossible to say whether these predicted results are a real, counterintuitive, physical behavior or simply an artificial result of the strip theory formulation in such seaways. Further efforts to resolve the validity of the decrease in roll, along with determining the exact portion of the formulation that causes the predicted decrease, would require experimental and numerical investigations along with a detailed examination of strip theory, all of which are not within the scope of this task. Without further information available it is recommended that a conservative approach be taken and to assume that the roll motion does not decrease between 75 and 105 degrees and instead reaches a maximum at 90 degrees and takes on a value slightly larger than the values at 75 and 105 degrees.

Survival Mission Assessment

The results of both the JHSS monohull and trimaran designs for the “survival” portion of the mission assessment study are presented here. The only parameter of interest in this portion of the mission assessment is the roll angle that disables the vessel. The deck edge of the trimaran will be submerged for any static heel greater than 30 degrees. Therefore, this value was chosen as the critical roll angle for this portion of the mission assessment.

Critical Roll

The results of the survival mission assessment roll angle are shown in Figure 25. The general trends are the same for both hull designs and show that the roll angle is below the limiting threshold in a general head or following seas orientation. However, there is a large change in roll angle for a small change in wave orientation such that both hulls begin to experience large roll angles as the wave heading begins to approach a general beam seas orientation. The trimaran does slightly better in this portion of the mission assessment than the monohull since it only technically exceeds the critical threshold value in pure beam seas. However, in any wave heading in a general beam seas situation, the roll is very large and close to the threshold value. For the monohull, any wave heading in the general beam seas situation will cause it to exceed the threshold criteria.

There is again a small unexpected downward spike in the roll angle, analogous to the “transfer” portion, right at pure beam seas for the monohull. This unexpected roll behavior was examined

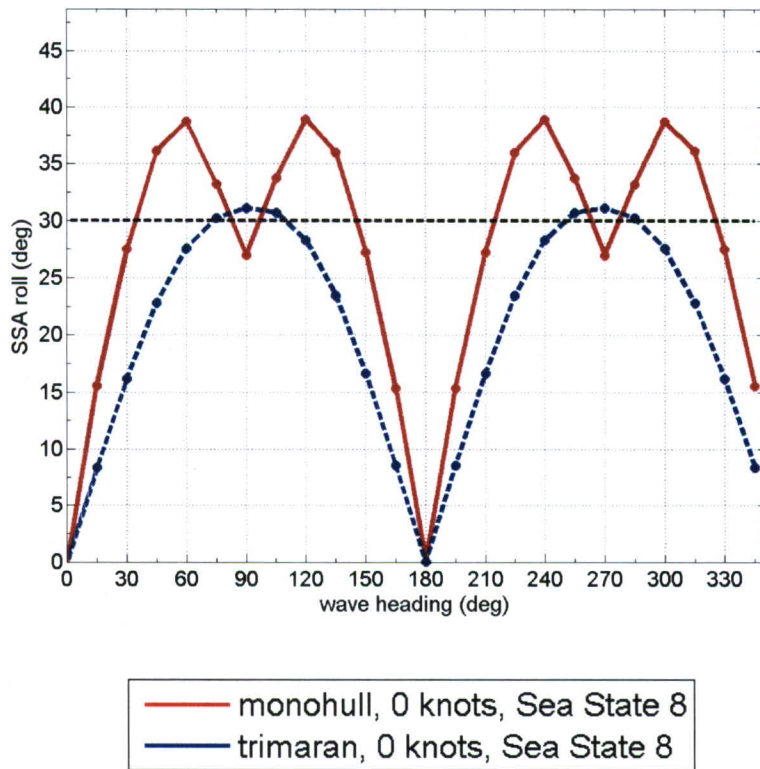


Fig. 25. Vessel roll results for both the JHSS monohull and trimaran during a simulated survival situation.

and discussed in detail in the **Roll and Pitch Motion Limits** section of the “transfer” portion of the mission assessment. As detailed in that section, this unexpected downward spike appears to be an artifact of traditional strip theory in beam seas with short wavelengths. However, since our previous conclusions were not dependent on the sea state, the recommendations given for the “transfer” portion in the previous section should also be used here for the “survival” portion. Thus, the expected roll magnitude around pure beam seas should be estimated as being slightly greater than the roll predicted at 75 and 105 degrees.

Sensitivity of Results

In this section we address the general topic of the sensitivity of the results. The task of completing a mission assessment study requires certain decisions to be made. These decisions are, in many cases, engineering judgments and introduce a degree of error into the results. A slightly different choice could conceivably change the results. This issue was addressed previously in Section **Mission Assessment Criteria**. Therefore, it is advantageous to have a understanding of how sensitive the simulated results are to such changes that result from different engineering judgments. A complete and exhaustive sensitivity study is beyond the time and financial restrictions of

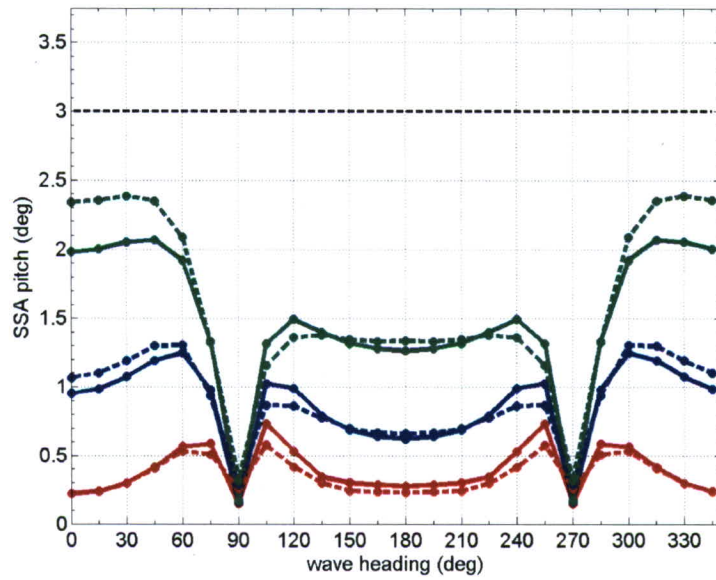
this, and most studies. However, the sensitivity of two important variables in this study, the use of the ordinary 2D compared to 2.5D strip theory and the critical velocity used to mark a slamming event, is explored.

First the difference between ordinary 2D strip theory compared to high-speed 2.5D strip theory is compared. As was discussed in Section **VERES Theory**, there is not a clear direction in the literature as to when one needs to use the 2.5D theory; only that somewhere between $F_n = 0.30$ and $F_n = 0.40$ the change in strip theory should be used. For a speed of 36 knots, the corresponding Froude number for the monohull is 0.347 and for the trimaran is 0.364. Therefore, this condition is subject to the choice of which strip theory to use. In order to assess the sensitivity of the results to the choice of strip theory, all 36-knot cases were simulated twice, once with the traditional strip theory and once with the high-speed theory, for both the monohull and trimaran. A sample comparison result is shown in Figure 26.

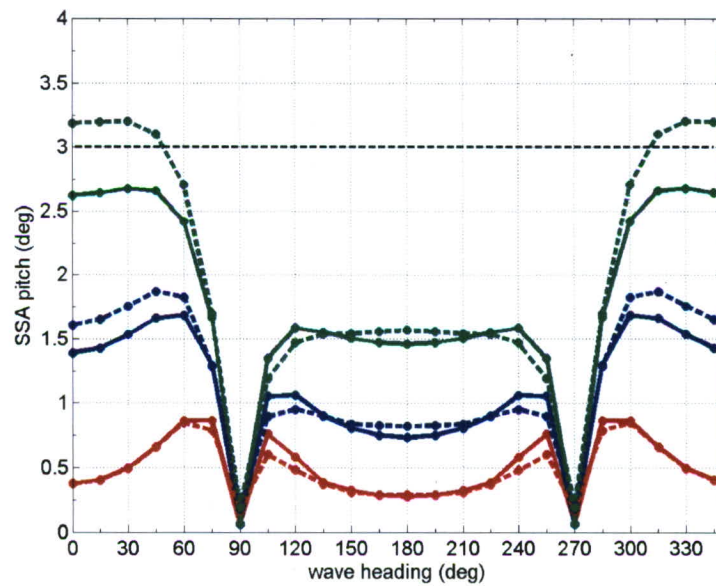
This sample result is typical of all the results seen for the monohull and trimaran, except for the results concerning bow slams. As a general rule, the high-speed 2.5D strip theory predicted that the value of the parameter of interest would be either equal to the corresponding parameter value obtained using the traditional 2D strip theory, or in some cases only slightly larger. This means that parameters that were well below the threshold criteria using the traditional strip theory remained well below the threshold criteria when the high-speed theory was used. The pitch angle of the vessel was purposely chosen to show that in some cases, the traditional theory was below the threshold criteria while the high-speed theory exceeded it. However, in those cases, the traditional theory predicted a parameter value that was extremely close to the threshold criteria in the first place. Therefore, that point would have already been a concern and the high-speed theory, by pushing it past the threshold criteria, did not dramatically change any previous conclusions. The complete results for the monohull can be found in Appendix C and for the trimaran in Appendix D.

The only parameter that did show a large sensitivity to the type of strip theory used was the number of slams per hour. The sensitivity of the number of slams for both the monohull and trimaran can be seen in Figure 27. The number of predicted bow slams for the monohull more than tripled, and more than doubled for the trimaran, when using high-speed strip theory instead of traditional strip theory. It should be noted that this sensitivity is only concerned with Sea State 7 conditions. In the lower sea states investigated, the number of slam events was approximately zero for both types of strip theories.

Due to the sensitivity of bow slams, the effect of the critical velocity on the number of slams was explored as well. The important role that critical velocity plays in the determination of whether a slam occurs or not was discussed earlier. The number of slams predicted using the Ochi criteria¹⁵ are compared with the number predicted using a critical velocity of zero in Figure 28(a) for the monohull and in Figure 28(b) for the trimaran. By assigning a critical velocity of zero the number of slams is bound. A critical velocity of zero will cause VERES to count every time the bow enters the water as a slam, and thus, the limiting case of the maximum number of slams is determined. The results show that, similar to the slamming sensitivity to the type of strip theory used, only the motions produced by Sea State 7 conditions matter. Not much motion occurs for the lower sea states so they are not sensitive. However, for Sea State 7, Figure 28 shows that the bows of both ships leave the water a large number of times. Therefore, the potential for a large number of slamming events. Due to the exponential dependence of slamming on the critical velocity, this parameter will always be fairly large.



(a) monohull



(b) trimaran

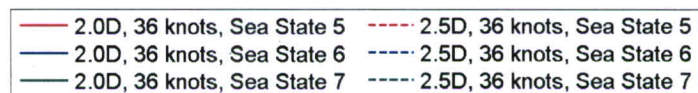
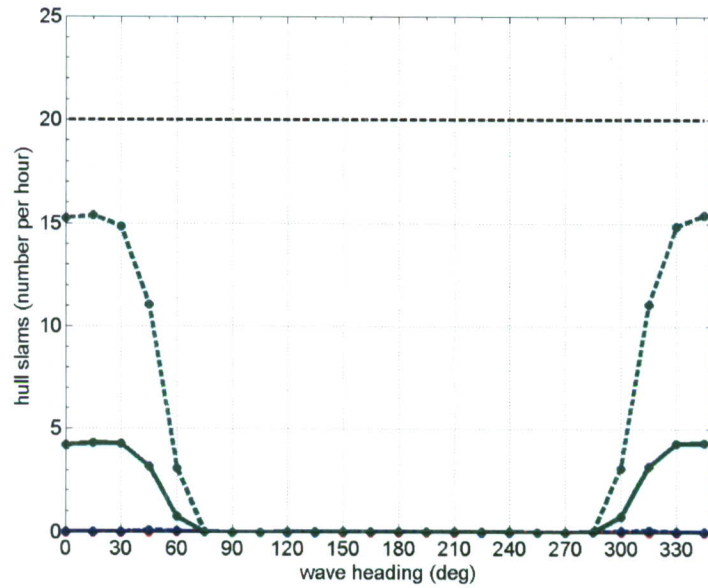
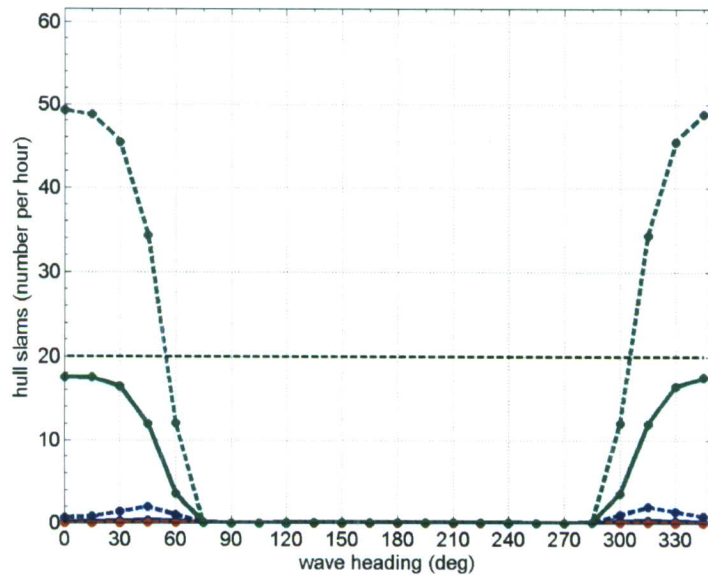


Fig. 26. Comparison of vessel pitch angles predicted using the traditional 2D strip theory and the high-speed 2.5D strip theory for a 36 knot simulation for both the JHSS monohull and trimaran.



(a) monohull



(b) trimaran

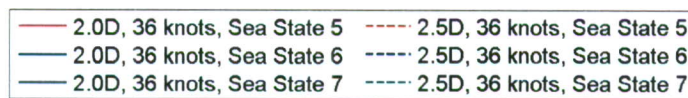
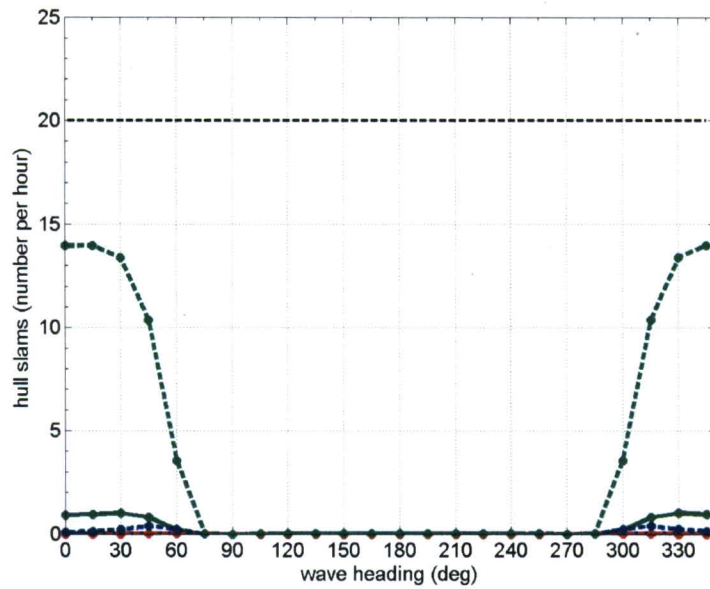
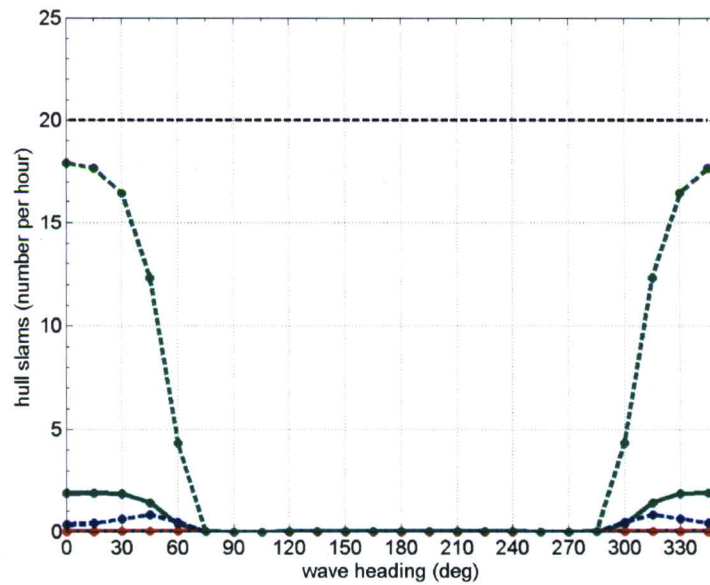


Fig. 27. Comparison of hull slams predicted using the traditional 2D strip theory and the high-speed 2.5D strip theory for a 36 knot simulation for both the JHSS monohull and trimaran.



(a) monohull



(b) trimaran

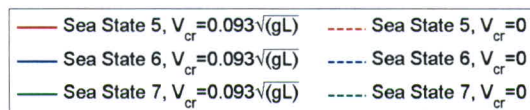


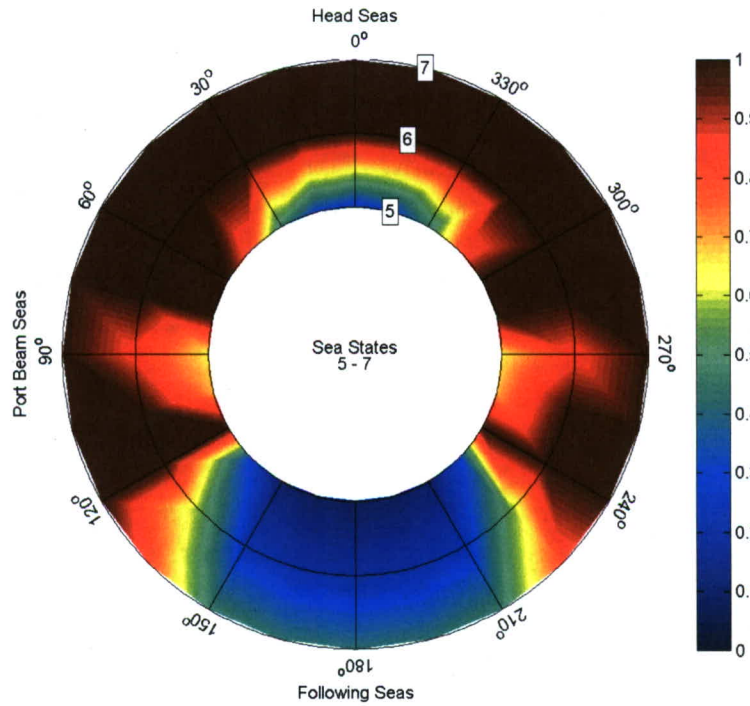
Fig. 28. Comparison of hull slams predicted using the traditional Ochi critical velocity relationship and a $V_{cr} = 0$ for a 20 knot simulation for both the JHSS monohull and trimaran.

Summary and Conclusions

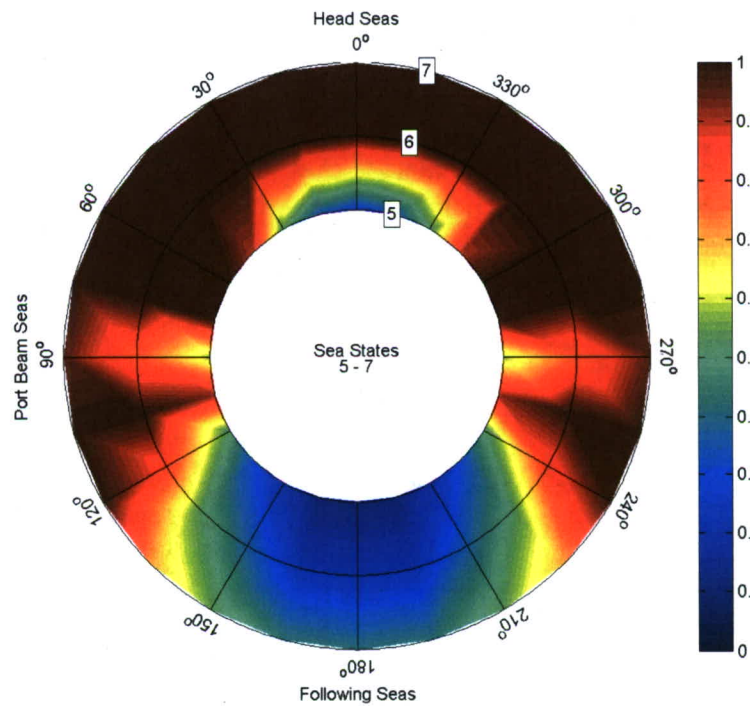
The numerous mission assessment criteria make it difficult to assess what the overall mission capability is when taking into account all the various acceleration, rotation angle, and motion event considerations. So for the purpose of this study, all the mission assessment parameters were combined to create a composite mission assessment figure. In such a framework, for the ship to be able to carry out the mission, *all* the parameters must be below their respective threshold criteria. If any parameter value is above the threshold, then the mission can not be accomplished. Therefore, for each speed, heading, and sea state, the parameter that comes closest to, or surpasses, the threshold criteria is the most important parameter for that speed, heading, and sea state combination. In order to compare all the parameters, we have normalized the results with respect to each parameter's threshold criteria. For instance, a nondimensional value of 0.5 would mean that that particular parameter of interest had a value that was half of the threshold criteria. The composite result then captures the single largest normalized value of all the parameters for each speed, heading, and sea state combination. A value of 1.0, or greater, means that at least one parameter surpassed the threshold criteria and the vessel is unable to perform the required mission under those conditions. For the sake of maintaining maximum resolution in the region below the threshold criteria, the upper limit on the following composite figures was capped at a value of 1. If one wanted to know the extent that a parameter exceeded the threshold criteria he or she could use the individual parameter figures earlier in the report. These composite mission assessments are presented as *sea state* polar plots. They are similar to traditional *speed* polar plots except that the speed axis has been replaced by the sea state and the figure represents a single ship speed.

Summary of Transit Mission Assessment

The transit mission assessment was conducted over three different sea states, Sea States 5-7, and at two different speeds, 20 and 36 knots. The composite results for the monohull can be seen in Figure 29(a) for 20 knots and Figure 29(b) for 36 knots. The composite results for the trimaran can be seen in Figures 30(a) and 30(b) for the same speeds. The first thing that stands out is how similar the composite mission assessments results are for both hull designs at both speeds. For the three sea states investigated, there is no sea state that allows for unrestricted headings of either of the designs. For both designs, general head seas are limited mainly by MSI considerations. Bow quartering and general beam seas are limited both by MII and roll considerations for both designs. The trimaran is also limited by transverse acceleration considerations in general beam seas. Each hull design failed at least one of the mission assessment criteria when operating in head seas all the way around to stern quartering seas. The best operating condition for both vessels is in following seas. Since during a transit mission the vessel may not have a choice in heading, if either vessel needed to operate in a heading other than following seas in Sea State 6 or 7, then completion of the mission may be possible by lowering the vessel speed below 20 knots. However, potential slower speeds, if any existed, would have to be simulated in order to verify that the threshold criteria were no longer exceeded. There are also some scattered pockets of mission capable operating areas such as beam and head seas in Sea State 5. It appears that the trimaran has a slightly larger head seas window to operate within at 20 knots in Sea State 5 than the monohull does. Also, for both hulls, if the vessel speed increases from 20 to 36 knots, then it appears that the best operating region in following seas also increases slightly.

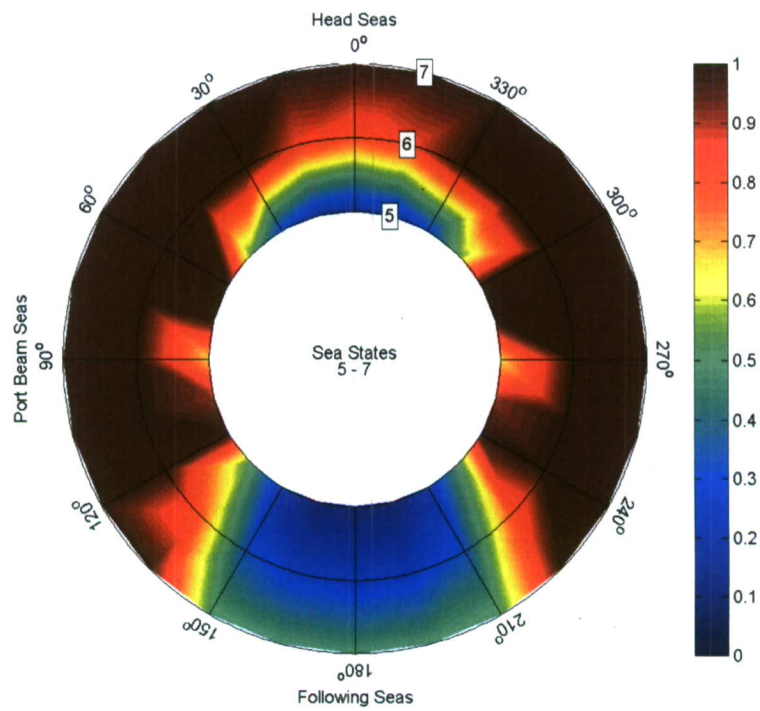


(a) 20 knots

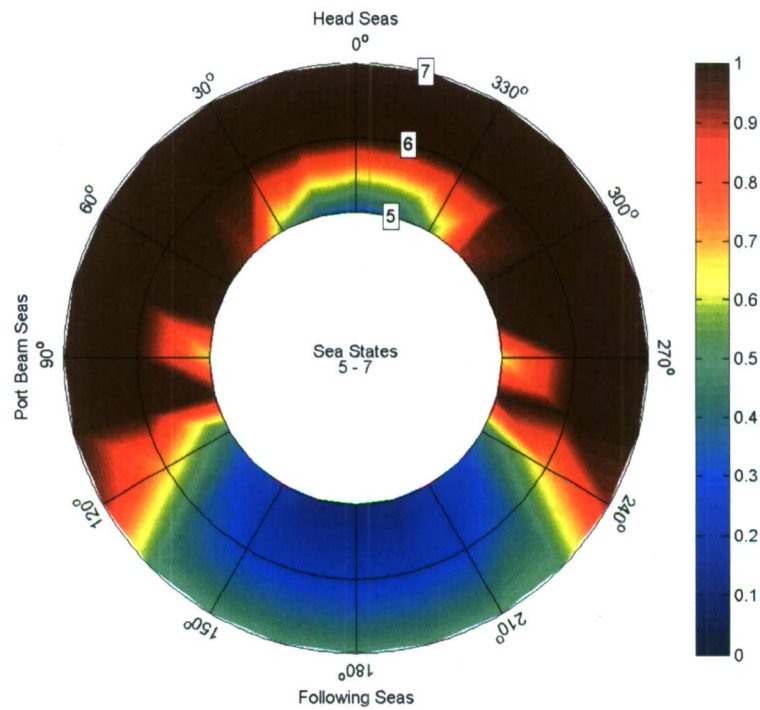


(b) 36 knots

Fig. 29. Composite results of the transit mission for the JHSS monohull.



(a) 20 knots



(b) 36 knots

Fig. 30. Composite results of the transit mission for the JHSS trimaran.

Summary of Transfer Mission Assessment

Similar composite mission assessment sea state polar plots were constructed for the cargo transfer mission assessment. However, since this mission assessment only involves one speed, zero knots, there is only one plot per hull design. The composite results for the monohull can be seen in Figure 31(a) and for the trimaran in Figure 31(b).

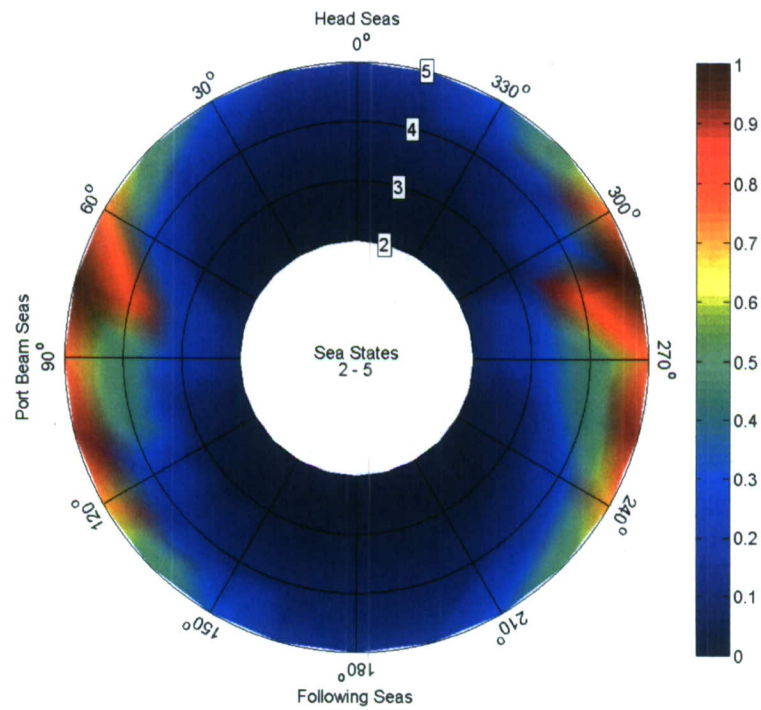
The composite results for the cargo transfer mission assessment of the two vessels are again very similar. Both hull designs appear able to remain below the composite threshold criteria for every parameter and at all headings in sea states 2 through 4. In Sea State 5, both vessels are below the composite threshold criteria in head and following seas; however, both vessels are not able to remain under the composite threshold criteria in the region of general beam seas. The major difference between the two hull designs in terms of the composite mission assessment is that the trimaran remains below 50 percent of the composite threshold criteria for all headings in Sea States 2 through 4 while the monohull has small pockets of headings in Sea State 4 where it approaches the composite threshold criteria. The trade-off appears to be that the monohull does have a few headings in the beam seas condition where it is able to fulfill the mission assessment requirements even in Sea State 5. The trimaran fails at least one parameter threshold in the entire beam seas region.

Summary of Survival Mission Assessment

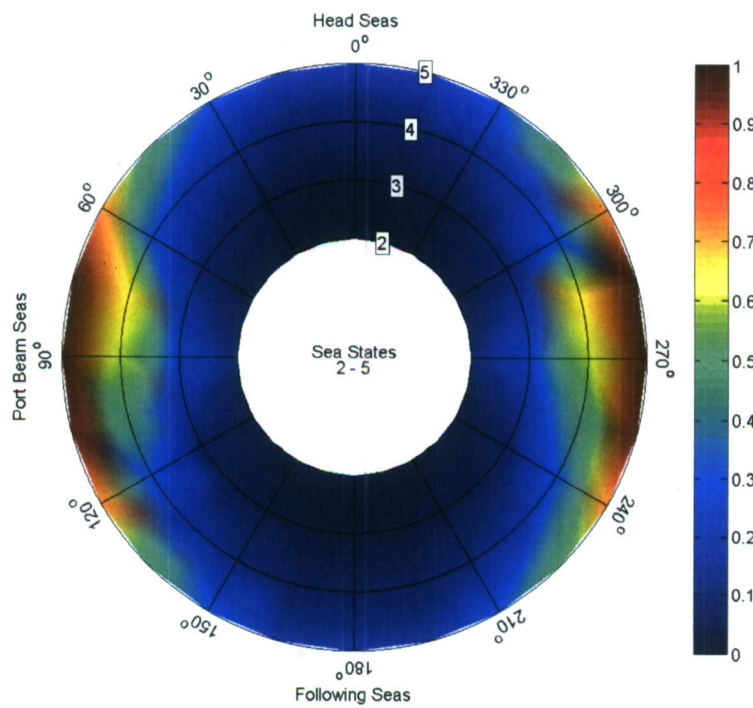
The final composite result is for the survival mission assessment. Since this mission only involved one speed, one sea state, and one parameter, the composite result is identical to Figure 25 except that now the lone parameter, roll angle, has been turned into a nondimensional percentage of the threshold value. This is shown in Figure 32.

Overall Conclusions

Although a large number of parameters and locations were examined for the transit portion of the mission assessment, the small area of mission capable operating conditions is due to only a few of the parameters. The MSI parameter at the pilothouse and forward helicopter spot caused the elimination of the head to bow quartering seas operating area. The MII parameter at the pilothouse and forward helicopter spot caused the elimination of the general beam seas operating area. The ship roll angle also caused the elimination of beam to stern quartering seas. This was the case for both hull designs. The trimaran also surpassed the threshold criteria of transverse acceleration in bow quartering to stern quartering seas as well. Therefore, dramatic improvements can be made in the amount of mission acceptable headings by simply targeting these few parameters. For instance, head seas operating conditions would be possible if MSI concerns would be addressed, for example, by moving the location of the crew to areas of the ship that experience smaller accelerations or limiting the exposure time of the crew. Furthermore, for the monohull design, if MII concerns were addressed, for example, by changing the location of where the tasks were performed to regions of the ship that experience smaller lateral and vertical accelerations, then the vessel could operate in bow quartering seas as well. The mission assessment analysis currently shows that the vessel is limited to very few operating conditions. However, this is due to only a single, or limited number, of parameters exceeding the threshold values. Addressing these limited points would greatly in-



(a) monohull



(b) trimaran

Fig. 31. Composite results of the transfer mission for both the JHSS monohull and trimaran.

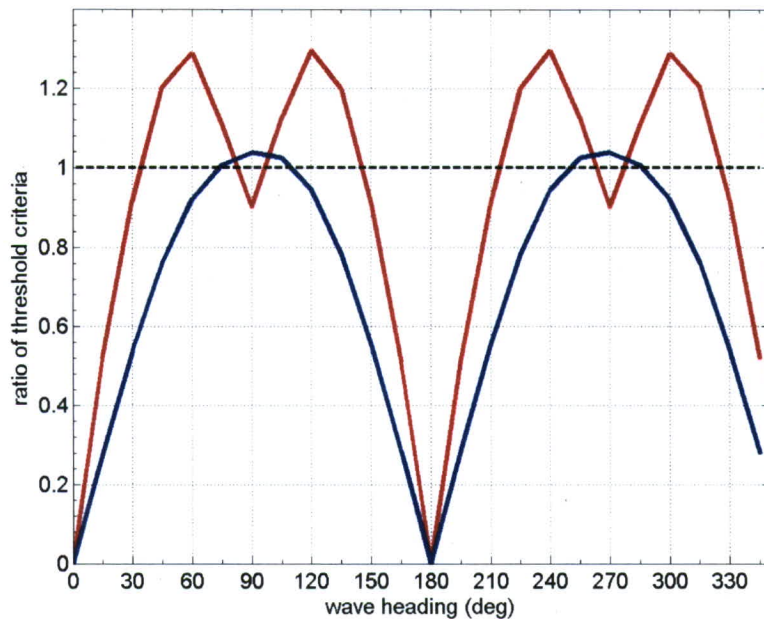


Fig. 32. Composite results for the survival mission for both the JHSS monohull and trimaran.

crease the potential operating conditions. Since only Sea States 5-7 were requested for the transit portion of the study, no definite statement can be made regarding where the design would fail in a lower sea state. Obviously more operating areas would presumably be available but the rate at which they become available as sea state decreases is not known. The cargo transfer assessment was done in Sea States 2-5, however, those results can not be combined with the higher sea state results for the transit portion because the underlying wave spectra were different. A Bretschneider spectral shape was used for the transit portion while a JONSWAP spectrum was used for the transfer portion.

The cargo transfer mission assessment showed that most headings and sea states were acceptable. Furthermore, the problematic areas were general beam seas in Sea States 4 and 5. If such a situation arose and the cargo transfer was urgent, the vessel should be able to be realigned such that the primary wave heading was either head or following seas, in which case, the cargo transfer should be able to continue even in Sea State 5.

Acknowledgements

The authors would like to acknowledge the support of Dr. Colen Kennel, Mr. Jack Offutt, and Mr. Andy Anderson for supplying all the information needed to characterize the monohull and trimaran configurations. We would also like to thank Dr. Michael Hughes for creating the VERES compliant geometry input files along with Mr. Rielly Conrad who established the locations of the points of interest on both vessels and helped with the establishment of the threshold criteria values. Both also participated in the investigation exploring the unexpected decrease in the predicted monohull roll motion in beam seas; their efforts are greatly appreciated. Finally, we thank Mr. Terrence Applebee for providing the results of the previous SMP monohull simulations.

Appendix A - Random Seaway Description

Random seaway spectra are calculated in VERES using the following formulation ³

$$S(\omega) = \frac{5}{16} \frac{H_s^2}{\omega_m} (1 - 0.287 \ln \gamma) \left(\frac{\omega_m}{\omega} \right)^5 e^{-\frac{5}{4} \left(\frac{\omega_m}{\omega} \right)^4} \Psi \quad (\text{A.1})$$

where $S(\omega)$ is the point spectrum, ω is the wave frequency, H_s is the significant wave height of the sea state, ω_m is the modal wave frequency of the sea state, γ is a peakedness parameter used in a Joint North Sea Wave Project (JONSWAP) type spectrum to determine the concentration of the spectral ordinates about the peak frequency, and Ψ is a frequency dependent scaling factor given by

$$\Psi = \gamma e^{-\frac{1}{2\sigma^2} \left(\frac{\omega}{\omega_m} - 1 \right)^2} \quad (\text{A.2})$$

where γ is again the peakedness parameter and σ is a spectral width parameter.

For a Bretschneider spectrum, γ is unity and the frequency dependent scaling factor does not influence the spectral shape. For the transit portion of the mission assessment study, a Bretschneider spectral shaped seaway was modeled for Sea States 5 through 7, shown in Figure A.1 through Figure A.3. For the survival portion of the mission assessment study a Sea State 8 Bretschneider seaway, shown in Figure A.4, was used. In these figures the red x's designate the periods at which the vessel transfer functions were computed at for use in the moment calculations of the response spectra. All the Bretschneider sea states used in the study are plotted on a common axis in Figure A.5 for comparison.

For a JONSWAP spectrum, σ , in Equation A.2, is 0.07 if the wave frequency is less than the modal frequency and 0.09 otherwise. The parameter γ can be set to a fixed value of 3.3 or a variable value based on the values of modal period and significant wave height. For all the JONSWAP spectra used in this mission assessment study, a fixed value of 3.3 for γ was used. The cargo transfer portion of the mission assessment study used a JONSWAP spectral shaped seaway for Sea States 2 through 5, as shown in Figure A.6 through Figure A.9. On these figures as well, the red x's designate the periods at which the vessel transfer functions were computed at for use in the moment calculations of the response spectra. As was done for the Bretschneider sea states, all the JONSWAP sea states used in the study are plotted on a common axis in Figure A.10 for comparison.

It is important to calculate the vessel transfer functions at frequencies that contain the energy for the given sea spectrum of interest. Equally important is to have an adequate resolution of the frequencies such that the important features and end behaviors are captured accurately when the transfer function and seaway spectrum are combined to obtain the vessel response, as shown by Equation 2 in Section **VERES Theory**. The frequency distribution and resolution that was used for each sea state can be seen in Figures A.1 through A.4 for the Bretschneider spectra and Figures A.6 through A.9 for the JONSWAP spectra. The points denoted by red x's correspond to the locations that motion transfer functions were calculated. In VERES, the distribution of points is input as modal periods so for consistency, the spectra are displayed over wave period compared to the more traditional angular frequency.

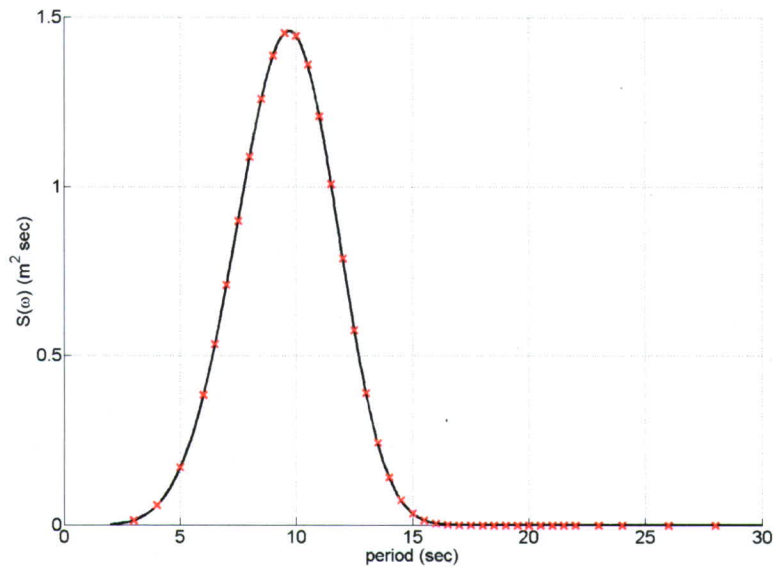


Fig. A.1. Bretschneider Sea State 5 spectral shape used in the “transit” portion of the mission assessment.

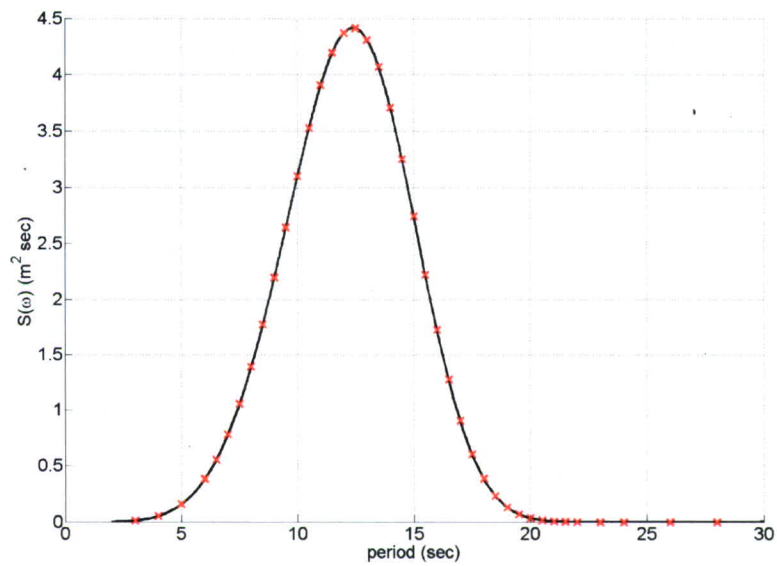


Fig. A.2. Bretschneider Sea State 6 spectral shape used in the “transit” portion of the mission assessment.

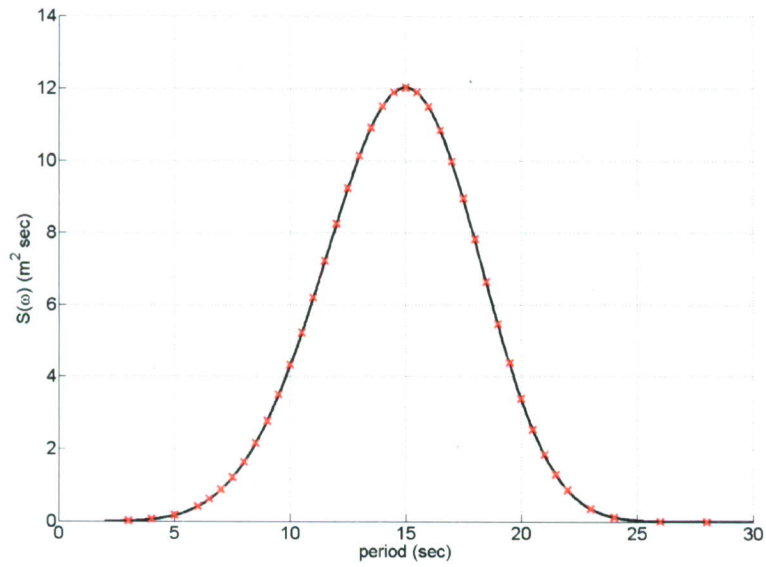


Fig. A.3. Bretschneider Sea State 7 spectral shape used in the “transit” portion of the mission assessment.

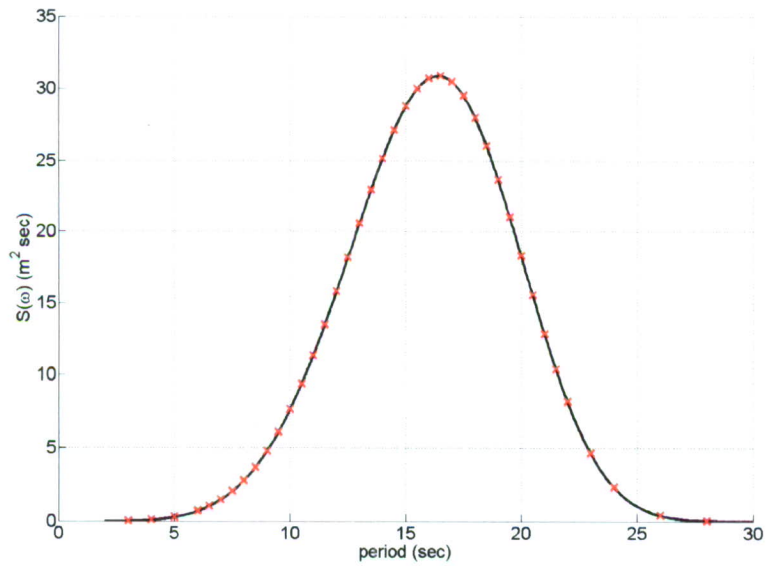


Fig. A.4. Bretschneider Sea State 8 spectral shape used in the “survival” portion of the mission assessment.

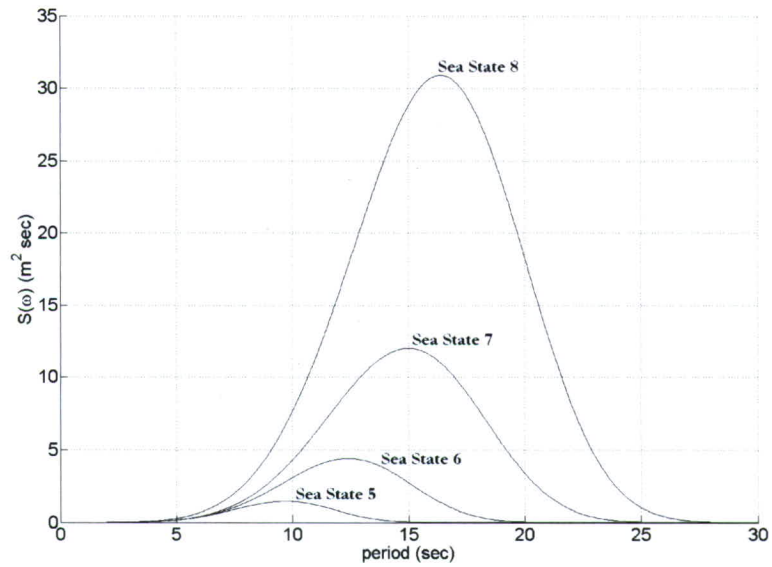


Fig. A.5. Comparison of the spectral shapes for Bretschneider Sea States 5 through 8 used during the “transit” and “survival” portion of the mission assessment study.

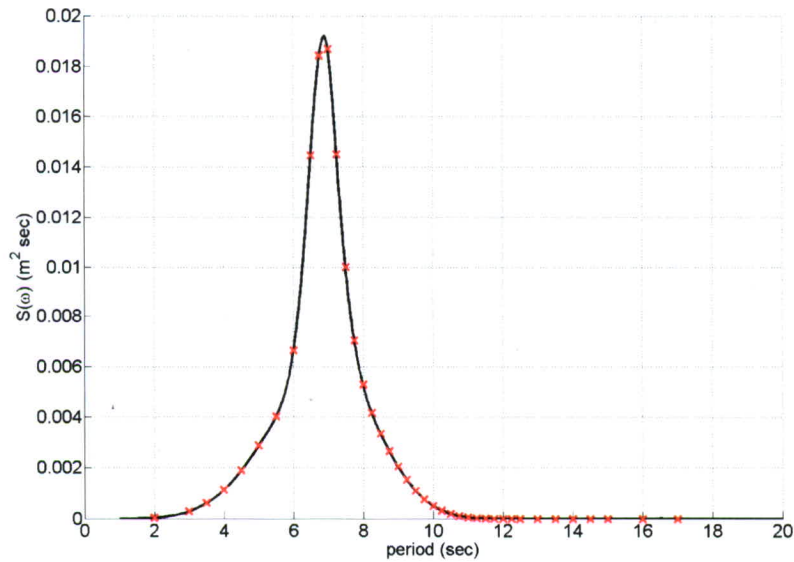


Fig. A.6. JONSWAP Sea State 2 spectral shape used in the “transfer” portion of the mission assessment.

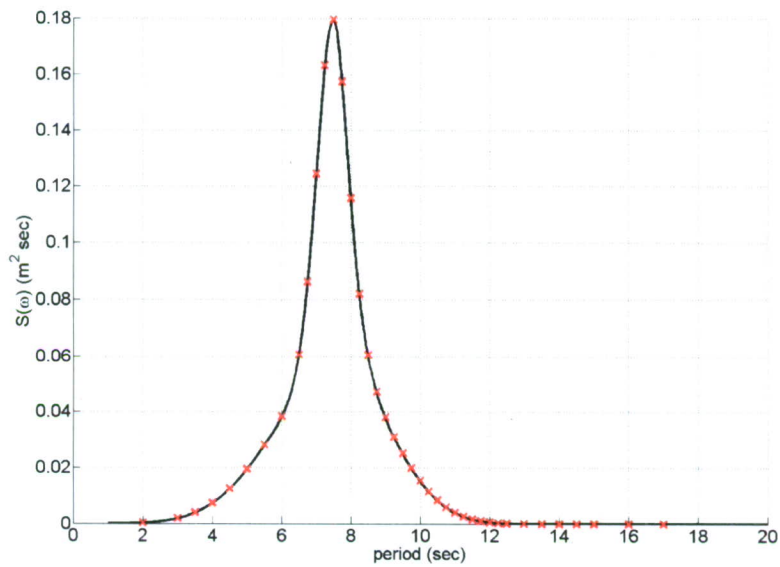


Fig. A.7. JONSWAP Sea State 3 spectral shape used in the “transfer” portion of the mission assessment.

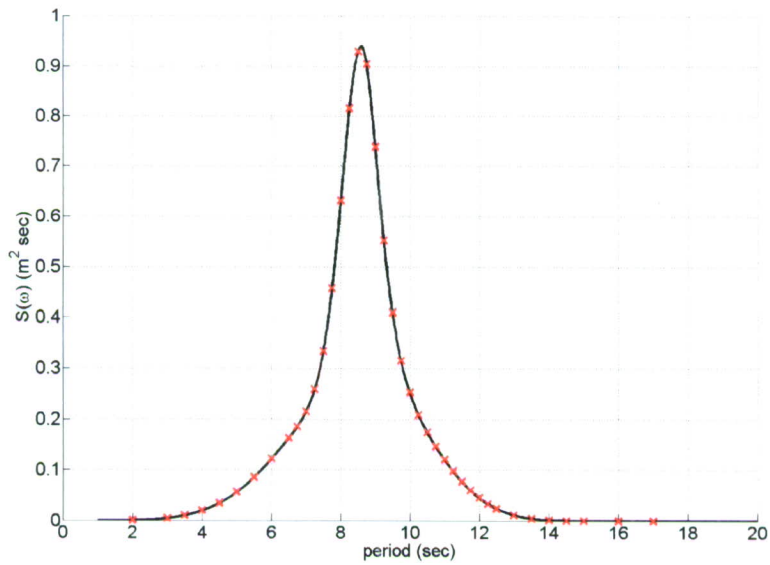


Fig. A.8. JONSWAP Sea State 4 spectral shape used in the “transfer” portion of the mission assessment.

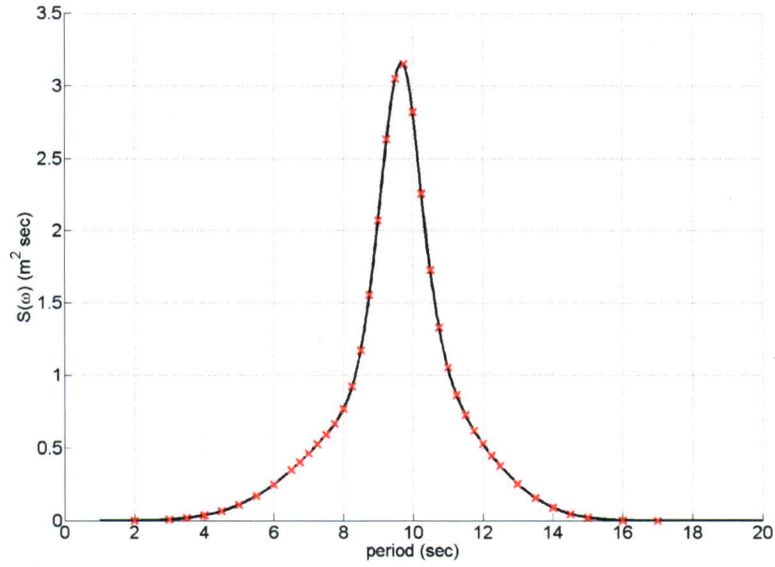


Fig. A.9. JONSWAP Sea State 5 spectral shape used in the “transfer” portion of the mission assessment.

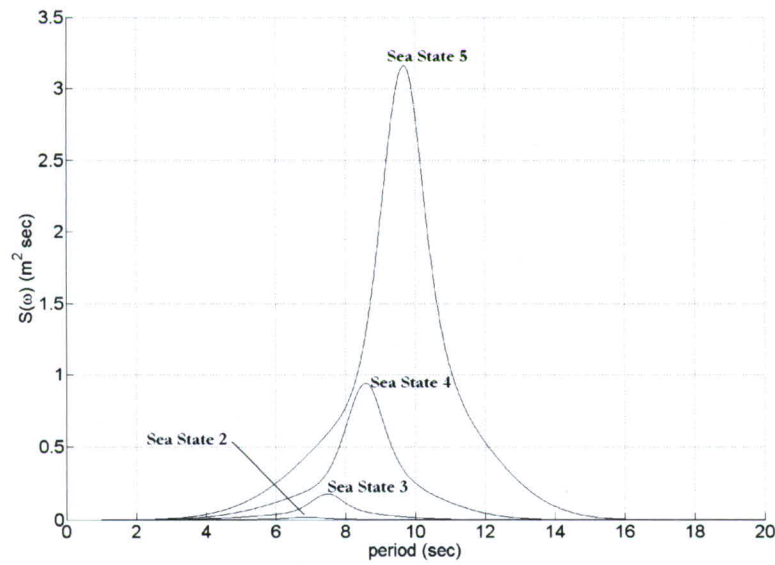


Fig. A.10. Comparison of the spectral shapes for JONSWAP Sea States 2 through 5 used during the cargo “transfer” portion of the mission assessment study. For these JONSWAP spectra, γ was fixed at 3.3 and modal period and significant wave height was specified.

Appendix B - Dynamic Sinkage and Trim Determination

The dynamic sinkage and trim values for the monohull geometry were based off an experimental model test conducted at the Naval Surface Warfare Center, Carderock Division involving the Joint High Speed Sealift Model 5653-3. These experimentally measured values can be seen in Figure B.1. The full details of the model test can be found in Cusanelli and Chesnakas¹⁰.

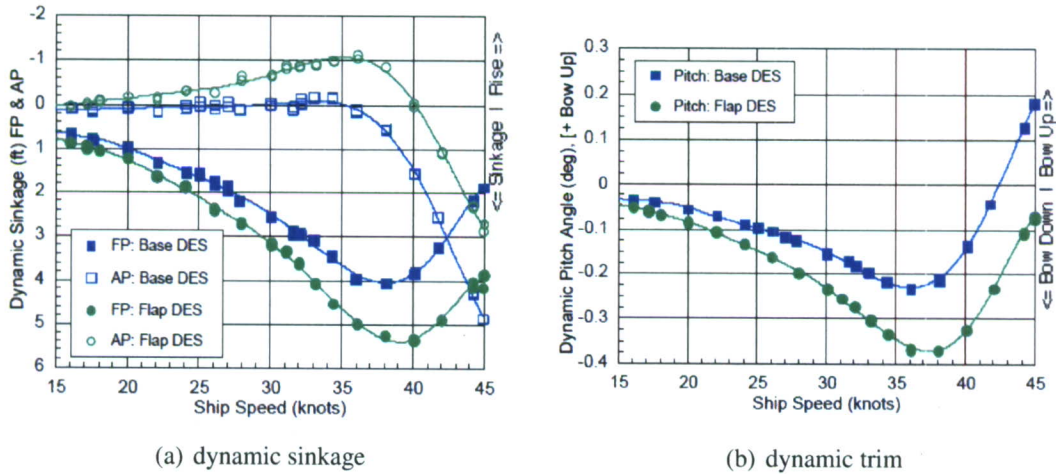


Fig. B.1. Experimentally measured dynamic sinkage and trim of the JHSS monohull. Figure from Cusanelli and Chesnakas¹⁰.

The dynamic sinkage and trim values for the trimaran geometry were estimates based on experimental results from a model test conducted at Webb Institute using a trimaran hull geometry similar to the one used for this mission assessment study. During this model test, the change in hull draft and trim, from their static values, was recorded over a range of speeds for different side hull locations. These experimentally measured values can be seen in Figure B.2. For the test conducted at Webb Institute, the standard convention is vessel center of gravity up is positive sinkage, and bow up is positive trim. The full details of the model test can be found in Carr and Dvorak¹¹.

The Carr and Dvorak test involved three transverse and three longitudinal side hull spacing arrangements for a total of nine unique configurations. The 30.9 percent transverse spacing arrangement tested, where the percentage is the ratio of the space between the main and side hulls to the beam of the main hull, is very similar to the transverse spacing of the JHSS trimaran side hulls. Unfortunately, the longitudinal spacing of the JHSS, the ratio of the distance from the stem to the midpoint of the side hull to the total length of the vessel, is approximately 56 percent. This is much lower than the three values tested at Webb Institute. Therefore, the three experimental runs at a transverse spacing of 30.9 percent were used to extrapolate what the change in hull draft and trim would be for a longitudinal space of roughly 56 percent. The results of this extrapolation can be seen in Figure B.3 for the change in hull draft and in Figure B.4 for the change in hull trim. The red and green data points represent the extrapolated values for the 20 and 36 knots cases, respectively.

The two extrapolated values for the change in draft were used as the dynamic sinkage for the JHSS hull at the corresponding speeds in the simulation. The two extrapolated values for the

change in trim were applied to the static trim that the JHSS trimaran is designed to have in order to approximate the dynamic trim at the corresponding simulation speeds.

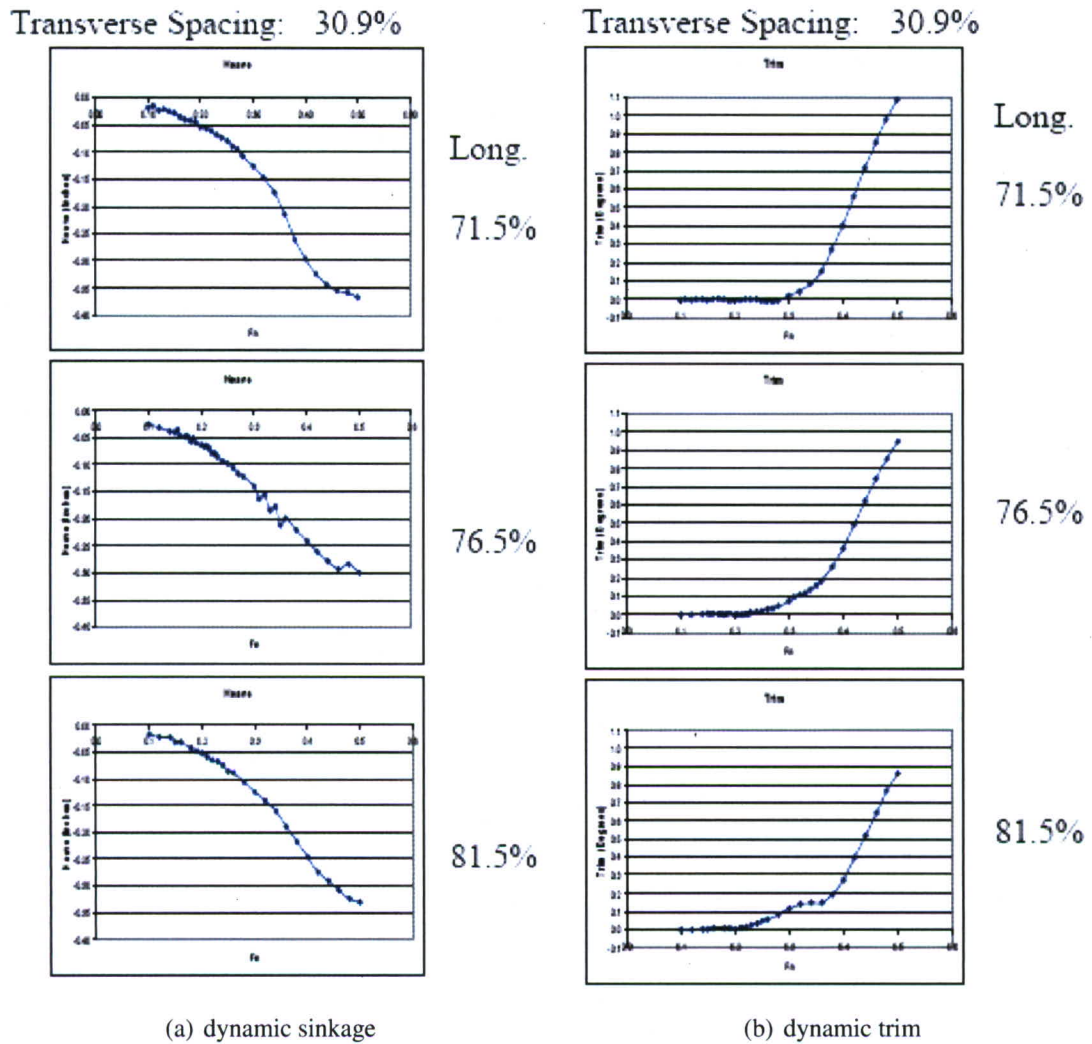


Fig. B.2. Experimentally measured dynamic sinkage and trim of a similar trimaran model to the JHSS trimaran. Transverse and longitudinal spacing refer to location of the side hulls as a percentage of the beam and length of the model. Figure from Carr and Dvorak¹¹.

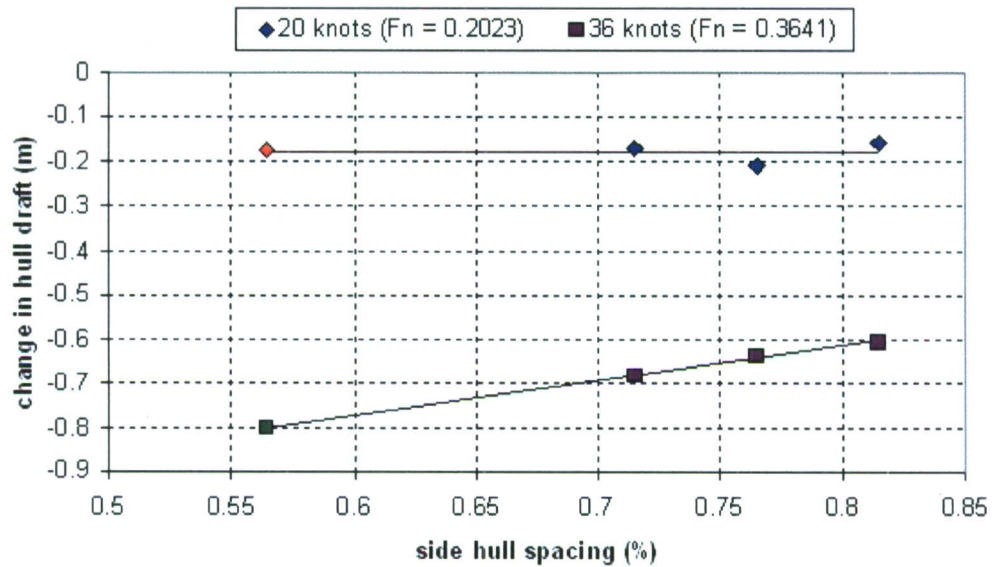


Fig. B.3. Extrapolated dynamic sinkage value for 20 and 36 knots for different longitudinal side hull spacing ratios. All results are for a transverse spacing of 30.9 percent.

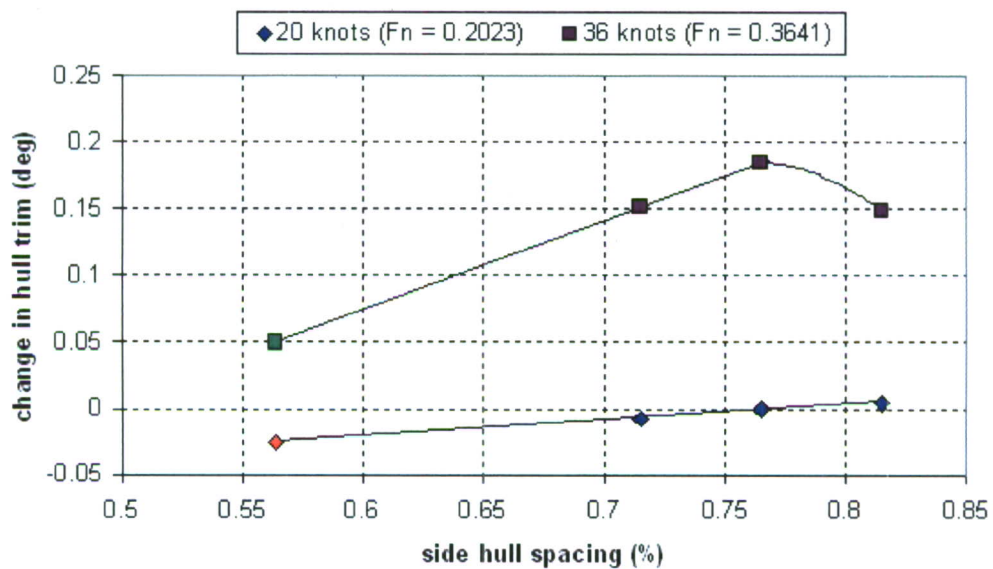


Fig. B.4. Extrapolated dynamic trim values for 20 and 36 knots for different longitudinal side hull spacing ratios. All results are for a transverse spacing of 30.9 percent.

THIS PAGE INTENTIONALLY LEFT BLANK

Appendix C - Comparison of 2D and 2.5D Strip Theory for the Monohull at 36 knots

The higher speed case, 36 knots, of the “transit” portion of the mission assessment for the monohull resulted in a $F_n = 0.347$ which is in the Froude number region of where traditional two-dimensional strip theory begins to need to be corrected for forward speed. However, there is not a clear distinct speed above which a 2.5D strip theory is required to be used. Therefore, in the mission assessment study, only traditional two-dimensional theory was used. However, in this appendix, we compare all the 36 knot speed monohull results that one would obtain using the two-dimensional strip theory compared to the 2.5D strip theory formulation in Figures C.1 through C.14.

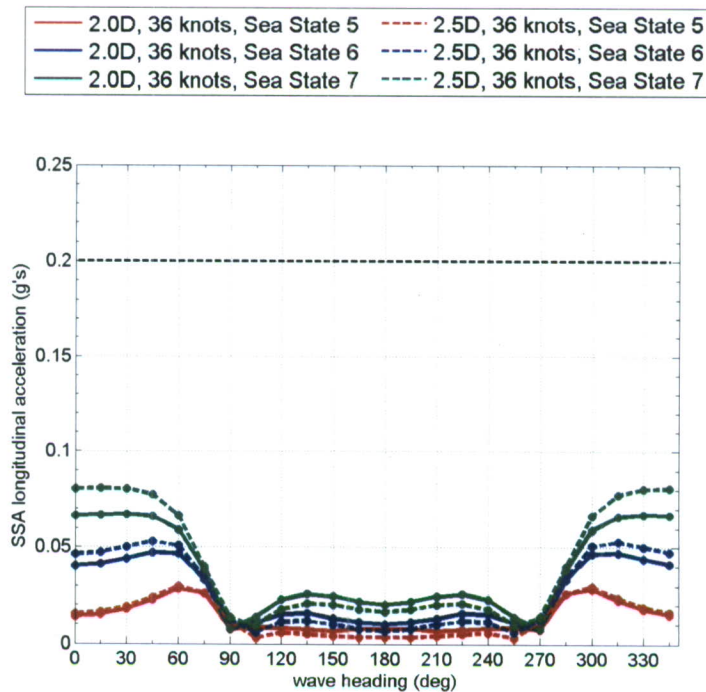


Fig. C.1. Comparison of longitudinal accelerations at the pilothouse for the JHSS monohull using 2D and 2.5D strip theory at $F_n = 0.347$.

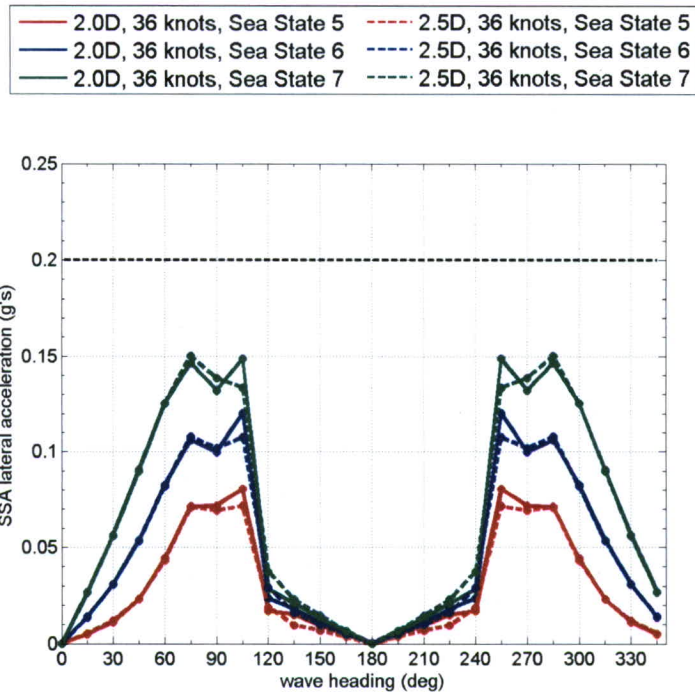


Fig. C.2. Comparison of lateral accelerations at the pilothouse for the JHSS monohull using 2D and 2.5D strip theory at $F_n = 0.347$.

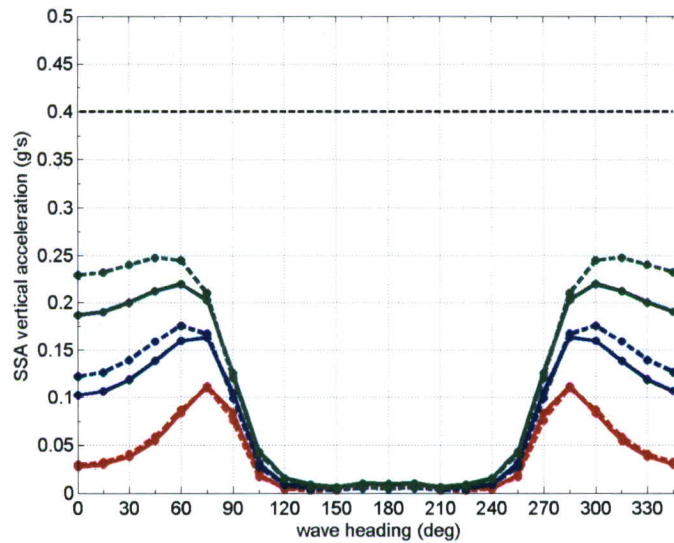


Fig. C.3. Comparison of the vertical accelerations at the pilothouse for the JHSS monohull using 2D and 2.5D strip theory at $F_n = 0.347$.

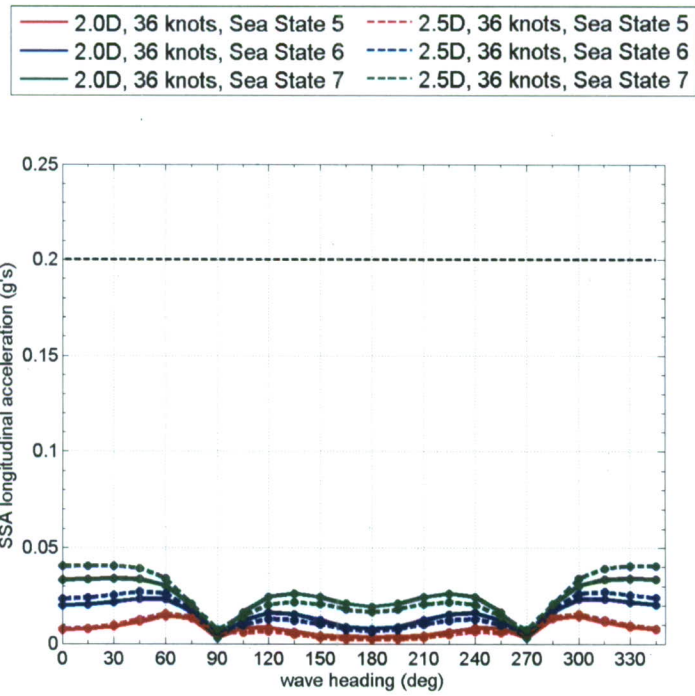


Fig. C.4. Comparison of longitudinal accelerations at the general helicopter spot for the JHSS monohull using 2D and 2.5D strip theory at $F_n = 0.347$.

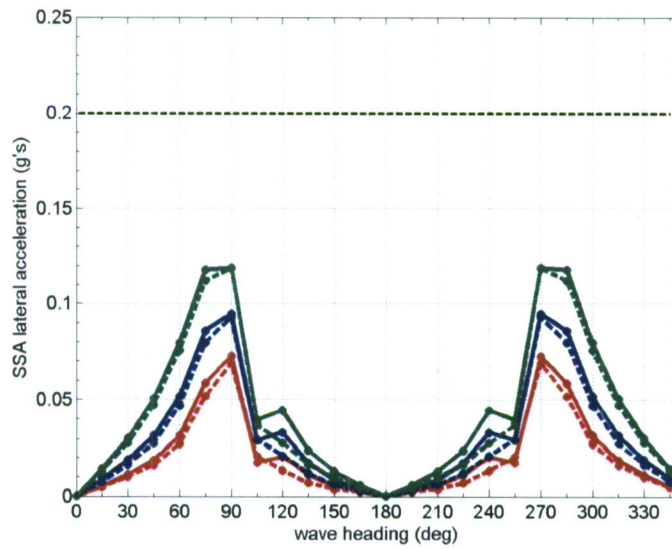


Fig. C.5. Comparison of lateral accelerations at the general helicopter spot for the JHSS monohull using 2D and 2.5D strip theory at $F_n = 0.347$.

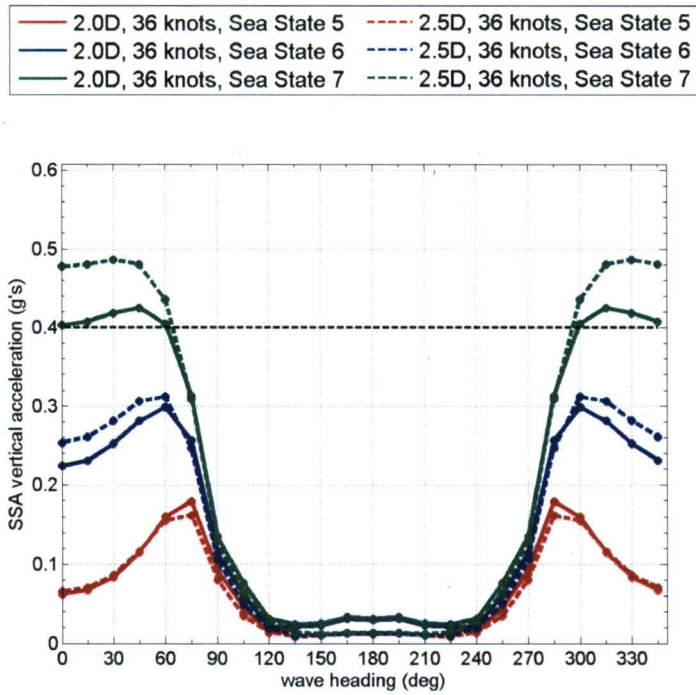


Fig. C.6. Comparison of vertical accelerations at the general helicopter spot for the JHSS monohull using 2D and 2.5D strip theory at $F_n = 0.347$.

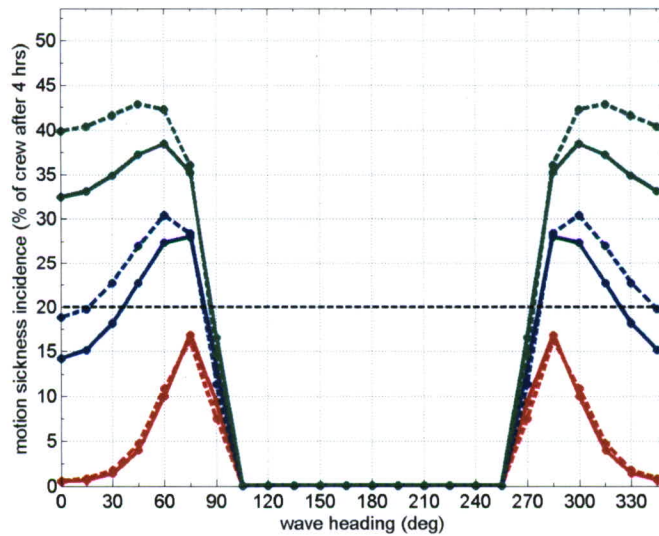


Fig. C.7. Comparison of MSI at the pilothouse for the JHSS monohull using 2D and 2.5D strip theory at $F_n = 0.347$.

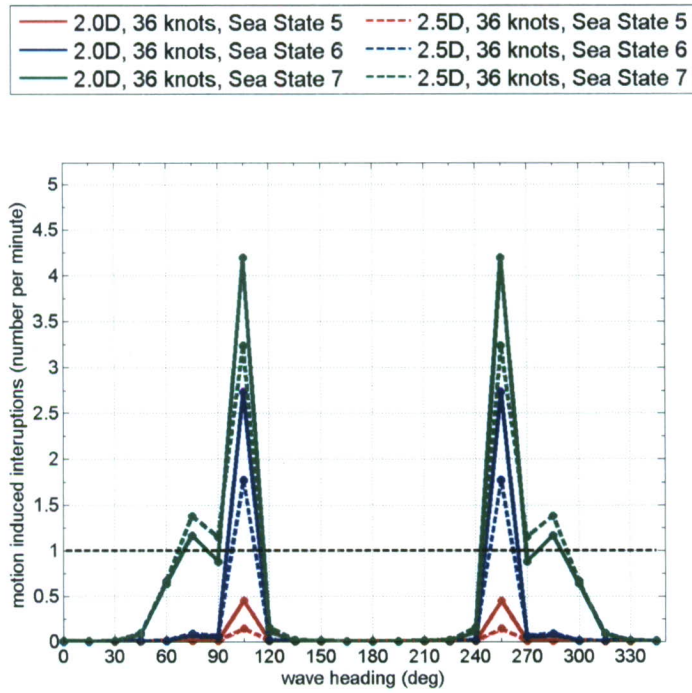


Fig. C.8. Comparison of MII at the pilothouse for the JHSS monohull using 2D and 2.5D strip theory at $F_n = 0.347$.

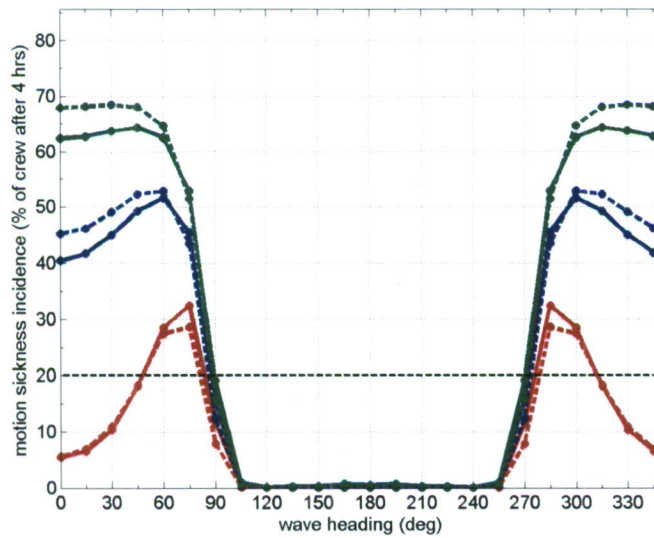


Fig. C.9. Comparison of MSI at the general helicopter spot for the JHSS monohull using 2D and 2.5D strip theory at $F_n = 0.347$.

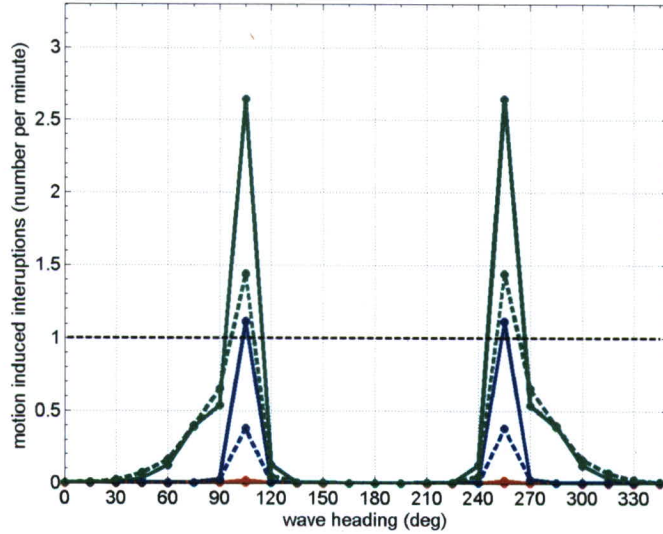
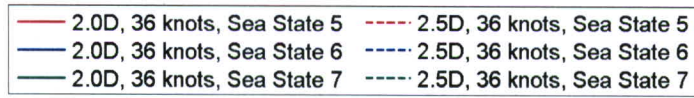


Fig. C.10. Comparison of MII at the general helicopter spot for the JHSS monohull using 2D and 2.5D strip theory at $F_n = 0.347$.

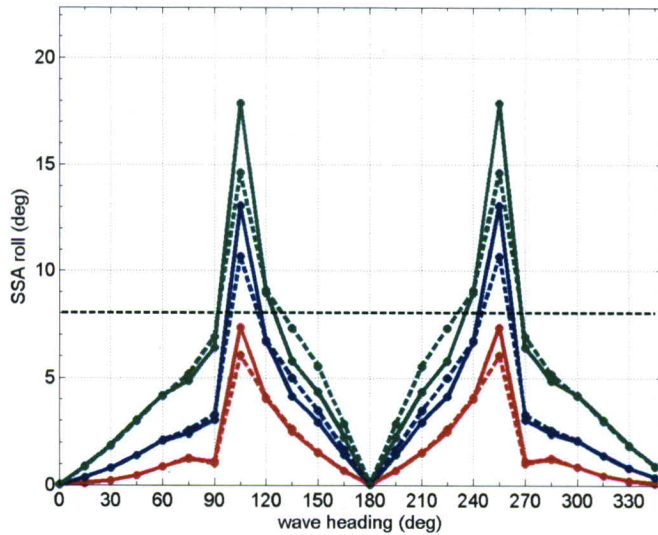


Fig. C.11. Comparison of vessel roll angles for the JHSS monohull using 2D and 2.5D strip theory at $F_n = 0.347$.

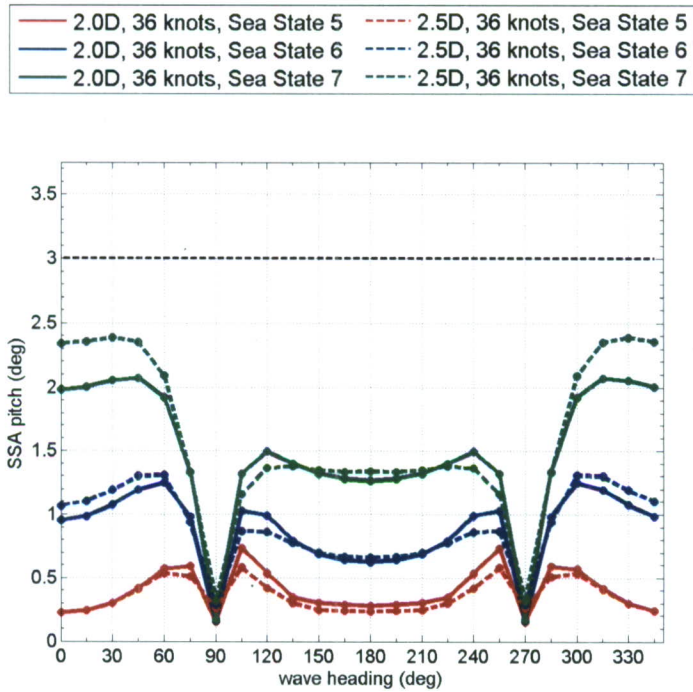


Fig. C.12. Comparison of vessel pitch angles for the JHSS monohull using 2D and 2.5D strip theory at $F_n = 0.347$.

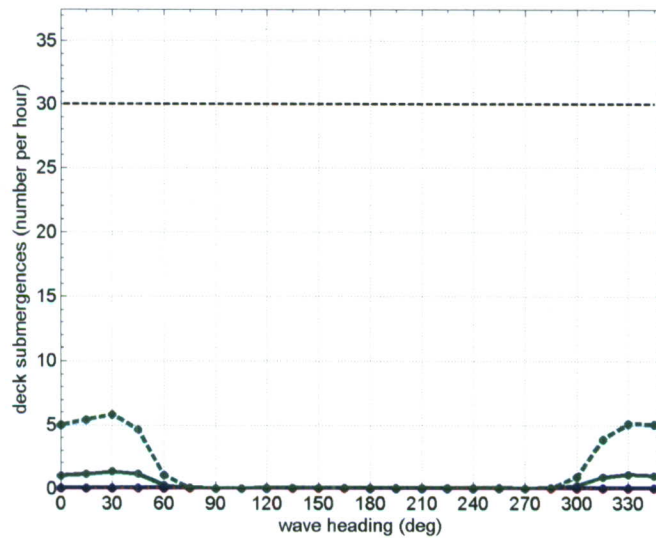


Fig. C.13. Comparison of deck wetness at the bow for the JHSS monohull using 2D and 2.5D strip theory at $F_n = 0.347$.

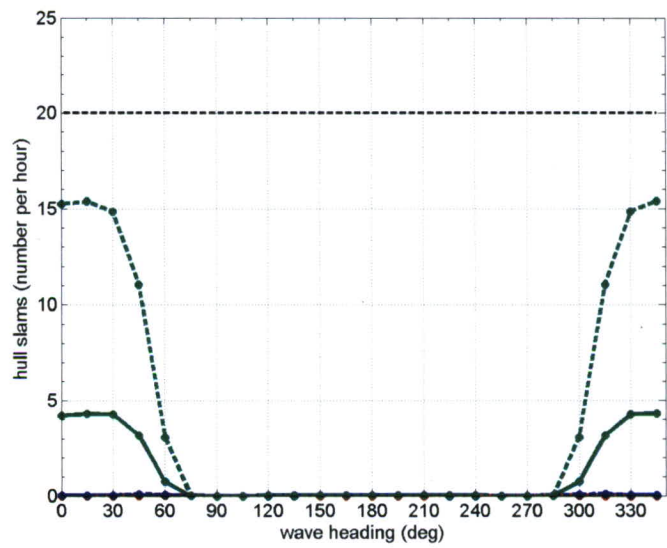
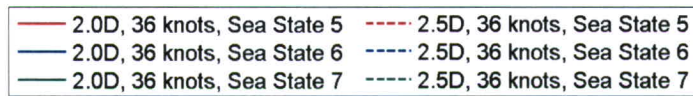


Fig. C.14. Comparison of hull slams at the bow for the JHSS monohull using 2D and 2.5D strip theory at $F_n = 0.347$.

Appendix D - Comparison of 2D and 2.5D Strip Theory for the Trimaran at 36 knots

The “transit” portion of the mission assessment involved a higher speed case, 36 knots, that for the trimaran resulted in a $F_n = 0.364$ which is in the Froude number region of where traditional two-dimensional strip theory begins to need to be corrected for forward speed. However, there is not a clear distinct speed above which a 2.5D strip theory must be used. Therefore, in the mission assessment study, only traditional two-dimensional theory was used. However, in this appendix, we compare all the 36 knot speed trimaran results that one would obtain using the two-dimensional strip theory compared to the 2.5D strip theory formulation in Figures D.1 through D.14.

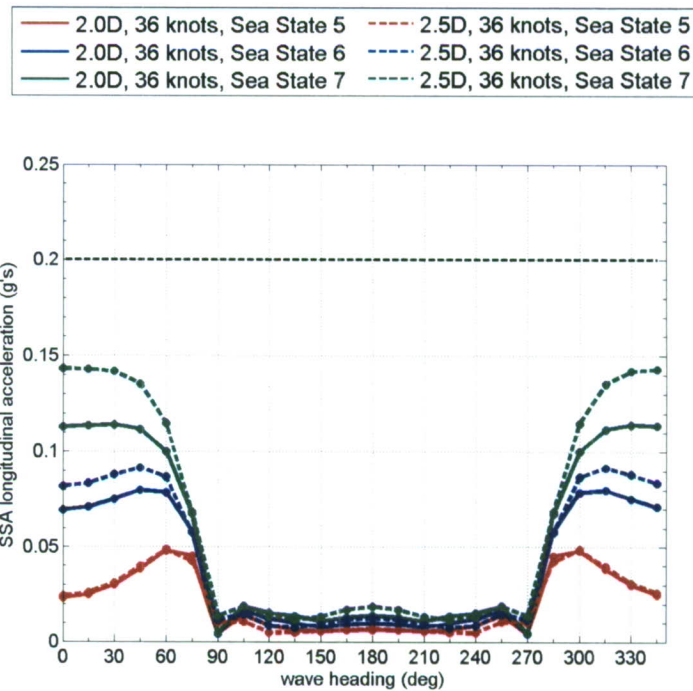


Fig. D.1. Comparison of longitudinal accelerations at the pilothouse for the JHSS trimaran using 2D and 2.5D strip theory at $F_n = 0.364$.

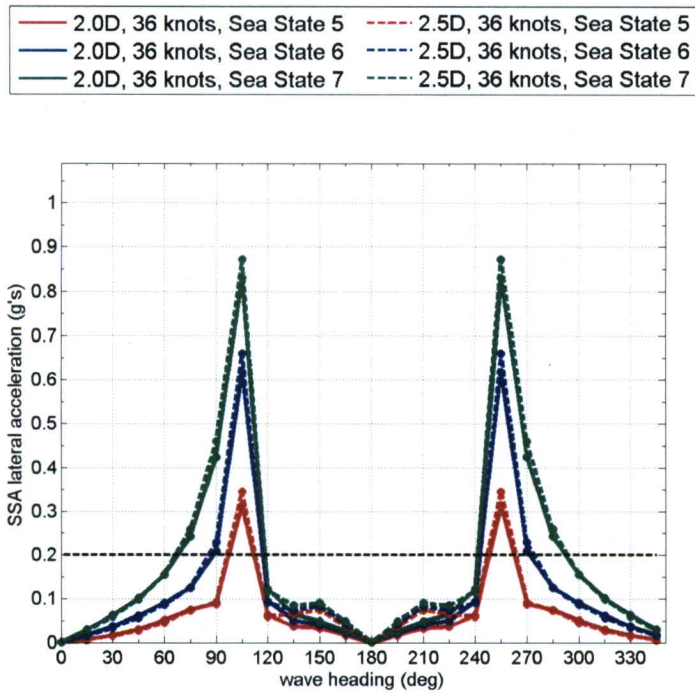


Fig. D.2. Comparison of lateral accelerations at the pilothouse for the JHSS trimaran using 2D and 2.5D strip theory at $F_n = 0.364$.

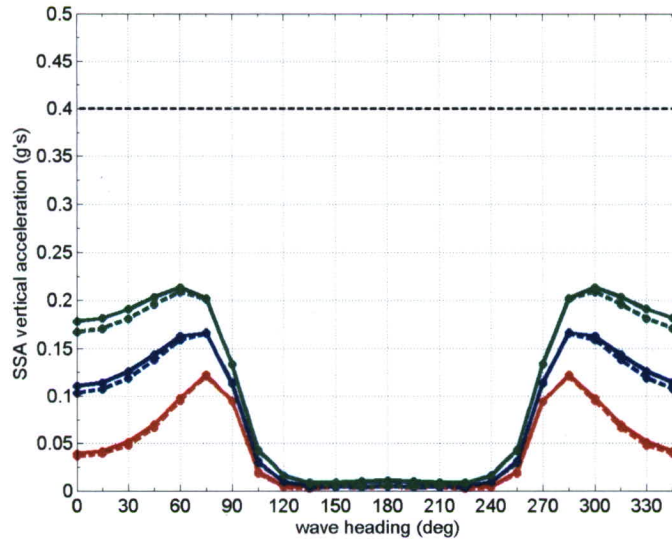


Fig. D.3. Comparison of vertical accelerations at the pilothouse for the JHSS trimaran using 2D and 2.5D strip theory at $F_n = 0.364$.

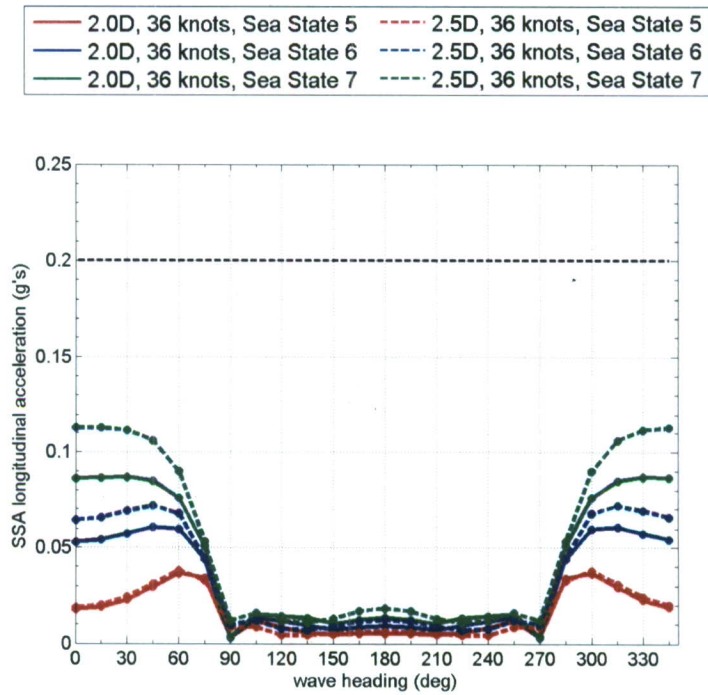


Fig. D.4. Comparison of longitudinal accelerations at the general helicopter spot for the JHSS trimaran using 2D and 2.5D strip theory at $F_n = 0.364$.

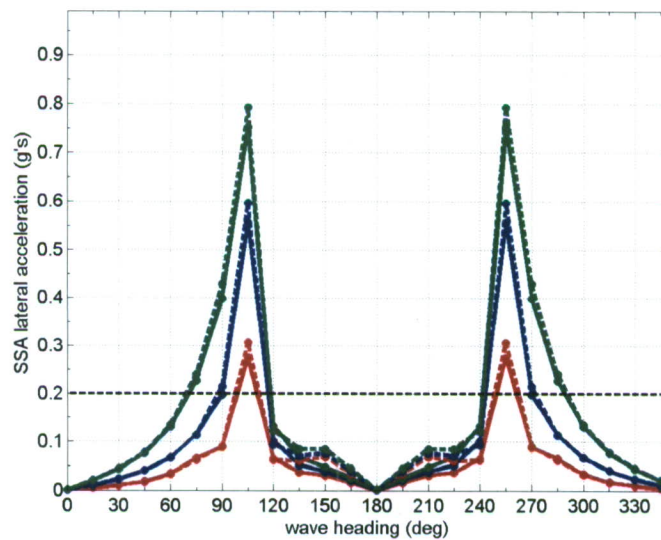


Fig. D.5. Comparison of lateral accelerations at the general helicopter spot for the JHSS trimaran using 2D and 2.5D strip theory at $F_n = 0.364$.

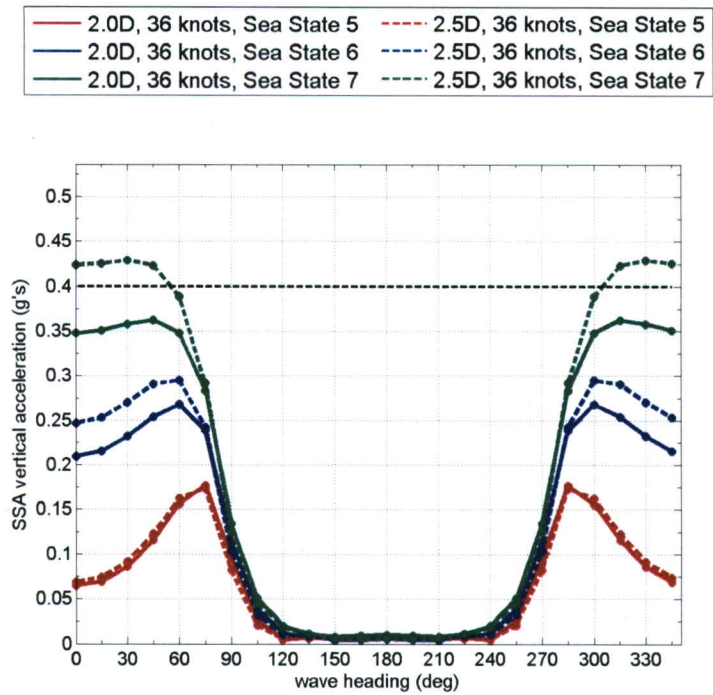


Fig. D.6. Comparison of vertical accelerations at the general helicopter spot for the JHSS trimaran using 2D and 2.5D strip theory at $F_n = 0.364$.

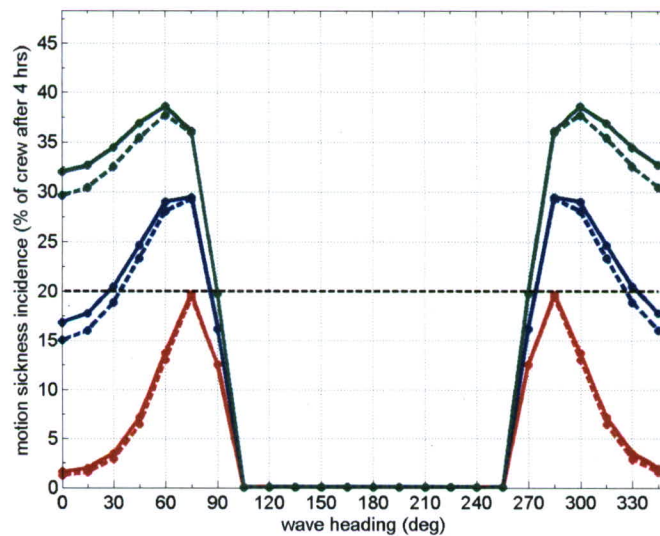


Fig. D.7. Comparison of MSI at the pilothouse for the JHSS trimaran using 2D and 2.5D strip theory at $F_n = 0.364$.

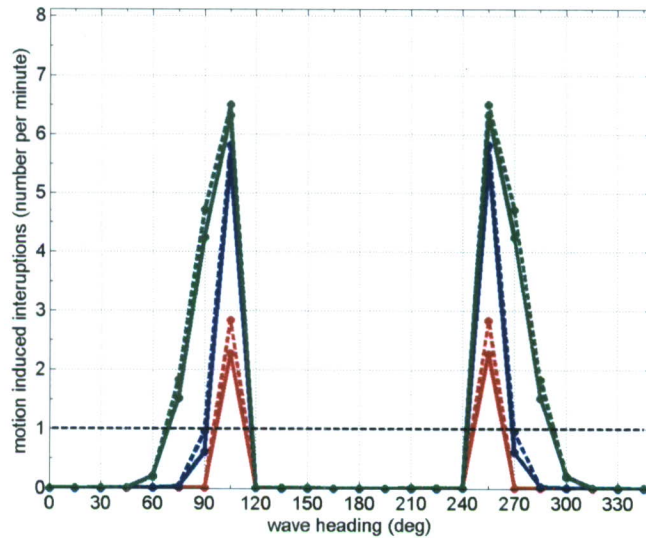
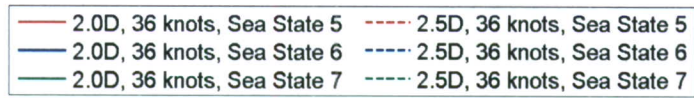


Fig. D.8. Comparison of MII at the pilohouse for the JHSS trimaran using 2D and 2.5D strip theory at $F_n = 0.364$.

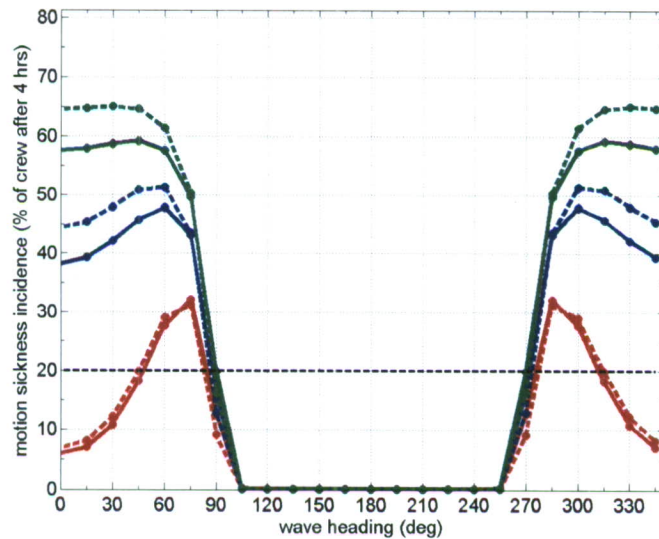


Fig. D.9. Comparison of MSI at the general helicopter spot for the JHSS trimaran using 2D and 2.5D strip theory at $F_n = 0.364$.

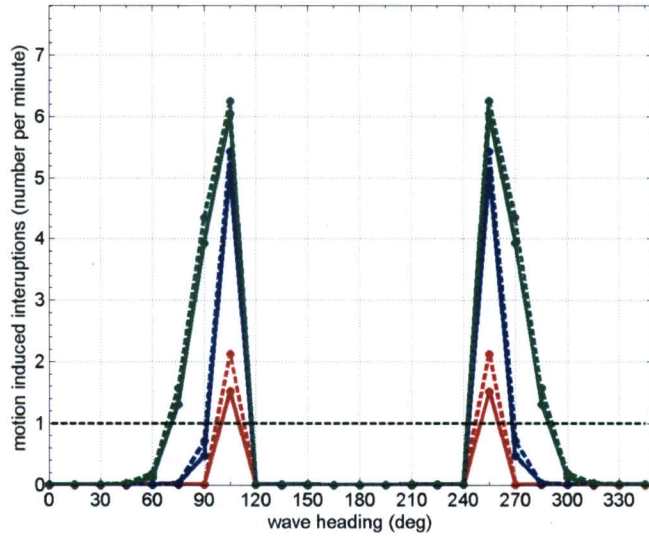
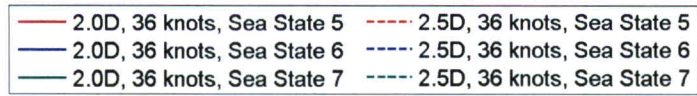


Fig. D.10. Comparison of MII at the general helicopter spot for the JHSS trimaran using 2D and 2.5D strip theory at $F_n = 0.364$.

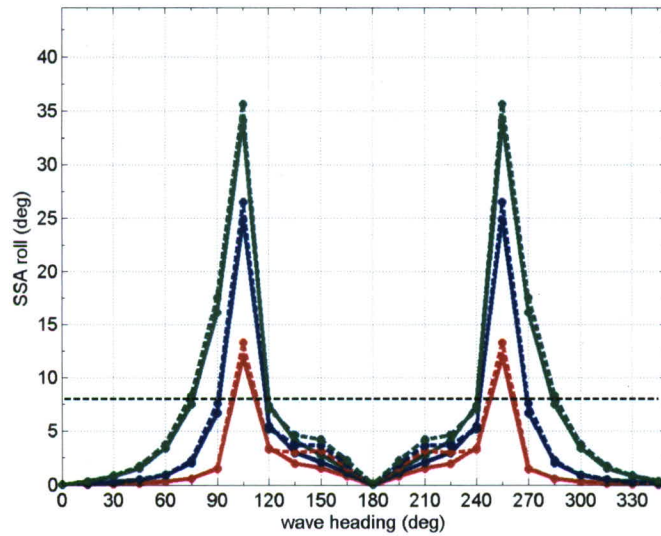


Fig. D.11. Comparison of vessel roll angles for the JHSS trimaran using 2D and 2.5D strip theory at $F_n = 0.364$.

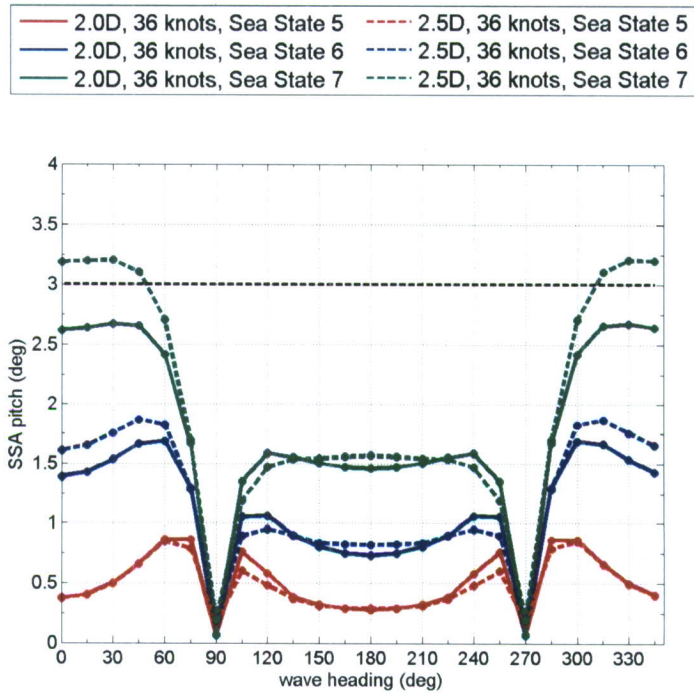


Fig. D.12. Comparison of vessel pitch angles for the JHSS trimaran using 2D and 2.5D strip theory at $F_n = 0.364$.

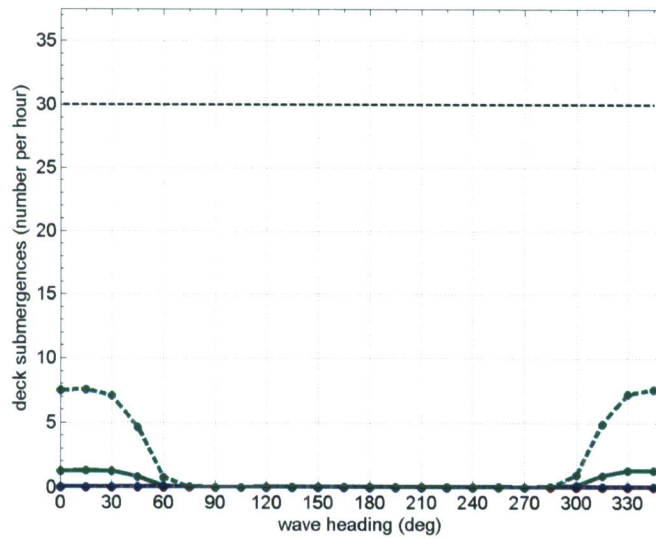


Fig. D.13. Comparison of deck wetness at the bow for the JHSS trimaran using 2D and 2.5D strip theory at $F_n = 0.364$.

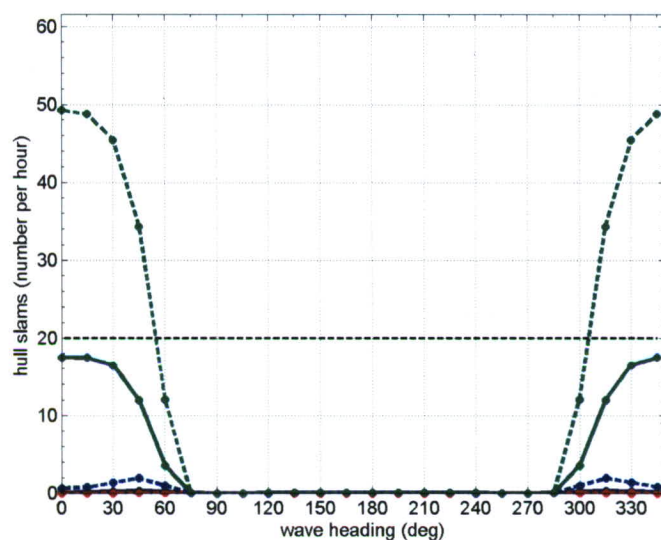
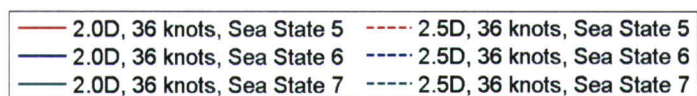


Fig. D.14. Comparison of hull slams at the bow for the JHSS trimaran using 2D and 2.5D strip theory at $F_n = 0.364$.

References

1. Salvensen, N., Tuck, E.O., and Faltinsen, O., "Ship Motions and Sea Loads," *Trans. SNAME* **78**, pp. 250-287 (1970).
2. Faltinsen, O.M. and Zhao, R., "Numerical Predictions of Ship Motions at High Forward Speed," *Phil. Trans. R. Soc. Lond. A* **334**, pp. 241-252 (1991).
3. Fathi, D., "ShipX Vessel Responses (VERES) ship motions and global loads users' manual," Project No. 609660, Norwegian Marine Technology Research Institute, Trondheim, Norway, October 2005.
4. O'Hanlon, J. and McCauley, M.E., "Motion sickness incidence as a function of the frequency and acceleration of vertical sinusoidal motion," *Aerospace Medicine*, pp. 366-369, April 1974.
5. McCauley, M.E., Royal, J.W., Wylie, C.D., O'Hanlon, J.F., and Mackie, R.R., "Motion sickness incidence: Exploratory studies of habituation, pitch and roll, and the refinement of a mathematical model," Technical Report 1733-2, Human Factors Research Inc., Goleta, California, April 1976.
6. Graham, R., "Motion-induced interruptions as ship operability criteria," *Naval Engineers Journal* **102**(2), pp. 65-71, March 1990.
7. NATO Standardization Agreement (STANAG) No. 4154 Edition 3, "Common Procedures for Seakeeping in the Ship Design Process," November 1997.
8. COMNAVAIRSYSCOM (AIR-4.0) letter 4760 Serial AIR-4.0/289 of 6 January 2004, "LHA(R) Ship Motion Design Criteria and Performance Requirements."
9. Lee, W.T. and Bales, S.L., "Environmental data for design of marine vehicles," *Ship Structure Symposium SNAME*, pp. 197-209 (1984).
10. Cusanelli, D. S. and Chesnakas, C. J., "Joint High Speed Sealift (JHSS) Baseline Shaft & Strut (BSS) Model 5653-3: Series 2, Propeller Disk LDV Wake Survey; and Series 3, Stock Propeller Powering and Stern Flap Evaluation Experiments," NSWCCD-50-TR-2007/084, (September 2007).
11. Carr, B. and Dvorak, R., "Investigation of trimaran interference effects," Bachelor of Science Degree thesis, Webb Institute, Glen Cove, NY (June 2007).
12. O'Dea, J.F., "Correlation of VERES Predictions for Multihull Ship Motions," NSWCCD-50-TR-2005/021, (September 2005).
13. Kato, H., "On the frictional resistance to the rolling of ships," *Journal of Zosen Kiokai* **102**(115), 1958.
14. Ikeda, Y., Himeno, Y., and Tanaka, N., "On eddy-making component of roll damping force on a naked hull," Technical Report 00403, Department of Naval Architecture, University of Osaka Prefecture, 1978.

15. Ochi, M. K., "Prediction of occurrence and severity of ship slamming at sea," In *Fifth Symp. on Naval Hydrodynamics*, pp. 545-596, Washington DC, 1964.

Initial Distribution List

Number of Hard Copies	Number of PDF Copies	Office	Individual
1	1	NAVSEA 05D	Wynn, S.
0	1	NAVSEA 05Z	Waters, R.
1	1	NAVSEA PMS 385	Fink, M.
1	1	DTIC	

Number of Hard Copies	Number of PDF Copies	NSWCCD Code	Individual
0	1	2410	Anderson, A.
0	1	2200	Kennel, C.
0	1	2200	Offutt, J.
0	1	3452	Library
1	1	5060	Walden, D.
1	1	5500	Applebee, T.
3	1	5500	Klamo, J.T.
1	1	5500	Lee, S.S.
3	1	5500	Silver, A.L.